



# DIGITAL ACCESS TO SCHOLARSHIP AT HARVARD

## Critical period plasticity and sensory function in a neuroligin-3 model of autism

The Harvard community has made this article openly available.  
[Please share](#) how this access benefits you. Your story matters.

Citation	No citation.
Accessed	February 19, 2015 1:04:28 PM EST
Citable Link	<a href="http://nrs.harvard.edu/urn-3:HUL.InstRepos:11158258">http://nrs.harvard.edu/urn-3:HUL.InstRepos:11158258</a>
Terms of Use	This article was downloaded from Harvard University's DASH repository, and is made available under the terms and conditions applicable to Other Posted Material, as set forth at <a href="http://nrs.harvard.edu/urn-3:HUL.InstRepos:dash.current.terms-of-use#LAA">http://nrs.harvard.edu/urn-3:HUL.InstRepos:dash.current.terms-of-use#LAA</a>

*(Article begins on next page)*

HARVARD UNIVERSITY  
Graduate School of Arts and Sciences



DISSERTATION ACCEPTANCE CERTIFICATE

The undersigned, appointed by the  
Division of Medical Sciences  
Program in Neuroscience  
have examined a dissertation entitled

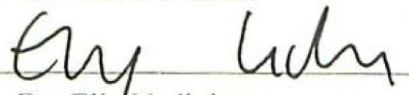
*Critical period plasticity and sensory function in a neuroligin  
-3 model of autism*

presented by Jocelyn Jacqueline LeBlanc

candidate for the degree of Doctor of Philosophy and hereby  
certify that it is worthy of acceptance.

Signature: 

Typed Name: Dr. Mustafa Sahin

Signature: 

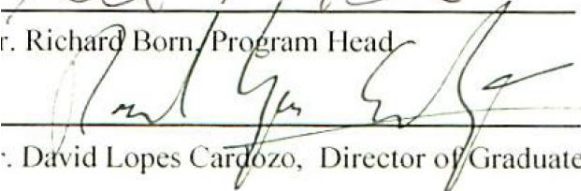
Typed Name: Dr. Elly Nedivi

Signature: 

Typed Name: Dr. Guoping Feng

  
r. Richard Born, Program Head

Date: February 25, 2013

  
: David Lopes Cardozo, Director of Graduate Studies



**Critical period plasticity and sensory function in a neuroligin-3 model of autism**

A dissertation presented

by

**Jocelyn Jacqueline LeBlanc**

to

The Division of Medical Sciences

in partial fulfillment of the requirements

for the degree of

Doctor of Philosophy

in the subject of

Neurobiology

Harvard University

Cambridge, Massachusetts

February 2013

© 2013 Jocelyn Jacqueline LeBlanc

All rights reserved.

## **Critical period plasticity and sensory function in a neuroligin-3 model of autism**

### Abstract

Extensive experience-dependent refinement of cortical circuits is restricted to critical periods of plasticity early in life. The timing of these critical periods is tightly regulated by the relative levels of excitatory and inhibitory (E/I) neurotransmission during development. Genetic disruption of synaptic proteins that normally maintain E/I balance can result in severe behavioral dysfunction in neurodevelopmental disorders like autism, but the mechanisms are unclear. We propose that abnormal critical periods of sensory circuit refinement could represent a key link between E/I imbalance and the cognitive and behavioral problems in autism.

In order to test this hypothesis, we characterized visual function and the critical period for ocular dominance in the neuroligin-3-R451C mouse model of autism. This autism-associated point mutation in the postsynaptic cell adhesion molecule neuroligin-3 (R451C) has been shown to enhance cortical inhibition. We first evaluated baseline vision using *in vivo* electrophysiological recording in the visual cortex (V1) of anesthetized adult mice. Many properties of V1 cells were normal, including retinotopy, ocular dominance, signal-to-noise ratio, and orientation and direction selectivity. Surprisingly, visual spatial acuity was unstable throughout development and dramatically increased in young adult mutant mice when compared with wild-type littermates, indicating abnormal local circuit processing.

Ocular dominance plasticity was tested over development with monocular deprivation at different ages. Plasticity was limited to the end of the first postnatal month in wild-type mice, but this

critical period was extended into adulthood in the mutants. This aberrant adult plasticity was measured by a reduction in deprived eye acuity and a shift in the ocular dominance of cells. These changes in visual function and plasticity were accompanied by increased GAD65 levels and enhanced parvalbumin-positive inhibitory circuitry in adult V1. Accordingly, we also observed a substantial enhancement of the inhibitory component of the visual evoked potential (VEP) waveform *in vivo*.

In this study, we identified novel effects of increased inhibition on visual processing and critical period plasticity in NL3-R451C mutant mice. These results provide evidence that vision can be used as a biomarker for autism, and offer insight into how E/I imbalance may alter cortical function and ultimately lead to behavioral impairments.

## TABLE OF CONTENTS

	Page
<b>Chapter 1. Introduction.....</b>	<b>1</b>
<b>Chapter 2. Methods.....</b>	<b>25</b>
<b>Chapter 3. Characterization of the visual pathway and processing.....</b>	<b>39</b>
Introduction.....	40
Results.....	42
Discussion.....	53
<b>Chapter 4. The critical period for ocular dominance plasticity.....</b>	<b>57</b>
Introduction.....	58
Results.....	59
Discussion.....	81
<b>Chapter 5. Discussion and Conclusions.....</b>	<b>85</b>
<b>References.....</b>	<b>100</b>



**TABLE OF FIGURES**

	<b>Page</b>
<b>Figure 1.1</b> .....	4
<b>Figure 1.2</b> .....	9
<b>Table 1.1</b> .....	14
<b>Figure 1.3</b> .....	20
<b>Figure 2.1</b> .....	29
<b>Figure 2.2</b> .....	31
<b>Figure 2.3</b> .....	33
<b>Figure 2.4</b> .....	36
<b>Figure 3.1</b> .....	43
<b>Figure 3.2</b> .....	44
<b>Figure 3.3</b> .....	46
<b>Figure 3.4</b> .....	48
<b>Figure 3.5</b> .....	51
<b>Figure 3.6</b> .....	52
<b>Figure 4.1</b> .....	61
<b>Figure 4.2</b> .....	62
<b>Figure 4.3</b> .....	64
<b>Figure 4.4</b> .....	65
<b>Figure 4.5</b> .....	67
<b>Figure 4.6</b> .....	69
<b>Figure 4.7</b> .....	70
<b>Figure 4.8</b> .....	72
<b>Figure 4.9</b> .....	73
<b>Figure 4.10</b> .....	76
<b>Figure 4.11</b> .....	78
<b>Figure 4.12</b> .....	80

<b>Figure 5.1</b> .....	87
<b>Figure 5.2</b> .....	96

## **ACKNOWLEDGEMENTS**

There are many people that I would like to acknowledge who have made this work possible. I would like to thank Takao Hensch and all of the past and present members of the Fagiolini and Hensch labs for their support over the years. It has been a pleasure sharing the experience of graduate school with all of my wonderful labmates and classmates, and I thank them for their friendship.

I would like to thank my dissertation advisory committee members, John Maunsell, Michael Greenberg, and Naoshige Uchida, for advising and guiding me throughout this whole process. I must give a special thank you to my dissertation exam committee members, John Maunsell, Mustafa Sahin, Elly Nedivi, and Guoping Feng, for offering their feedback during this final stage of my graduate career.

I also must thank Pamela Lynn for first igniting my passion for neuroscience, and Andrea Tilden, Leonard Zon, Teresa Bowman, and Xiaoying Bai for building the foundation for the scientist I have become. Thank you to my incredibly supportive parents, Denise and Denis LeBlanc, and to my family, friends, and husband Rodney Yeoh. I could not have done any of this without their encouragement.

Finally, I would like to thank Michela Fagiolini for being a wonderful mentor and role model. This dissertation is a testament to her wisdom, passion, and encouragement.

## **CONTRIBUTIONS**

Y. Kate Hong designed, performed, and analyzed the retinal histology and eye-specific LGN segregation experiments presented in Figures 3.1- 3.3 while in the laboratories of Josh Sanes and Chinfai Chen. All other experiments were designed by Jocelyn LeBlanc and Michela Fagiolini, and performed and analyzed by Jocelyn LeBlanc. Portions of the text were reproduced or adapted from LeBlanc and Fagiolini (2011).

# **CHAPTER 1**

## **INTRODUCTION**

Neuronal cortical circuits are refined by experience during critical periods early in postnatal life. The relative levels of excitatory and inhibitory (E/I) neurotransmission tightly regulate the timing of these sensitive periods during development. This makes them vulnerable to disruption if E/I balance is tipped in either direction without compensatory homeostatic changes. There is now increasing evidence that neurodevelopmental disorders of early postnatal development, such as autism spectrum disorder (ASD), are accompanied by genetic disruption of synaptic proteins responsible for proper E/I equilibrium. How this imbalance results in abnormal sensory, cognitive and social behavior is still largely unclear.

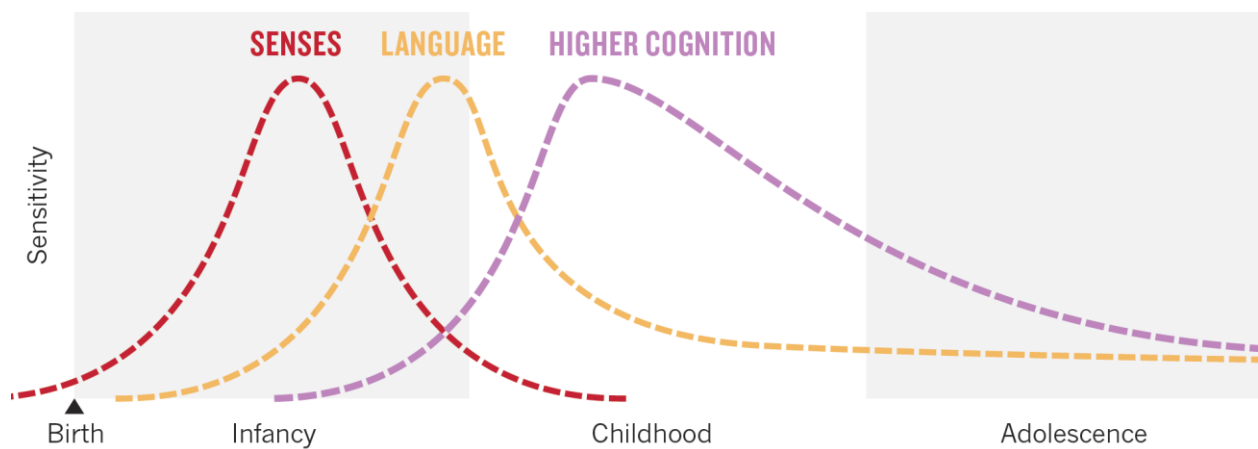
Here, we propose that alteration of the expression and/or timing of critical period circuit refinement could represent a key link between E/I imbalance and the cognitive and behavioral problems found in ASD. In this chapter, I will review what is currently known about critical periods, focusing in particular on the well-characterized critical period for ocular dominance plasticity. Next, I will explore the emerging view that autism is a synaptic disorder that results from cortical E/I imbalance, concentrating on the role that neuroligins may play in autism. Finally, I will discuss evidence of sensory processing abnormalities in autism.

The remaining chapters will describe the approach I took to address our hypothesis and potential implications of our results. Chapter 2 outlines in detail the different methods used throughout my thesis work. In Chapter 3, we characterize the visual system of the NL3-R451C mutant mice in order to understand sensory processing in autism. In Chapter 4, we evaluate ocular dominance plasticity, map the critical period, and begin to investigate the connectivity of specific GABAergic circuits in order to better understand the effect of this mutation on local circuits. To conclude, Chapter 5 contains an in depth discussion of our results and their broader implications.

## **Early brain development and circuit refinement**

The developing brain is remarkably malleable, capable of restructuring synaptic connections in response to changing experiences. The basic layout of the brain is first established by genetic programs and intrinsic activity, and is then actively refined by the environment in which the individual is immersed (Katz and Shatz, 1996). This experience-dependent sculpting of neuronal circuits occurs during distinct time windows called critical periods (Hensch, 2004). There is evidence of independent postnatal critical periods for different modalities, ranging from basic visual processing to language and social skills. They occur sequentially in a hierarchical manner, beginning in primary sensory areas (Fig. 1.1).

These sensitive periods of elevated plasticity are times of opportunity, but also of great vulnerability, for the developing brain. As many have experienced, it is easier to learn a new language, musical instrument, or sport as a child rather than in adulthood. On the other hand, early disruption of proper sensory or social experiences can result in miswired circuits that will respond suboptimally to experience in the future. The devastating effects of early deprivation are scientifically documented (Harlow et al., 1965; Nelson et al., 2007). A study of socially and emotionally-deprived children raised in Romanian orphanages demonstrated that neglect causes severe developmental delay, mental retardation, and neuropsychiatric symptoms (Nelson et al., 2007). This study showed that orphans need to be placed with caring foster families before two years of age in order to develop cognitive, social, and intellectual skills. Otherwise, neglected children are unable to recover normal function even if they are placed in similar foster homes later in life.



*Adapted by permission from Macmillan Publishers Ltd: NATURE Vol. 487 (2012)*

**Figure 1.1. Critical periods occur in succession over the course of development.**

Sensitivity to experience peaks during critical periods. The timing and duration of these windows differs depending on the domain. Critical periods for senses, like vision and hearing, occur early during infancy and have definitive closures. Critical periods for language and higher cognition occur later and do not close all of the way, permitting some plasticity to persist late in life. This sequence allows for more complex skills to build on a stable foundation of basic processing.

Comparable effects are evident for the development of senses as well. Conductive hearing loss often associated with childhood ear infections can produce long-lasting deficits in auditory perceptual acuity if not treated before the age of seven (Popescu and Polley, 2010; Harrison et al., 2005; Svirsky et al., 2004). Similarly, if binocular vision is compromised by strabismus or cataract in one eye and is not treated during early childhood, loss of acuity in the deprived eye is permanent and irreversible (Banks et al., 1975; Mitchell and Mackinnon, 2002). However, if corrected promptly, restoration of normal binocular vision is possible.

Why is this type of large-scale plasticity robust early in life but restricted in adulthood? What are the mechanisms underlying experience-dependent circuit refinement? If the timing of critical periods is disrupted, how might perception and behavior be affected? These intriguing questions prompted the birth of a whole field in neuroscience dedicated to understanding critical periods. In recent years, it has been discovered that a precise balance of cortical E/I neurotransmission regulates critical period plasticity (reviewed in Hensch, 2005; Le Magueresse and Monyer, 2013).

### **The critical period for ocular dominance**

One of the most mechanistically well-characterized critical periods is for ocular dominance plasticity in the mammalian visual cortex. Here, I will focus my discussion on the ocular dominance critical period because the underlying molecular and cellular mechanisms have been extensively dissected, making it the best model system for testing our hypothesis that critical periods may be abnormal in autism.

Abnormal visual input to one eye during infancy results in permanent loss of visual acuity, or amblyopia, if not corrected during childhood. If perturbation of vision occurs in adulthood, the visual



impairments are significantly milder or absent (Lewis and Maurer, 2009). This observation in humans inspired the development of a simple laboratory paradigm to test for the existence of a critical period in animals. David Hubel and Torsten Wiesel began investigating ocular dominance plasticity in a series of Nobel Prize-winning experiments in the 1960s (reviewed in Hubel and Wiesel, 1998). They found that the closure of one eye (monocular deprivation) in kittens during a specific time window early in postnatal life results in an experience-dependent loss of visual acuity from the deprived eye, despite no physical damage to the eye itself (Wiesel and Hubel, 1963; Hubel and Wiesel, 1970). This is due to a competitive invasion of cortical territory previously responsive to the deprived eye by inputs from the nondeprived eye. A functional loss of responsiveness to the deprived eye and an increase of responsiveness to the open eye are followed first by pruning and then regrowth of dendritic spines on cortical pyramidal neurons (Oray et al., 2004; Mataga et al., 2004). Further structural reorganization takes place in the form of shrinkage of thalamocortical projections (ocular dominance columns) serving the deprived eye and expansion of those serving the open eye (LeVay et al., 1978; LeVay et al., 1980; Antonini and Stryker, 1996; Antonini et al., 1998; Antonini et al., 1999).

This type of large-scale plasticity is only present during a restricted critical period (Hubel and Wiesel, 1970; Daw et al., 1992; Gordon and Stryker, 1996; Prusky et al., 2000b). However, plasticity is possible at other points during life. The visual cortex maintains the ability to detect changes in sensory experience, such as monocular deprivation, in adulthood as well (Lehmann et al., 2012; reviewed in Morishita and Hensch, 2008; Sato and Stryker, 2008; Chen and Nedivi, 2010). This adult plasticity can be measured using methods that are sensitive to subthreshold synaptic changes, such as imaging of intrinsic activity, activation of immediate early genes like *Arc* and *cfos*, and the contralateral/ipsilateral ratio of visual evoked potential (VEP) amplitude in response to low spatial frequency stimuli (reviewed in Morishita and Hensch, 2008). We can differentiate juvenile "critical period" plasticity from adult

plasticity by the presence of permanent suprathreshold functional changes in vision, including loss of acuity, a shift in the ocular dominance of single cells, and the rearrangement of thalamocortical axons.

The ocular dominance critical period is present in all mammals tested so far, from humans to mice, and the duration of the critical period correlates with lifespan and brain weight (Berardi et al., 2000). The establishment of rodents as models of amblyopia has made possible a fine dissection of the mechanisms underlying critical period expression. In particular, by taking advantage of genetically modified mouse models, a specific inhibitory circuit has been identified that controls the timing of ocular dominance plasticity (Fagiolini et al., 2004). Historically, the postnatal development of inhibitory neurotransmission was believed to progressively restrict plasticity, but the following key experiments proved that GABA is actually necessary for a normal ocular dominance critical period, prompting further investigation into the role of inhibition in brain plasticity.

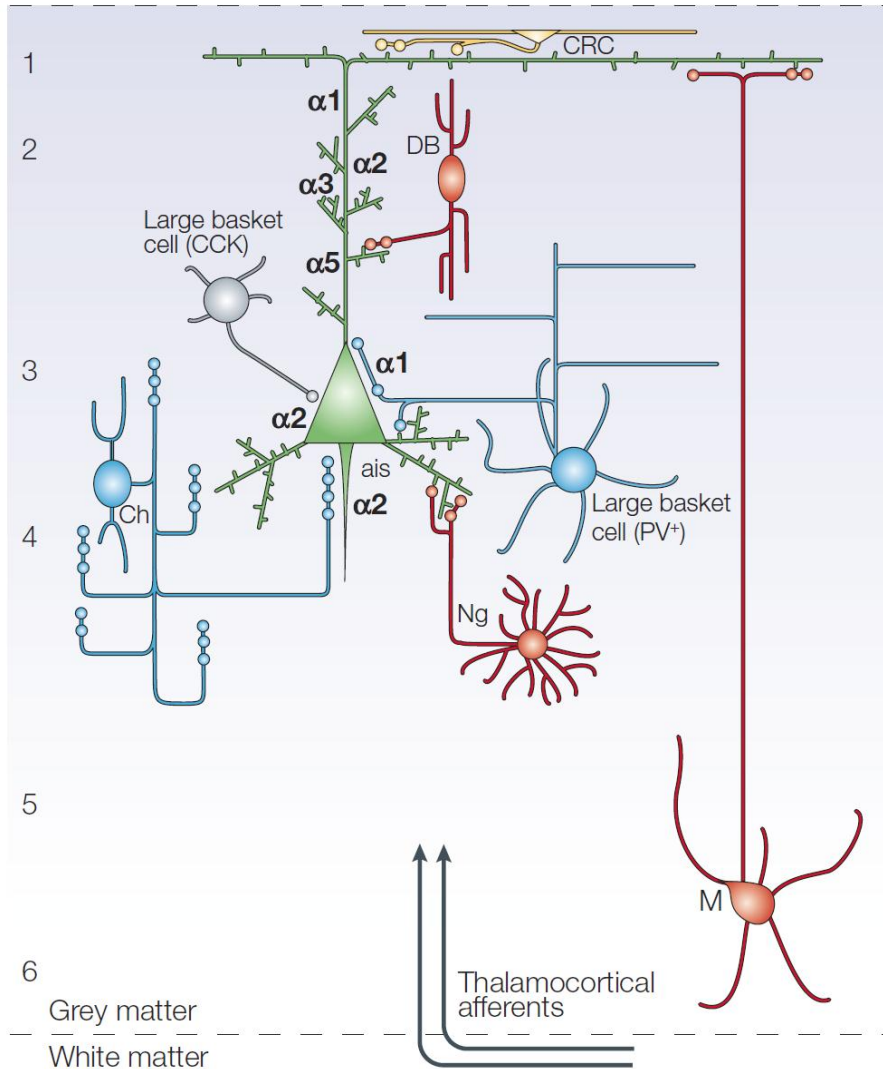
Manipulation of inhibitory transmission is difficult *in vivo* because enhancing inhibition silences the brain, while reducing inhibition can trigger seizures. With the generation of a mouse lacking only one of the two enzymes that synthesizes GABA (GAD65), researchers were able to titrate down the level of inhibition and test its role in the ocular dominance critical period (Hensch et al., 1998). Strikingly, the visual cortex of *GAD65* knockout mice remains in an immature, pre-critical period state throughout life (Fagiolini and Hensch, 2000). At any age, functionally enhancing GABAergic transmission with benzodiazepine (diazepam) treatment triggers the onset of a normal-length critical period. In addition, administering diazepam to pre-critical period age wild-type mice can cause the critical period to open prematurely (Fagiolini and Hensch, 2000). Diazepam binds to the  $\alpha$ -subunits of the GABA<sub>A</sub> receptor and increases channel open probability. Further studies revealed that plasticity is induced through the binding of diazepam to  $\alpha$ 1 and not  $\alpha$ 2 subunits (Fagiolini et al., 2004). GABA<sub>A</sub> receptors containing the  $\alpha$ 1 subunit are found on the soma and proximal dendrite region of pyramidal cells, and they are

targeted by parvalbumin-positive basket cells (Nusser et al., 1996; Klausberger et al., 2002).

Consequently, these results launched a series of studies investigating the role of parvalbumin cells in critical period regulation.

### **Parvalbumin cell regulation of critical periods**

Inhibitory interneurons account for approximately 20% of cortical neurons and exhibit heterogeneous morphological and physiological characteristics (Markram et al., 2004). Included in this large variety of inhibitory interneurons is a specific subset of GABAergic neurons that expresses the calcium-binding protein parvalbumin (Fig 1.2). Fast-spiking parvalbumin-positive basket cells (PV cells) develop with a late postnatal time course in anticipation of critical period onset across brain regions (del Rio et al., 1994; Chattopadhyaya et al., 2004). In the visual cortex, PV cells mature in an experience-dependent manner, and dark-rearing delays their maturation and critical period expression (Huang et al., 1999; Sugiyama et al., 2008). On the other hand, overexpression of brain-derived neurotrophic factor (BDNF) promotes the maturation of PV cells and speeds up the onset of the critical period (Huang et al., 1999; Hanover et al., 1999). Di Cristo et al. (2007) found that premature removal of polysialic acid (PSA), a carbohydrate polymer presented by the neural cell adhesion molecule (NCAM), results in a precocious maturation of perisomatic innervation of pyramidal cells by PV cells, enhanced inhibitory synaptic transmission, and an earlier onset of the critical period. Recent results indicate that PV cell maturation is regulated by the Otx2 homeoprotein, an essential morphogen for embryonic head formation (Sugiyama et al., 2008). Otx2 is stimulated by visual experience to pass from the retina to PV cells in the visual cortex, thereby promoting PV cell maturation and consequently triggering the onset of the ocular dominance critical period in the visual cortex.



*Adapted by permission from Macmillan Publishers Ltd: NATURE Vol. 877 (2005)*

**Figure 1.2. Local inhibitory circuits in the cortex.**

A diversity of interneurons exists in the cortex. Specific subtypes can be identified by their morphology, connectivity, intrinsic properties, and calcium binding protein or neuropeptide expression. The parvalbumin-positive large basket cell targets GABA<sub>A</sub> receptors containing the α1 subunit on the soma of pyramidal cells (shown in green). 1-6, cortical layers; Ais, axon initial segment; CRC, Cajal-Retzius cell; DB, double bouquet cell; CCK, cholecystokinin expressing cell; Ch, chandelier cell; Ng, neurogliaform cell; PV, parvalbumin-positive cell; M, Martinotti neuron.

PV cells receive direct thalamic input and connect to each other in large networks across brain regions by chemical synapses and gap junctions (Cruikshank et al., 2007; Galarreta and Hestrin, 1999). Moreover, PV cells form numerous synapses onto the somata of pyramidal cells, which in turn enrich these sites with GABA<sub>A</sub> receptors containing the  $\alpha$ 1-subunit (Fagiolini et al., 2004; Hensch, 2005; Katagiri et al., 2007; Sugiyama et al., 2008; Klausberger, 2009). This makes PV cells perfectly situated to detect changes in sensory input, to regulate the spiking of excitatory pyramidal cells, and to synchronize brain regions (DeFelipe and Farinas, 1992; Kawaguchi and Kubota, 1997; Somogyi et al., 1998).

### **Closure of the critical period**

Once the critical period is initiated, plasticity is only possible for a set length of time, and then the critical period closes (Hubel and Wiesel, 1970; Daw et al., 1992; Gordon and Stryker, 1996; Prusky et al., 2000b). Functional and structural brakes on plasticity have been identified in recent years (reviewed in Bavelier et al., 2010), and disruption of these brakes in the adult brain allows critical periods to reopen and neuronal circuits to be reshaped by experience. Interestingly these brakes share a common theme of regulating E/I balance, and particularly the GABAergic system. Locally reducing inhibition in adulthood restores plasticity in visual cortical circuits (He et al., 2006; Harauzov et al., 2010). Treatment with the antidepressant drug fluoxetine also reopens plasticity, potentially by increasing BDNF levels and altering inhibitory transmission (Maya Vetencourt et al., 2008; Chen et al., 2011). Finally, knocking out lynx1, an endogenous prototoxin that promotes desensitization of the nicotinic acetylcholine receptor (nAChR), extends the critical period into adulthood (Morishita et al., 2010). Lynx1 likely modulates E/I balance because treatment with diazepam in lynx1 knockout mice abolishes adult plasticity by restoring E/I balance to normal adult levels. On the other hand, transplanting immature GABAergic cells into the visual cortex can allow for ocular dominance plasticity later in life (Southwell et al., 2010). This second

sensitive period only emerges once the newly transplanted GABAergic cells reach a certain stage of connectivity. This study reveals that the level of maturation of inhibitory cells plays a crucial role in creating an environment that is permissive for plasticity.

Structural factors also restrict remodeling of circuits with the closure of critical periods. For example, PV cells become increasingly enwrapped in perineuronal nets (PNN) of extracellular matrix with the progression of the critical period, and enzymatic removal of these nets or disruption of their formation restores plasticity in adulthood (Sugiyama et al., 2008; Pizzorusso et al., 2002; Carulli et al., 2010). PNNs are hypothesized to regulate the firing of PV cells by controlling extracellular ion concentrations, or by sequestering molecules, like Otx2 (Beurdeley et al., 2012), that influence PV cell maturation. In addition, myelination throughout the layers of the visual cortex increases as the critical period closes, as measured by the levels of myelin basic protein (MBP) (McGee et al., 2005). Myelin signaling through Nogo receptors (NgRs) limits plasticity in adulthood, and genetic or pharmacological disruption of these receptors allows for persistent ocular dominance plasticity later in life (McGee et al., 2005; Morishita et al., in review). In addition to reopening plasticity, disruption of some of these brakes also allows for recovery from deprivation-induced loss of acuity in adulthood. This includes enzymatic degradation of PNNs (Pizzorusso et al., 2006), disruption of NgR signaling (Morishita et al., in review), administration of fluoxetine (Maya Vetencourt et al., 2008), and enhanced cholinergic signaling by *lynx1* knockdown or treatment with acetylcholinesterase inhibitors (Morishita et al., 2010). Treatment with fluoxetine and acetylcholinesterase inhibitors offers particularly promising therapeutic potential because these drugs are already FDA-approved for human use.

The exquisite care with which critical periods are regulated suggests that their proper expression is crucial for normal brain function. Disruption of E/I balance could lead to poorly refined or consolidated circuits, ultimately resulting in neurodevelopmental disorders like autism. Dissection of the

cellular and molecular mechanisms governing well-established critical periods represents a powerful tool with which to identify potential therapeutic targets to normalize plasticity and function in affected neuronal circuits.

### **Excitatory/inhibitory imbalance in autism**

Signal transmission in the postnatal central nervous system is ultimately regulated by the opposing forces of excitatory glutamatergic (E) and inhibitory GABAergic (I) inputs. Individual neurons and circuits must maintain a proper E/I balance for normal function, and the exact nature of this balance varies depending on the brain region, neuronal subtype, and developmental stage (Gatto and Brodie, 2010). This is a dynamic process, and the brain has developed mechanisms to modulate synaptic strength in order to maintain homeostasis (reviewed in Turrigiano and Nelson, 2004; Maffei and Fontanini, 2009). However genetic alterations that affect the transcriptional or translational control of synaptic molecules can disrupt homeostatic processes by altering synapse formation, organization, maintenance, or function. Such uncorrected E/I imbalance is implicated in a range of neural disorders, including autism.

The symptoms of ASD arise within the first three years of life, during a time of intense synaptogenesis and experience-dependent circuit refinement (Huttenlocher, 1990; Hensch, 2004), and include abnormal socialization, impaired communication, repetitive behaviors, and increased or decreased sensitivity to sensory stimuli (APA-DSMIV, 1994; APA-DSM5, 2011). Autistic individuals range from intellectually disabled to high-functioning, and exhibit a wide range in the manifestation and severity of symptoms. Despite a recent surge in the incidence of ASD (currently 1 in 88 children, [www.cdc.gov](http://www.cdc.gov), 2012), there is relatively little known about the neurobiological basis of autism.

In the study of human diseases, the generation and characterization of animal models is an essential bridge between understanding the molecular features of the disease and the development of therapeutics. The idea of autism mouse models has been controversial because of the difficulty in recapitulating the construct, face, and predictive validity of autism in mice (Crawley, 2004). There is, however, a genetic basis to autism, which allows for the introduction of ASD mutations into mice. There is a 70-90% concordance rate between monozygotic twins, a 10% rate for dizygotic twins, and siblings of children with autism are 25 times more likely to develop ASD (Abrahams and Geschwind, 2008; Geschwind, 2008). There is also a high incidence of ASD in some monogenetic neurodevelopmental disorders, including Rett, Fragile X, Tuberous Sclerosis, and Angelman syndromes, which are known to be caused by genetic mutations in *MeCP2* (Amir et al., 1999), *Fmr1* (Verkerk et al., 1991), *Tsc1/2* (van Slechtenhorst et al., 1997; European Chromosome 16 Tuberous Sclerosis Consortium, 1993), and 15q11-13/*Ube3a* (Magenis et al., 1987; Kishino et al., 1997; Matsuura et al., 1997), respectively. The most well-accepted ASD mouse models have been generated based on mutations associated with autism and have show some evidence of altered behavior, like abnormal communication or socialization (reviewed in Robertson and Feng, 2011; Crawley, 2012).

Many ASD-linked genes converge on common pathways that regulate synapse function and experience-dependent plasticity (reviewed in Rubenstein and Merzenich, 2003; Walsh et al., 2008; Betancur et al., 2009; Ye et al., 2010; Zoghbi and Bear, 2012; Peça and Feng, 2012). Thus, ASD is often considered to be a synaptic disorder. The most striking outward indication of E/I imbalance in autism and its associated disorders is a shared susceptibility to epilepsy (Gillberg and Billstedt, 2000). Many studies demonstrate broad alterations in both glutamatergic and GABAergic systems in ASD humans and animal models (Table 1; reviewed in Gatto and Brodie, 2010; LeBlanc and Fagiolini, 2011; Le Magueresse and Monyer, 2013).



**Table 1.1 Evidence of excitatory/inhibitory imbalance in autism spectrum disorder.**

Some examples of excitatory and inhibitory signaling alterations in syndromic and non-syndromic ASD, based on studies across different ages and brain regions in human patients (denoted with an asterisk\*) and animal models.

Disorder	Gene	Evidence of changes in excitation and inhibition	References
ASD	Unknown - general studies of autism patients	<ul style="list-style-type: none"> <li>*Elevated plasma GABA levels</li> <li>*Reduced GAD65 and GAD67 levels</li> <li>*GABA<sub>A</sub> and GABA<sub>B</sub> receptor disruption</li> <li>*Altered modulation of GABA<sub>A</sub> receptors in the presence of GABA</li> <li>*Increased number and decreased width of neocortical minicolumns</li> <li>*Increased dendritic spine density in cortex</li> </ul>	Dhossche et al., 2002; Dhossche et al., 2005 Fatemi et al., 2002; Yip et al., 2007 Collins et al., 2006; Fatemi et al., 2009a; Fatemi et al., 2009b; Fatemi et al., 2010 Guptill et al., 2007  Casanova et al., 2002; Casanova et al., 2003 Hutsler and Zhang, 2010
ASD	Neurologin-3	Increased spontaneous and evoked inhibitory transmission in cortex Increased excitatory transmission in hippocampus	Tabuchi et al., 2007  Etherton et al., 2011
ASD	Neurologin-1	Reduced NMDA/AMPA ratio at cortico-striatal synapses	Blundell et al., 2010
ASD	Neurexin-1	Reduced excitatory synaptic strength	Etherton et al., 2009
ASD	Shank3	Reduced cortico-striatal neurotransmission Altered postsynaptic density composition	Peça et al., 2011
Rett	Mecp2	Altered somatosensory evoked potentials Abnormal EEG recordings Decreased cortical minicolumn size Reduced dendritic spine number  *Altered glutamate and GABA receptors Decreased spontaneous activity  Increased PV cell innervation of excitatory cells Enhanced inhibitory gating LTP deficits  Reduced GABA <sub>A</sub> receptor subunit levels	Moser et al., 2007  Casanova et al., 2003 Belichenko et al., 1994; Chapleau et al., 2009 Blue et al., 1999 Durand et al., 2012; Dani et al., 2005 Durand et al., 2012  Moretti et al., 2006; Dani and Nelson, 2009 Medrihan et al., 2008
Fragile X	Fmr1	*Long, thin dendritic spines  Reduced AMPAR levels and LTP	Hinton et al., 1991; Irwin et al., 2000 Li et al., 2002;

**Table 1.1 (Continued)**

		<p>Increased mGluR-dependent LTD</p> <p>Increased glutamatergic vesicle fusion frequency and enhanced exocytic vesicle cycling</p> <p>Increased intrinsic excitability of excitatory cortical neurons</p> <p>Decreased number of parvalbumin interneurons</p> <p>Decrease in GABA<sub>A</sub>R subunit mRNA and decreased tonic inhibition</p>	<p>Zhao et al., 2005; Desai et al., 2006; Wilson and Cox, 2007</p> <p>Nosyreva and Huber, 2006; Zhang et al., 2009</p> <p>Zhang et al., 2001; Gatto and Broadie, 2010</p> <p>Gibson et al., 2008</p> <p>Selby et al., 2007</p> <p>Curia et al., 2009</p>
<b>Tuberous sclerosis</b>	Tsc1/2	<p>Thickened dendritic arbors of cortical pyramidal cells</p> <p>Increased excitability of cortex</p> <p>Decreased cerebellar purkinje cell excitability</p>	<p>Meikle et al., 2007</p> <p>Tsai et al., 2012</p>
<b>Angelman</b>	Ube3a, 15q11-13	<p>Abnormal spine morphology and spine density</p> <p>Defective experience-dependent development of excitatory circuits</p>	<p>Dindot et al., 2008</p> <p>Yashiro et al., 2009</p>

## **The autistic synapse: disruption of common synaptic cell adhesion pathways**

Synapse formation is an elaborate process that requires initial cell contact, differentiation of pre- and postsynaptic terminals, and organization of many different proteins. On the presynaptic side, neurotransmitter, vesicles, and release machinery must be assembled at the terminal. At the postsynaptic density, scaffolding molecules must anchor receptors and signaling proteins. After a synapse is formed, it must be stabilized and mature in order to function properly. Cell adhesion molecules (CAMs) can signal in a bidirectional manner across the synapse through their intracellular and extracellular domains, and have been shown to play roles in all stages of the life of a synapse (reviewed in Bukalo and Dityatev, 2012). CAMs play a crucial role in synaptic development by initiating contact between pre- and postsynaptic cells, maintaining adhesion, and anchoring scaffolding proteins that assemble the essential components of a synapse. CAMs can determine the identity and function of synapses, thereby having a direct influence on E/I balance.

It is estimated that a significant proportion of the genes linked to ASD encode CAMs or CAM-related molecules, establishing them as an important subset of ASD risk factors (reviewed in Betancur et al., 2009; Ye et al., 2010; Van Spronsen and Hoogenraad, 2010). These ASD-associated genes encode for include members of the immunoglobulin family (CNTN3-4, NRCAM, CADM1, ROBO1-4), cadherin family (CDH9-10, CDH18, PCDH9-10), integrin family (ITGB3, ITGA4), neurexin family (NX1, CNTNAP2, CNTNAP5), neuroligin family (NL1, NL3-4), and others (ASTN2, SHANK1-3, SLC6A4, LAMB1) (Ye et al., 2010). The neurexin (NX) and neuroligin (NL) genes are considered strongly associated with ASD and are among the most extensively studied CAMs. Much recent work has focused on understanding how mutations in these molecules can lead to autism.

## Neuroligins

Neuroligins are type I membrane proteins that are composed of an extracellular non-functional esterase homology domain, a single transmembrane domain, and a short cytoplasmic tail with a PDZ-binding motif (Ichtchenko et al., 1996). There are 4 genes encoding NLs in mice (NL1-4) that undergo alternative splicing (Ichtchenko et al., 1996). Using immunostaining and electron microscopy, the location of each isoform has begun to be elucidated. NL1 is primarily located at excitatory synapses (Song et al., 1999; Chih et al., 2005) and NL2 at inhibitory synapses (Varoqueaux et al., 2004; Chih et al., 2005). The localization of NL3 is less clear due to the poor quality of existing antibodies, but there is evidence that it can be found at both inhibitory and excitatory synapses (Budreck and Scheiffle, 2007; Heller et al., 2012). NL4 localizes to glycinergic inhibitory synapses in the retina and inhibitory synapses throughout the central nervous system (Hoon et al., 2011). Alternative splicing in the extracellular domain of both NLs and NXs can create a diverse code and can also influence whether an excitatory or inhibitory synapse is formed (Dalva et al., 2007).

Studies of NL function *in vitro* initially suggested a crucial role in synapse formation. Heterologous expression of NLs in non-neuronal cells induces morphological and functional presynaptic differentiation in axons contacting these cells (Scheiffele et al., 2000; Graf et al., 2004). Likewise, heterologous expression of neurexins in non-neuronal cells induces the formation of postsynaptic specializations in co-cultured neurons (Dean et al., 2003; Graf et al., 2004; Nam and Chen, 2005). Overexpression of NLs in cultured neurons increases the total number of synapses (Chih et al., 2005), while RNAi knockdown decreases synapse number (Chih et al., 2005). Together, these studies suggest that NLs are sufficient to induce synapse formation.

However, subsequent analysis of the function of NLs *in vivo* revealed that synapses can be established even in the absence of NLs. Thus, they are sufficient but not necessary for synapse

formation. Instead, NLs are crucial for normal functioning of synapses, playing roles in the maturation, maintenance, and function of synapses (reviewed in Sudhof, 2008). NL1-2-3 triple knock-out mice die within 24 hours of birth, and although they form typical numbers of morphologically normal synapses, there are severe deficits in synaptic transmission and reduced expression of synaptic proteins (Varoqueaux et al., 2006). Analysis of neurotransmission in single NL KO mice has allowed for a more nuanced investigation of the functional role of different NL isoforms. In the hippocampus, NL1 KO mice have impaired excitatory NMDA receptor signaling (Chubykin et al., 2007), but there is very little effect on inhibitory signaling (Chubykin et al., 2007; Gibson et al., 2009). NL2 KO mice have impaired inhibitory transmission, selectively affecting input from parvalbumin fast-spiking neurons and not somatostatin-positive interneurons (Chubykin et al., 2007; Gibson et al., 2009). Accordingly, NL1 and NL2 overexpression in cultured hippocampal neurons increases excitatory and inhibitory synaptic transmission, respectively (Chubykin et al., 2007). NL3 KO mice show a decrease in mEPSC frequency and increase in mIPSC frequency in the hippocampus (Etherton et al., 2011), but no changes in the somatosensory cortex (Tabuchi et al., 2007).

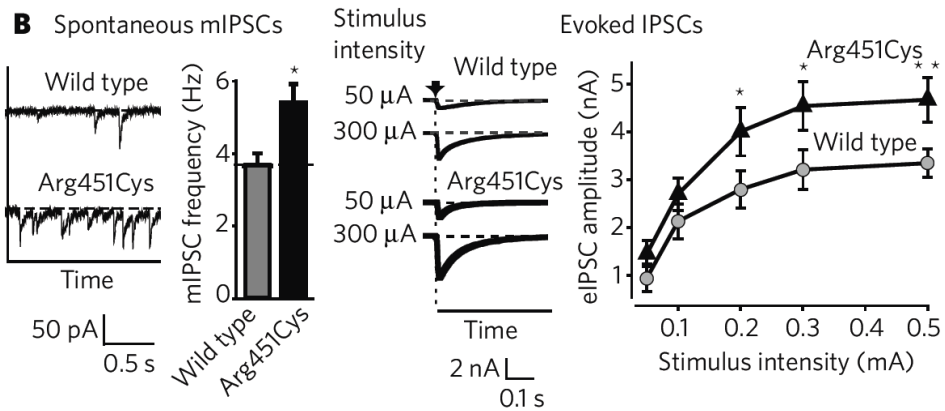
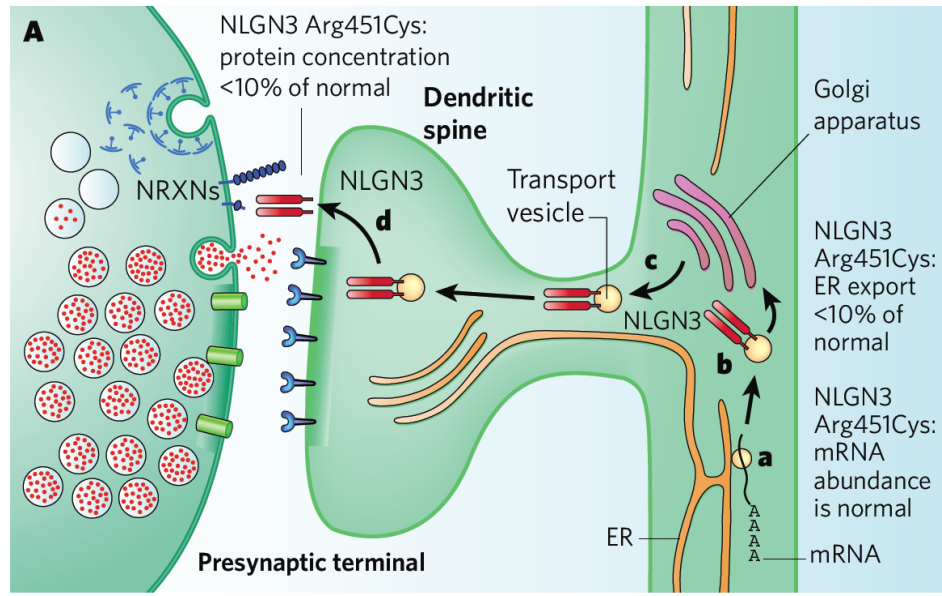
NLs bind to presynaptic NXs with different affinities depending on the isoform and alternative splicing pattern (Koehnke et al., 2010). Signaling via the NL-NX complex assembles the presynaptic and postsynaptic machinery of the synapse (Scheiffele et al., 2000; Dean et al., 2003; Graf et al., 2004; Nam and Chen, 2005). Consistent with their localization, NL1 interacts with PSD95 (Prange et al., 2004; Levinson et al., 2005) and NL2 interacts with gephyrin and collybistin (Poulopoulos et al., 2009). In fact, intracellular scaffolding proteins may play an important role in recruiting the appropriate NL isoform to excitatory or inhibitory synapses (Levinson et al., 2010).

Interest in NLs has grown recently due to their association with autism (reviewed in Sudhof, 2008; Van Spronsen and Hoogenraad, 2010; Ye et al., 2010; Jun-Yu et al., 2012). The first report of

autism-related NL mutations was by Jamain et al. (2003), when they identified one mutation in NL3 (R451C) and one in NL4 (D396X) in two different families. Since then, many other studies have also identified genetic disruption of NL1 (Glessner et al., 2009), NL3 (Yu et al., 2011), and NL4 (Laumonnier et al., 2004; Yan et al., 2005; Talebizadeh et al., 2006; Yan et al., 2008; Lawson-Yuen et al., 2008; Zhang et al., 2009; Daoud et al., 2009; Yanagi et al., 2012) (but see Vincent et al., 2004; Gauthier et al., 2005; Ylisaukko-oja et al., 2005; Blasi et al., 2006; Wermter et al., 2008). Given the crucial role that NLS play in synaptic function, much work in the past few years has focused on understanding the neurobiological consequences of ASD-associated mutations in NLS using mouse models. Many studies have focused on the R451C point mutation in NL3.

### **The autism-associated neuroligin-3 R451C point mutation**

The R451C mutation was discovered in a Swedish family, where it was present in two brothers and inherited from the mother (Jamain et al., 2003). The older brother was diagnosed at 3-years-old with typical autism and severe mental retardation, and later developed epilepsy, whereas the younger brother was diagnosed at 10-years-old with Asperger's syndrome. *In vitro* cell culture studies found that this single amino acid change (arginine to cysteine) in the extracellular portion of NL3 results in a trafficking defect where 90% of the protein is retained in the endoplasmic reticulum (ER) and degraded (Chih et al., 2004; Comoletti et al., 2004; Chubykin et al., 2005; De Jaco et al., 2006). This trafficking defect may result from local protein misfolding or altered interaction with ER chaperones (De Jaco et al., 2006; De Jaco et al., 2010). The small percent of the protein (10%) that reaches the cell surface is still able to induce synapse formation (Chubykin et al., 2005) and form heterodimers with NL1 (Poulopoulos et al., 2012), but has been reported to exhibit diminished NX1 $\beta$  binding (Comoletti et al., 2004), even though the mutation maps to a location that is distinct from the NX1 $\beta$  binding site (De Jaco et al., 2010).



Adapted by permission from Macmillan Publishers Ltd: NATURE Vol. 455 (2008)

**Figure. 1.3. The NL3-R451C mutation enhances inhibitory neurotransmission *in vitro*.**

- A. Schematic of a synapse that demonstrates the effect of the R451C mutation on NL3 protein. (a) NL3 transcription is normal, as mRNA levels do not change. More than 90% of mutated NL3 protein does not pass quality control in the endoplasmic reticulum (ER) (b) and consequently less than 10% of NL3 protein exits the ER and is inserted into the membrane (c, d).
- B. Inhibitory signaling is enhanced in the somatosensory cortex *in vitro*. Spontaneous miniature synaptic events (mIPSCs) are increased in frequency (left), and evoked responses (eIPSCs) in response to current injection are increased in amplitude (right).

Tabuchi et al. (2007) introduced this mutation into the mouse genome by gene targeting and found an increase in inhibitory synaptic transmission with no apparent changes in excitatory signaling in the somatosensory cortex (Fig. 1.3). Spontaneous miniature synaptic events (mIPSCs) occurred more frequently, and the amplitude of evoked inhibitory responses (eIPSCs) was increased. Surprisingly, subsequent analysis revealed a contrasting phenotype in a different brain region. While inhibition was enhanced in the somatosensory cortex, excitation was enhanced in the hippocampus (Etherton et al., 2011). Specifically, the frequency of mEPSCs was higher, AMPA and NMDA receptor-mediated synaptic transmission was increased, and long-term potentiation (LTP) was enhanced. Thus, the consequences of the R451C mutation are not uniform for all synapses and instead depend on region and context.

Interestingly, these NL3-R451C mutant mice also exhibit changes in behaviors relevant to autism (Tabuchi et al., 2007; Etherton et al., 2011; but see Chadman et al., 2008). In the 3-chamber socialization test, wild-type and mutant mice showed a similar preference for interacting with a visiting mouse over an object (Etherton et al., 2011). When the object was replaced a novel mouse, wild-type mice preferred to spend time with the new mouse but mutant mice failed to distinguish between the novel and familiar mouse. Perhaps due to enhanced excitatory signaling and LTP in the hippocampus, the NL3-R451C mice also showed evidence of enhanced spatial learning and memory in the Morris water maze (Tabuchi et al., 2007).

It is currently unclear how changes in E/I balance, as a result of mutations like NL3-R451C, ultimately contribute to the expression of autistic behaviors. The execution of normal cognition and behavior relies on a meaningful and accurate representation of the external environment. Incidentally, the experience-dependent development of sensory processing, which is the link between the environment and the brain, is regulated by cortical E/I balance. Therefore, we believe that in depth



study of sensory processing will provide us with valuable insight into the neurobiological mechanisms underlying autism.

### **Sensory function in autism**

Much research has focused on understanding cognitive processing in the autistic brain. However, it is important to recognize that these higher order brain functions rely on integration of inputs from lower cortical regions, building off a reliable and accurate representation of the world generated by primary sensory areas. Critical period disruption, resulting in a slight degradation in the quality of any or all of these senses, would compromise the ability to successfully execute behaviors relying on this information. Indeed, sensory abnormalities have been reported in autistic individuals, indicating improper sensory perception (reviewed in Marco et al., 2011).

Common features of autistic individuals include aggressively avoiding or actively seeking out sensory stimulation, demonstrating a spectrum of hyper- or hyposensitivity to sensory input in multiple domains (Marco et al., 2011; Kanner, 1943; APA-DSM5, 2011). There are many anecdotal accounts of sensory processing disruption in autism (Grandin, 1992; Grandin, 2009; Williams, 1998; Bogdashina, 2003). A recent meta-analysis of 14 parent-report studies on sensory modulation suggests that autistic individuals exhibit significantly more sensory symptoms than control groups, particularly between the ages of 6 and 9 (Ben-Sasson et al., 2009). Interestingly, it is suggested that sensory processing is more commonly disrupted in autism than in other developmental disorders, that these symptoms lessen with age, and that their severity correlates with the degree of social impairment (Simmons et al., 2009).

Many studies of sensory phenotypes in autism have focused on the auditory system because of the language deficits characteristic of patients. There do appear to be lower-level cortical auditory

processing abnormalities as measured by electroencephalograms (EEG) and magnetoencephalography (MEG), but the nature of these differences is variable and depends on the specifics of each experiment (Marco et al., 2011). For example, while some studies have found that autistic subjects have increased latency of cortical response to tones (Ferri et al., 2003; Martineau et al., 1984), others observed a decreased latency of cortical response (Bruneau et al., 2003; Oram Cardy et al., 2008; Roberts et al., 2010). These contrasting results may reflect the different experimental paradigms used, or could simply reflect the wide spectrum of autism phenotypes.

Abnormal somatosensory experiences are commonly reported in autistic individuals (Cascio, 2010). One psychophysical study by Tommerdahl et al. (2007) tested the ability of a small group of autistic subjects to spatially discriminate two vibrotactile stimuli applied to the skin of the hand. After a priming stimulus, subsequent spatial discrimination in that same area of skin improved for controls but not for autistic subjects, due to recruitment of inhibitory circuits. The authors suggested that this may reflect a deficit in cortical inhibition of neighboring minicolumns, but this claim was not directly tested. Psychophysical studies rely on the behavioral report of the subject, and therefore may be complicated by behavioral impairments in autistic subjects. Several somatosensory studies have directly measured brain activity instead as a means to evaluate sensory processing. Miyazaki et al. (2007) found abnormal short-latency somatosensory evoked potentials (S-SEPs) in response to median nerve stimulation in about half of the autistic patients they tested. However, it must be noted that there were no controls tested in this study, and instead autistic S-SEPs were compared to S-SEPs from controls in a previous study. Another group used MEG to map the cortical representation of the hand and face regions of high-functioning autistic and control subjects (Coskun et al., 2009). Brain activity was recorded in response to physical stimulation of the skin. Interestingly, autistic subjects had a spatially distorted cortical representation of the hand and face compared with controls. Overall, abnormal somatosensory processing may play a large role in the avoidance of affective contact in autism (Cascio, 2010).

Abnormal processing of visual information may also contribute to deficient social and communicative behavior in autism. Autistic individuals exhibit particular impairments in the processing of socially-relevant visual information. For example, children with ASD fail to show an orienting preference towards biologically-relevant motion (Klin et al., 2009). The lack of this instinctual response could deprive these children of critical social experiences during sensitive windows of development. In addition, it has been found that lower-order visual abnormalities may contribute to the impairment of higher-order visual processing of faces (Simmons et al., 2009; Behrmann et al., 2006). A study by Vlamings et al. (2010) recorded visual evoked potentials (VEPs) in autistic and control children while they looked at two types of stimuli—simple horizontal gratings, and faces with neutral or fearful expressions. The gratings or faces were composed of either high or low spatial frequency lines. Autistic children, as opposed to controls, had an enhanced VEP response to high spatial frequencies and performed better at facial expression categorization when the faces were high-pass filtered. In contrast, non-autistic children generally used low spatial frequency information to categorize the emotions of the facial expressions. This difference observed in autistic children is in agreement with previous findings that autistic perception is more detail-oriented (Dakin and Frith, 2005; Happe and Frith, 2006; Mottron et al., 2006; Behrmann et al., 2006).

In addition to atypical unisensory experiences in autism, growing evidence points towards abnormalities in multisensory processing, which is the integration of information from different senses into one perceptual experience (Marco et al., 2011). Considering that the development of different sensory modalities share common mechanisms (Hensch, 2004), it would make sense that cortical E/I imbalance in autism might also affect the integration of senses. The development of senses, as well as their integration into meaningful behavior, requires experience-dependent plasticity. A disruption of neuronal circuit refinement during critical periods may represent the mechanistic link leading to the abnormal behaviors in autism.

## **CHAPTER 2**

### **METHODS**

## **Animals**

Neurologin-3-R451C and knock-out (KO) mice were provided by Dr. Thomas Sudhof (Stanford School of Medicine) (Tabuchi et al., 2007). Heterozygous R451C female and wild-type (WT) male crosses produced WT (Y/+) and mutant (Y/R451C) male littermate mice that were used for experiments. For the KO experiments, heterozygous females were crossed with WT males to produce WT (Y/+) and KO (Y/-) male mice. Animals were raised in a 12/12 h light/dark cycle in standard housing. All procedures were approved by the Institutional Animal Care and Use Committee (IACUC) at Boston Children's Hospital. Experiments and analysis were performed blind to genotype. In the text and figures, the term "juvenile" refers to 1-month-old mice and "young adult" refers to 2-3-month-old mice.

## **Retinal histology**

These experiments were performed by Y. Kate Hong in the laboratories of Dr. Joshua Sanes and Dr. Chinfai Chen. Detailed histology methods have been previously described (Kim et al., 2010; Hong et al., 2011). Retinae were dissected from perfused 2-3-month-old NL3-WT and R451C mutant mice and post-fixed for 20-30 min in 4% paraformaldehyde (PFA) in 0.1 M phosphate buffered saline (PBS). For whole-mount retinae, tissue was rinsed and incubated with mouse IgG1 anti-Brn3a antibody (1:500, Millipore) for 1-2 days at 4°C, rinsed in PBS, and incubated in Alexa 488-conjugated goat anti-mouse secondary antibody (Invitrogen) for 2-3 hrs at room temperature (RT). For retinal cross-sections, retinae were incubated with 30% sucrose in PBS for 1 hr, frozen, and cut on a cryostat into 16-18 µm thick sections. Sections were blocked with 2% donkey serum/0.1% Triton X-100/PBS for 30 min, followed by primary antibody incubation at 4°C overnight. The sections were then washed in PBS and incubated in secondary antibody for 2 hrs at RT. Primary antibodies included mouse anti-Bassoon (1:500, Enzo Life Sciences), rabbit-anti glutamate decarboxylase (GAD65/67) (1:1000, Millipore), mouse IgG2a antibody

Znp1 for labeling synaptotagmin II (1:100, Zebrafish International Resource Center), and rabbit anti Calbindin (1:3000, Swant). Secondary antibodies were conjugated to Alexa 488 (Invitrogen) and used at 1:500. Images were acquired on a confocal microscope (Zeiss LSM700) with a 25X oil objective and 0.5X zoom.

### **Retinal ganglion cell (RGC) density analysis**

These experiments were performed by Y. Kate Hong in the laboratories of Dr. Joshua Sanes and Dr. Chinfei Chen. The density of Brn3a-positive RGCs was compared in WT and mutant retinae overall and in 3 regions based on the distance from the optic head (center, middle, and edge). A 500x500  $\mu\text{m}$  window of tissue was imaged in each zone. In order to count the density of Brn3a-positive nuclei, images were processed and analyzed in ImageJ using the intermodes method of thresholding and the Particle Analysis feature.

### **Eye-specific segregation in the lateral geniculate nucleus (LGN)**

These experiments were performed by Y. Kate Hong in the laboratories of Dr. Joshua Sanes and Dr. Chinfei Chen. Young adult NL3-WT and R451C mutant mice were anesthetized by intraperitoneal injection of ketamine/xylazine. Eyes were injected with 1.5  $\mu\text{l}$  of cholera toxin B subunit conjugated to Alexa-488 in one eye and Alexa-594 in the other (1 mg/ml, Invitrogen). Animals were allowed to recover and were perfused 2-3 days later. Brains were dissected, post-fixed overnight at 4°C, and washed in PBS. Then 50  $\mu\text{m}$  sagittal sections were cut with a vibratome. Fluorescence images were taken with a 5X objective (Nikon 80i) at sub-saturation levels. Images were analyzed using a threshold-independent quantitative method as previously described (Torborg and Feller, 2004). Colocalization was determined

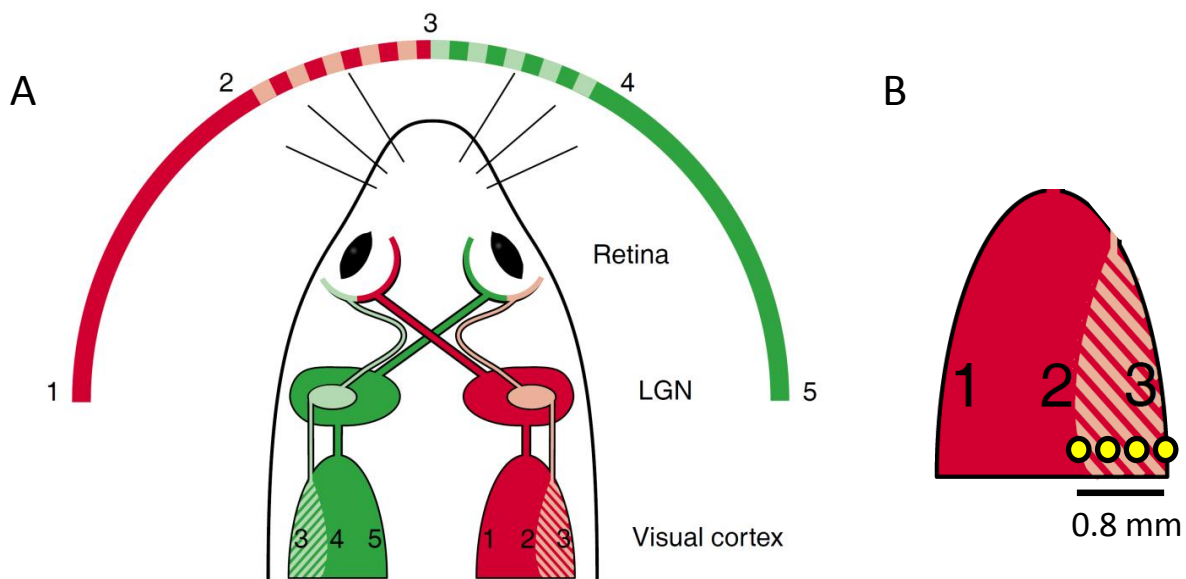
by finding the variance of R values for each pixel, where R is the log of the ratio of ipsilateral to contralateral pixel intensities in the axons ( $R = \log(I_{\text{ipsi}}/I_{\text{contra}})$ ). The variance, defined as the width of the distribution of R values, was used to compare the level of colocalization or segregation across different samples.

## **Electrophysiology**

Electrophysiological recordings were made from the binocular visual cortex (V1b) of anesthetized mice (50 mg/kg nembutal and 0.12 mg chlorprothixene) using standard methods (Gordon and Stryker, 1996; Hensch et al., 1998). Light anesthesia was maintained throughout the duration of the experiment with an isoflurane/oxygen mixture delivered to the mouse through a trachea tube. Visual stimuli were presented on a cathode ray tube (CRT) computer monitor placed in front of the mouse.

### Multi-channel single-unit recordings

A 16-channel probe spanning all layers of the cortex (Neuronexus Technologies, A1x16-3mm50-177) was lowered into V1b at 3 to 4 different locations between 2.6 and 3.4 mm lateral to the midline in each mouse (Fig. 2.1). Signals were filtered from 400 to 5000 Hz and amplified 5000 times, and a threshold was set to separate spikes from noise (SortClient, Plexon Technologies). Visual stimuli were delivered to the contralateral eye and consisted of 3-second-long presentations of drifting (2 Hz) black and white bars (100% contrast, 0.025 cpd) at 12 different orientations (0-360°) spaced 30° apart. Each orientation presentation was repeated 8 times in random order. Eight repetitions of a blank stimulus of intermediate luminance were interspersed throughout the session in order to evaluate spontaneous activity.



Reprinted from *Curr. Opin. Neurobiol.*, Vol. 13, M. Hubener, *Mouse Visual Cortex*, pp. 413-420, 2003, with permission from Elsevier.

**Figure 2.1. Schematic of the mouse visual system and V1b electrophysiological recording sites.**

- A. Visual information enters the visual system through the retina and is transmitted to the lateral geniculate nucleus (LGN) through the optic nerve. The majority of optic nerve fibers cross the midline at the optic chiasm. Inputs from the two eyes are distinctly segregated in the LGN (contralateral inputs in red and green and ipsilateral inputs in pink and light green). The visual cortex (V1) is separated into a medial monocular zone (solid red and green) that receives exclusive input from the contralateral eye, and a lateral binocular zone (striped red and green) that receives input from both eyes. V1 is retinotopically organized to represent different locations in the visual field, as indicated by the numbers 1-5. The lateral edges of the visual field are represented by cells in the monocular zone and the center is represented by cells in the binocular zone.
- B. Diagram of V1 showing the monocular zone (V1m, red) and the binocular zone (V1b, striped red). The yellow circles indicate electrophysiological recording sites across the extent of V1b.



Spikes were sorted based on waveform characteristics (Offline Sorter, Plexon Technologies), and a minimum interstimulus interval of 1.5 ms was imposed to ensure single unit isolation. Spiking rates in response to visual stimuli were determined using Matlab via SigTOOL (Lidierth, 2009). Spontaneous activity (SA) was calculated as the mean firing rate in response to blank stimuli. Maximum evoked response ( $R_{max}$ ) was defined as the maximum firing rate during any stimulus presentation. Signal-to-noise ratio =  $(R_{max}-SA)/R_{max}$ . The orientation selectivity index (OSI) =  $(R_{max}-R_{ortho})/(R_{max}+R_{ortho})$ , where  $R_{ortho}$  was the response to the orientation that was orthogonal ( $\pm 90^\circ$ ) to the preferred orientation. The direction selectivity index (DSI) =  $(R_{max}-R_{opp})/(R_{max}+R_{opp})$ , where  $R_{opp}$  was the response to the direction that was opposite ( $\pm 180^\circ$ ) to the preferred direction. Only visually responsive cells were included in the analysis ( $R_{max} \geq 1.5 \times SA$ ;  $R_{max} \geq 0.5$  spikes/s, unless  $OSI \geq 0.33$ ). Fast-spiking putative inhibitory cells were excluded from analysis based on trough to peak time  $\leq 0.37$  ms and peak to trough amplitude ratio  $\geq 0.43$  (Fig. 2.2; Bartho et al., 2004; Hasenstaub et al., 2005; Niell and Stryker, 2008).

### Extracellular recording

Multiple penetrations (3 to 4) across the lateral extent of V1b were made with a tungsten electrode (FHC, Inc.) and 5 to 8 cells spaced at least 70  $\mu\text{m}$  apart were recorded for each penetration (Fig. 2.1). The stimulus was a vertical bar of light,  $3^\circ$  wide, moving horizontally across the screen at a velocity of  $19^\circ/\text{s}$ . The signal was filtered from 300 to 5000 Hz and amplified 1000 times. The stimulus was repeated 6 times for each cell and for each eye, and the responses were averaged across all repetitions (software developed by C. Orsini, Pisa, Italy). Baseline activity was determined based on spiking during 2.5 seconds of blank screen between each repetition of the stimulus.

The ocular dominance score of each cell was calculated based on the relative spiking in response to stimulation of each eye. Ocular dominance score =  $[(PI-BI) - (PC-BC)] / [(PI-BI) + (PC-BC)]$ , where P=peak, B=baseline, C=contralateral eye, and I=ipsilateral eye (Hensch et al., 1998). Each cell was also

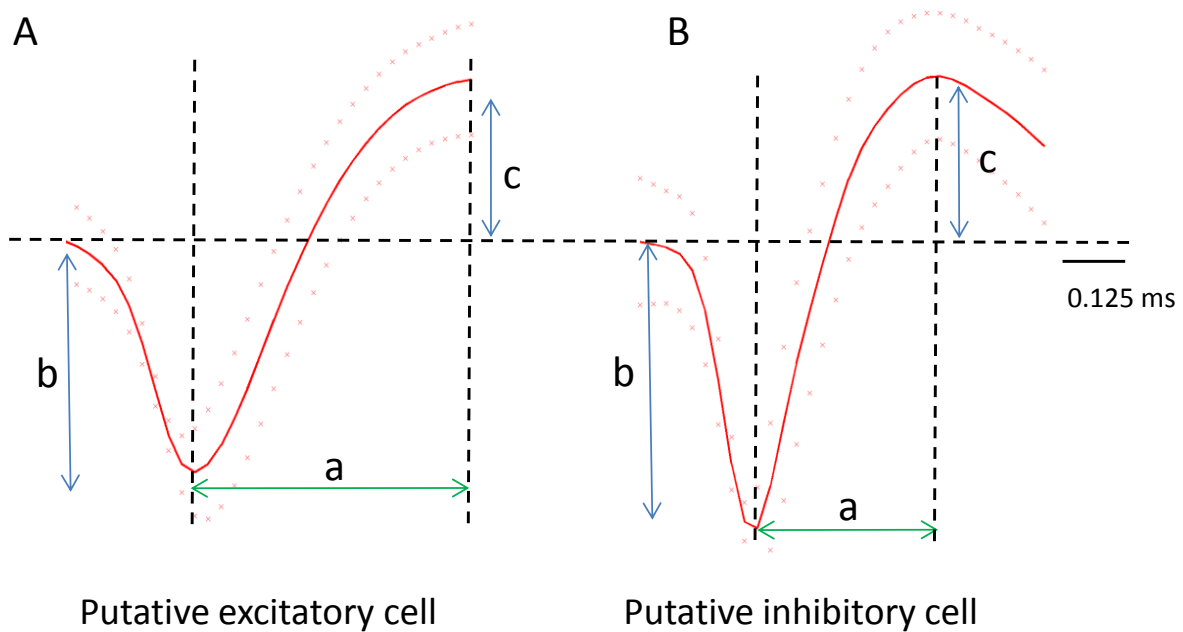


**Figure 2.2. Putative excitatory vs. inhibitory cell sorting based on waveform shape**

Schematic of the waveform parameters used to sort putative inhibitory from excitatory cells (Bartho et al. 2004, Hasenstaub et al. 2005, Mitchell et al. 2007, Niell and Stryker 2008). The blue arrows indicate the amplitude of the trough (b) and peak (c) and the green arrows indicate the trough to peak time (a).

- A. Putative excitatory cells had a trough to peak time (a) that was greater than 0.37 ms and a ratio of peak to trough amplitude (c/b) that was less than 0.43.
- B. Putative inhibitory cells had a trough to peak time (a) that was less than or equal to 0.37 ms and a ratio of peak to trough amplitude (c/b) that was greater than or equal to 0.43.

assigned a value on the qualitative 7-point ocular dominance classification scale originally developed by Hubel and Wiesel (1962). A cell would be ranked 1 if it only responded to the contralateral eye, 4 if it responded equally to both eyes, 7 if it only responded to the ipsilateral eye, and so on. A contralateral bias index (CBI) was calculated to represent the weighted average of overall ocular dominance in a population of cells.  $CBI = [(n_1 - n_7) + 2/3(n_2 - n_6) + 1/3(n_3 - n_5) + N] / 2N$ , where  $N$  = total number of cells and  $n_x$  = number of cells with a ranking of  $x$  on the 7-point scale (Gordon and Stryker, 1996). The receptive field locations of a subset of cells were determined by the location in degrees from the vertical meridian of the visual field where the maximum firing rate was evoked by the passing bar of light.

#### Visual evoked potential recordings

VEP recordings were performed as previously described (Porciatti et al., 1999). A tungsten electrode (FHC, Inc.) was placed at 2.8 mm from the midline in V1b where the visual receptive field was approximately 20° from the vertical meridian (Fig. 2.1). The contralateral eye of the mouse was presented with horizontal black and white sinusoidal bars that alternated contrast (100%) at 1 Hz (square wave). Local field potentials were recorded by filtering the signal from 0.1 to 100 Hz and amplifying 10,000 times. Signals were averaged over 20 repetitions of the visual stimulus (software developed by C. Orsini, Pisa, Italy). Acuity was measured at the cortical depth where the largest amplitude signal was obtained in response to a 0.05 cpd stimulus (Fig. 2.3). For each different spatial frequency ranging from 0.05 to 0.9 cpd, 3 to 4 trials consisting of 20 contrast reversals each were performed in random order. The mean peak amplitude of the negative component of the waveform (NC) was plotted against the log of the spatial frequency, and the threshold of visual acuity was determined by linear extrapolation to 0 mV.

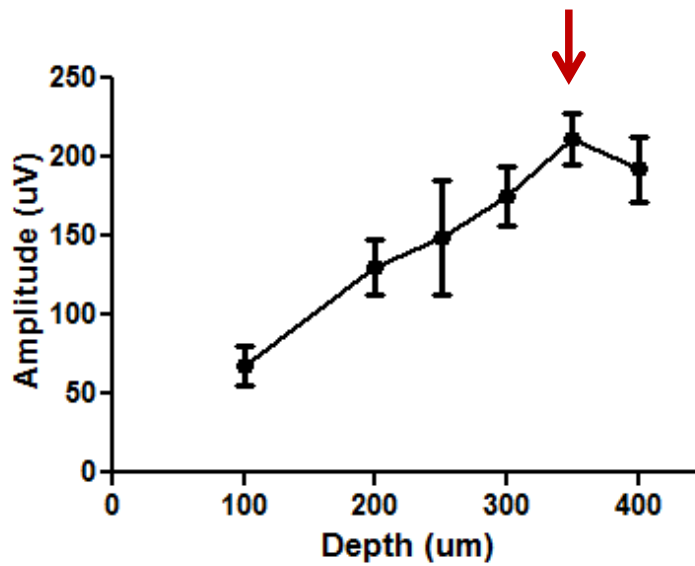


**Figure 2.3. VEP signal amplitude throughout the depth of the cortex in one mouse.**

For each VEP recording, the response of the contralateral eye to a low spatial frequency stimulus (0.05 cpd) was tested at multiple depths. The depth at which the largest amplitude response was recorded was used for the remainder of the recording. In this example it is 350  $\mu\text{m}$  (marked by the red arrow).

## Ocular Deprivation

Eyelids were trimmed and sutured under isoflurane anesthesia as previously described (Gordon and Stryker, 1996). The integrity of the suture was checked daily and mice were used only if the eyelids remained closed throughout the deprivation period. The eyelids were reopened immediately before recording and the cornea was checked for clarity. Depending on the experiment, either one eye was closed (monocular deprivation) or both eyes were closed (binocular deprivation). The duration of deprivation was either 4 days (short-term) or more than 1 month (long-term). To test the permanence of acuity loss, the eye was reopened at P33 or P40 following long-term deprivation and checked daily (for 25 to 40 days) to ensure the pupil remained unobstructed until the day of recording.

## Western Blot

The brain was quickly removed and both hemispheres of V1b (2-4 mm lateral, 0-2 mm posterior) of each animal were dissected and combined in one tube. The tissue was flash-frozen in liquid nitrogen and homogenized by sonication in RIPA-NaPO<sub>4</sub> lysis buffer. The samples were centrifuged at 4 °C at 13,200 rpm for 10 min to isolate the supernatant. The concentration of protein in each sample was determined using a micro BCA protein assay kit (Thermo Scientific). Equal amounts of protein (20-60 ug) were separated by size by 8-18% SDS-PAGE. Proteins were transferred overnight at 4°C at 50 mA onto nitrocellulose membranes (Whatman). Membranes were blocked in 5% milk in TBST for 1 h at RT, incubated with primary antibody for 2 hrs at RT, and with secondary horseradish peroxidase-conjugated antibodies (1:5000, abcam) for 45 min at RT. Bands were visualized using enhanced chemiluminescence (ECL) reagents (VisiGlo) and exposure to film. The mean intensities of the bands were quantified using MacBiophotonics ImageJ software (<http://www.Macbiophotonics.ca/imagej/>) and normalized to the GAPDH levels of each sample. Primary antibodies included mouse anti-Neuroigin-1 (1:5, Neuromab);

goat anti-Neurologin-2 (1:750, Abcam); mouse anti-Neurologin-3 (1:500, Neuromab); mouse anti-GAD67 (1:5000, Chemicon); mouse anti-GAD65 (1:200, Abcam); rabbit anti-VGAT (1:2500, GeneTex); mouse anti-PSD95 (1:500, Thermoscientific); rabbit anti-NR2A (1:1000, Frontier Science); rabbit anti-NR2B (1:1000, Frontier Science); rabbit anti-GABAA  $\gamma$ 2 (1:1000, Thermoscientific); rabbit anti-GABAA  $\alpha$ 2 (1:500, Alomone); mouse anti-GAPDH (1:50,000, Abcam); rabbit anti-Calbindin (1:5000, Swant); rabbit anti-Calretinin (1:2500, Swant); rabbit anti-Kv3.1 (1:100, Alomone); rabbit anti-Vglut1 (1:1000, Abcam); rabbit anti-GluR2/3 (1:1000, Millipore); rabbit anti-gephyrin (1:1000, Chemicon).

### **Immunohistochemistry**

Mice were anesthetized with 50 mg/kg nembutal and transcardially perfused with ice-cold 0.9% saline followed by 50 mL of 4% PFA. Brains were post-fixed for 3 h at 4°C, cryoprotected in 30% sucrose for 24 hrs, and frozen in OCT resin. Coronal sections 30  $\mu$ m thick were cut on a cryostat and frozen in PBS. Free-floating V1b sections were incubated in blocking solution (10% NGS, 0.5% Triton-X in PBS) for 30 min at RT, primary antibody overnight at RT, and secondary antibody for 1 h at RT in the dark. Sections were mounted in DAPI Fluoromount-G mounting medium (Southern Biotech) onto glass slides. Primary antibodies included rabbit anti-PV (1:000, Swant); mouse anti-GAD65 (1:1000, Developmental Studies Hybridoma Bank). Secondary antibodies included Alexa Fluor 488 goat anti-rabbit (1:1000, Invitrogen) and Alexa Fluor 594 goat anti-mouse (1:500, Invitrogen).

### **Confocal microscopy**

Sections were imaged with a laser scanning confocal microscope (Olympus FluoView, FV1000) using the multi-channel acquisition mode. All imaging and analysis was done blind to genotype. Images in V1b (Fig. 2.4) were taken with 1024x1024 pixel resolution and the same acquisition parameters were

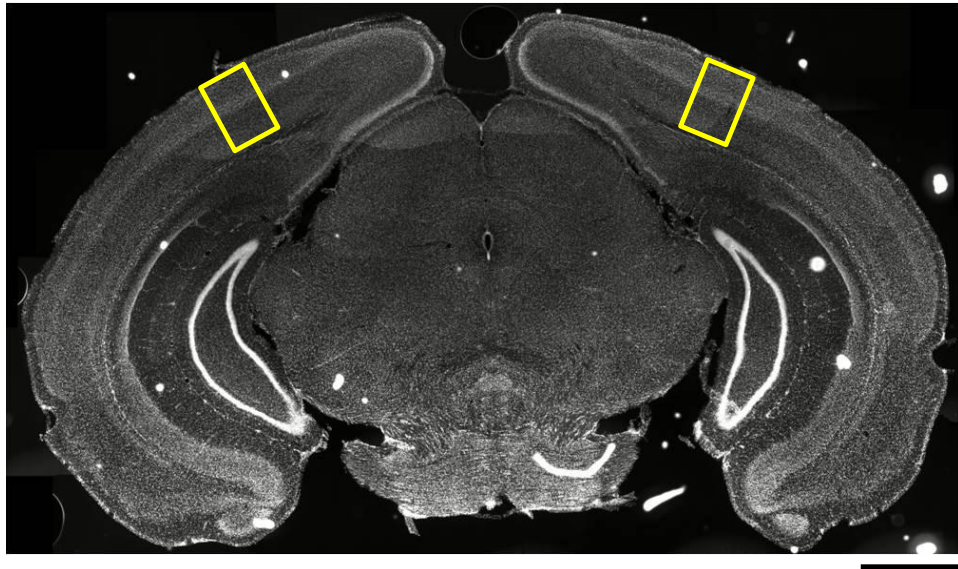


**Figure 2.4. Location in binocular visual cortex used for immunostaining studies.**

A composite of 10X images covering a 50  $\mu\text{m}$  thick coronal slice in a NL3-WT brain is shown. Cell nuclei are labeled with DAPI. The yellow boxes indicate the location inV1b that was used for immunostaining analysis. Interaural location, -0.24 mm; bregma location, -4.04 mm (Figure 64 in Paxinos and Franklin, 2001). Scale bar=1 mm.

used for all sections stained with the same antibodies. At 20X, a 0.75 numerical aperture and 1 Airy unit pinhole were used. At 100X, a 1.4 numerical aperture and 1 Airy unit pinhole were used. Images were analyzed using MacBiophotonics ImageJ software. Overall mean pixel intensity of PV and GAD65 staining were measured on 20X images.

#### Analysis of perisomatic puncta

Individual pyramidal cells innervated by PV cells in layer 2/3 or layer 5 within V1b were identified by their triangular-shaped morphology and imaged at 100X (oil immersion). Approximately 35 cells were imaged and analyzed for each animal across multiple sections. Cells were included in the analysis if the soma was DAPI-positive, PV-negative, and was encircled entirely by PV- and GAD65-positive boutons. The cell perimeter was measured and the numbers of PV-positive and GAD65-positive boutons were counted independently of each other by eye. The puncta density was calculated by dividing the number of boutons for each cell by the mean perimeter of the cells within each genotype. Finally, each PV+/GAD65+ bouton was traced and the mean pixel intensity was measured for both PV and GAD65.

#### **Statistical analysis**

Statistical analysis was performed with GraphPad Prism software. Data are represented in the figures as the mean  $\pm$  the standard error of the mean (SEM). All data were initially analyzed with the d'Agostino & Pearson omnibus normality test. For data consisting of 2 groups, an unpaired t-test was performed for normally distributed data and a Mann-Whitney test was performed for data that were not normally distributed. Continuous cumulative distributions were compared with the Kolmogorov-Smirnov test and categorical distributions were compared with the Chi-squared test. Three or more



groups were compared using a one-way ANOVA (Kruskal-Wallis test with Dunn's comparisons) or two-way ANOVA with Bonferroni post-tests. Correlation analysis was performed with the Pearson r test. The following symbols were used to indicate the level of significance: \* $P < 0.05$ ; \*\* $p < 0.01$ ; \*\*\* $p < 0.001$ . All statistical information is included in the figure legends.

## **CHAPTER 3**

# **CHARACTERIZATION OF THE VISUAL PATHWAY AND PROCESSING**

## INTRODUCTION

The proper execution of cognitive behaviors depends on normal processing of sensory information (Belmonte et al., 2004). Behaviors relevant to autism, such as communication and socialization, involve integration of auditory, visual, and somatosensory input. Indeed, abnormal sensitivity to sensory stimuli is an important component of the symptoms that comprise autism (Kanner, 1943; Marco et al., 2011), and is now proposed to be included as one of the key diagnostic criteria (APA-DSM5, 2011). The severity of sensory symptoms often correlates with the level of social impairment in autistic individuals (Simmons et al., 2009).

Different sensory domains have been reported to be affected in autism, including somatosensation, hearing, vision, and multisensory integration (Kanner, 1943; Marco et al., 2011). Of these domains, many studies have focused on vision because of its relevance to socialization and communication. In addition, many tools exist for noninvasively assessing visual function in autistic children, including eye tracking, psychophysical tasks, fMRI, and visual evoked potentials (VEP) (Simmons et al., 2009; Jeste and Nelson, 2009). Therefore, studying senses in autism could help to identify key alterations in basic brain function that then may cumulate to cause deficits in higher order cortical processes.

The rodent visual system is an excellent model with which to study sensory function in autism models because the basic organization and response properties are well-characterized and can be readily tested. Visual information from the outside world enters the visual system of the mouse through the retina. The retina is organized into multiple layers that contain different cell types (reviewed in Wässle, 2004; Sanes and Zipursky, 2010). The outer-most layer of the retina, or the outer nuclear layer (ONL), contains rod and cone granules. The inner nuclear layer (INL) is composed of interneurons, which include horizontal, amacrine, and bipolar cells, and is separated from the ONL by the inner plexiform

layer (IPL). Finally, the ganglion cell layer (GCL) is separated from the INL by the outer plexiform layer (OPL) and contains ganglion cells, which project to the lateral geniculate nucleus (LGN) of the thalamus and other targets via the optic nerve.

The majority of fibers in the optic nerve cross sides at the optic chiasm and innervate the contralateral LGN. Initially, projections from the contralateral and ipsilateral eye overlap significantly in the dorsal LGN (Godement et al., 1984; Penn et al., 1998; Shatz and Kirkwood, 1984), but through a process of activity-dependent synaptic pruning, eventually segregate into a distinct ipsilateral patch surrounded by a larger contralateral region (Fig. 2.1; reviewed in Torborg and Feller, 2005). This process of refinement takes place during the first week of life, before eye opening, and is guided by intrinsic patterned spontaneous activity called retinal waves. Total blockade or de-correlation of retinal activity results in incomplete eye-specific segregation (Shatz and Stryker, 1988; Bansal et al., 2000; Chapman, 2000; Rossi et al., 2001; reviewed in Torborg and Feller, 2005).

From the LGN, visual information is transmitted to the primary visual cortex (V1) and then to higher visual areas (Wang and Burkhalter, 2007). Mouse V1 is separated into a medial monocular zone that receives exclusive input from the contralateral eye, and a lateral binocular zone that receives mostly contralateral and some ipsilateral input (Fig. 2.1). Visual cortical cells are organized in a topographic fashion. Cells in the monocular zone respond best to stimulation of the lateral edge of the contralateral visual field, whereas cells in the binocular zone represent the central portion of the visual field (Drager, 1975; Gordon and Stryker, 1996; Schuett et al., 2002; reviewed in Hubener, 2003). The receptive field properties of V1 cells, including ocular dominance, receptive field location, orientation selectivity, and direction selectivity, can be measured in mice using electrophysiological recording of cell spiking in response to varied visual stimuli (Drager, 1975; Gordon and Stryker, 1996).

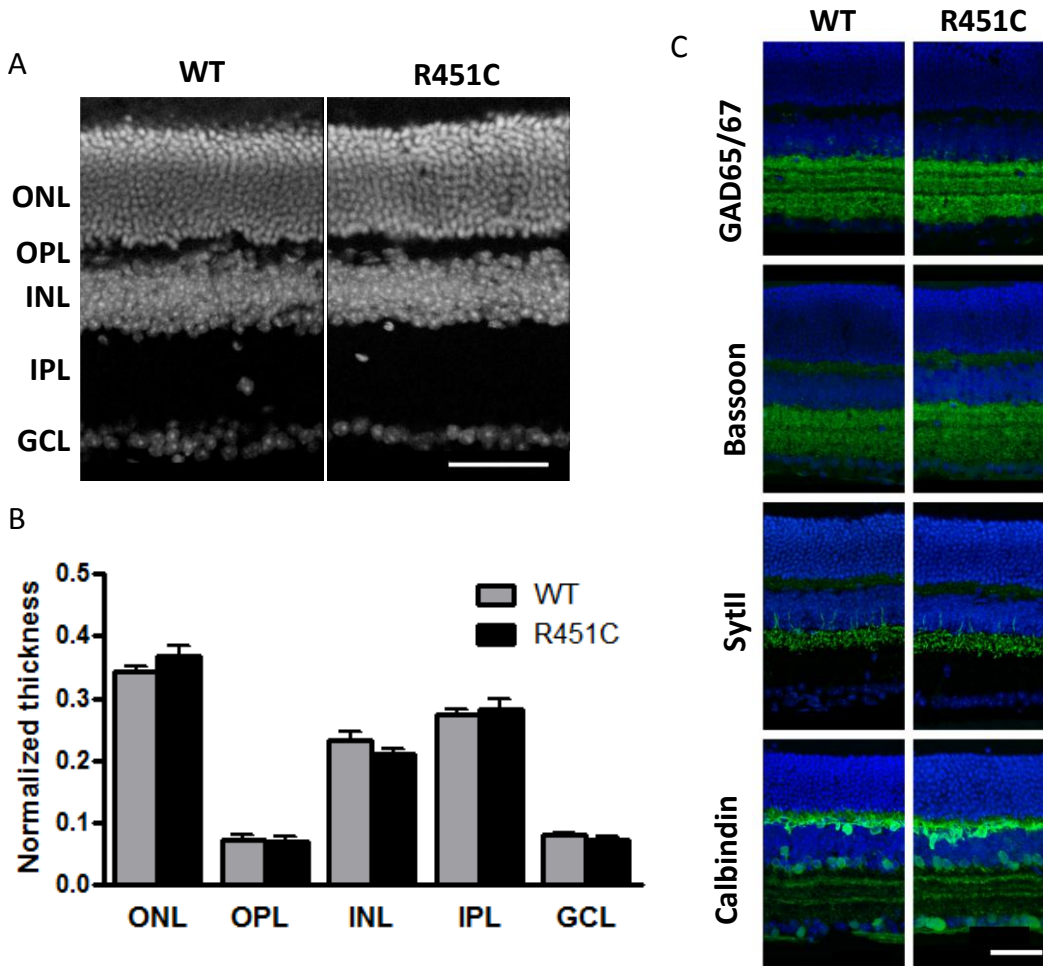
Neurologin-3 is expressed throughout the visual system (<http://www.brain-map.org>), but it is currently unknown if disruption of this cell adhesion molecule affects vision. Here, we thoroughly examined the organization of the retina, LGN, and cortex in young adult NL3-R451C and wild-type littermate mice to fully characterize baseline vision. We then tested the functional output of the visual cortex by measuring acuity.

## **RESULTS**

### **Retinal lamination and ganglion cell density analysis**

We examined the composition and organization of the retina in young adult (2-3-month-old) NL3-R451C WT and mutant mice by staining retinal cross sections for different synaptic and cellular markers. First, frozen sections of retinae were stained with DAPI to label the nuclei of all cells in order to distinguish the layers (Fig. 3.1A). The thickness of each cellular and synaptic layer was measured, including the ONL, INL, GCL, OPL, and IPL. The thickness of each layer was normalized to the total thickness of the retina, from the GCL to the outer edge of the ONL. There were no significant differences between the WT and mutant mice (Fig. 3.1B).

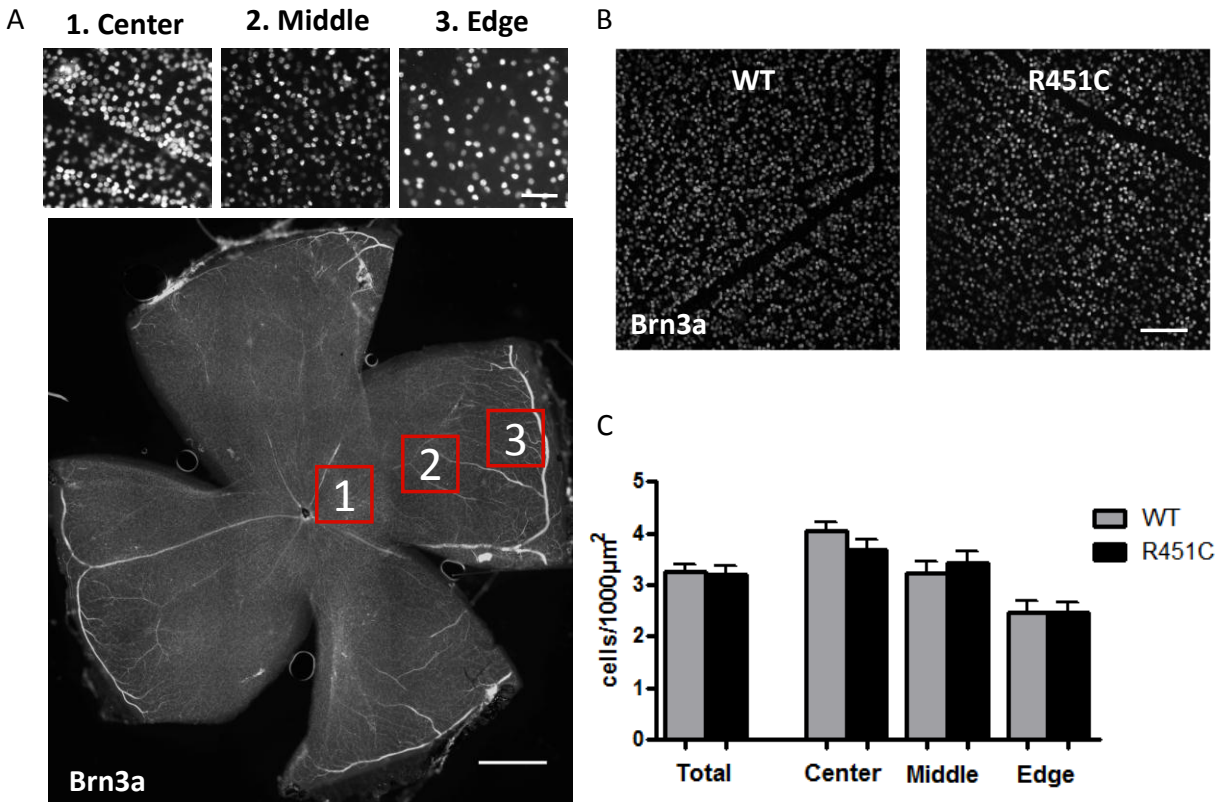
Next, retinal sections were stained with markers for specific cell and synapse types (Fig. 3.1C). GABAergic amacrine cells were labeled with GAD65/67, the two GABA-synthesizing enzymes. Photoreceptor ribbon synapses were labeled with Bassoon and OFF bipolar cells were marked with Synaptotagmin II (SytlI) (Fox and Sanes, 2007). Finally, Calbindin was used to label horizontal cells, as well as cholinergic amacrine cells and a smaller subset of non-cholinergic amacrine and retinal ganglion cells (RGCs) (Haverkamp and Wässle, 2000). Calbindin staining resulted in a characteristic pattern of 3



(Y. Kate Hong)

**Figure 3.1. No differences were detected in the cellular or synaptic lamination of the retina in young adult NL3-R451C mutant mice.**

- Sample cross sections of one WT and one mutant retina stained with DAPI in order to distinguish the retinal layers. ONL, outer nuclear layer; OPL, outer plexiform layer; INL, inner nuclear layer; IPL, inner plexiform layer; GCL, ganglion cell layer. Scale bar=50  $\mu$ m.
- Thickness measurements are normalized to the total thickness of the retina at each sampled location. Mann-Whitney or unpaired t-test between genotypes for each layer, no significance. N=2 mice, 6 sections (WT); n=3 mice, 9 sections (R451C).
- Sample retinal sections stained for markers of the different cell and synapse types of the retina. GAD65/67 (GABAergic amacrine cells), Bassoon (ribbon synapses), SytII (Synaptotagmin II, OFF lamina of IPL), Calbindin (horizontal and amacrine cells). Scale bar=50  $\mu$ m.



(Y. Kate Hong)

**Figure 3.2. Retinal ganglion cell density is normal in young adult NL3-R451C mutant mice.**

- A. Images of a sample whole-mount retina stained with Brn3a to label RGCs. The bottom image is an overall view of the retina and indicates the location of the center (1), middle (2), and edge (3) regions used for quantification. Scale bar=500 µm. The top shows zoomed in images of each region. Scale bar=50 µm.
- B. Representative images of one WT and one mutant whole-mount retina section showing Brn3a-labeled retinal ganglion cells. Scale bar=100 µm.
- C. The density of cells was quantified in the total retina and in the center, middle and edge sections of the retina. Unpaired t-tests between genotypes for each region, no significance. N=5 mice and 25-30 images for WT and R451C.

bands in the IPL. Comparison of these markers did not reveal any notable differences in laminar organization between WT and mutant mice.

The density of RGCs can influence aspects of visual function like spatial acuity (Wässle, 2004). We labeled RGCs in young adult NL3-WT and R451C mutant retinæ with Brn3a, which marks the majority of RGCs in the postnatal retina that specifically project to the LGN and the superior colliculus (Xiang et al., 1995; Badea et al., 2009; Quina et al., 2005). Because RGC density decreases significantly with eccentricity, we quantified the density in 3 regions (center, middle, edge; Fig. 3.2A), as well as overall RGC density. There were no significant differences between WT and mutant mice (Fig. 3.2C).

### **Eye-specific segregation in the lateral geniculate nucleus of the thalamus**

Axons from the retina project to the dorsal LGN in a characteristic pattern that is refined over development. In order to characterize LGN eye-specific segregation, we injected each eye of multiple young adult WT and mutant mice with labeled tracers (cholera toxin B conjugated to Alexa-488 or 594). The extent of overlap between the two eyes was quantified using the threshold-independent Torborg and Feller method (Torborg and Feller, 2005; see Chapter 2). Briefly, the R value for each pixel was calculated by taking the log of the ratio of ipsi to contra fluorescence intensities, and the variance of each R-distribution was calculated. A high R variance means that there are more pixels that are dominated by one eye or the other, and therefore indicates more segregation. On the other hand, a low R variance means that more pixels are double-positive and therefore the LGN is less segregated. Although there was a slight decrease in mean R variance in the mutants, indicating a possible increase in overlap, this difference did not reach significance (Fig. 3.3).



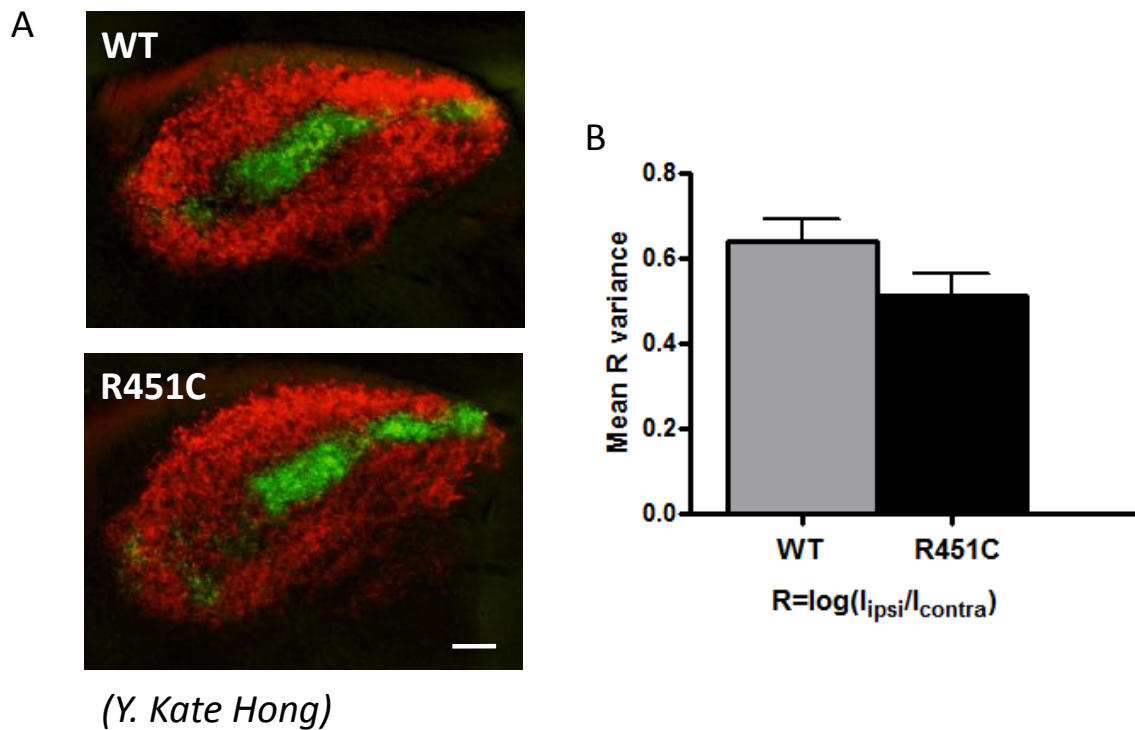


**Figure 3.3. Eye-specific segregation in the LGN is not significantly different in young adult NL3-R451C mutant mice.**

- A. Representative 5x images of sagittal sections of the dorsal LGN in mice that received retinal injections of cholera toxin B subunit conjugated to Alexa-488 in one eye and Alexa-594 in the other. Contralateral and ipsilateral retinal projections are labeled in red and green, respectively. Scale bar=100  $\mu\text{m}$ .
- B. Colocalization analysis was done using a threshold-independent method (Torborg and Feller, 2004). Colocalization was determined by finding the variance of R values across pixels, where R is the log of the ratio of ipsilateral to contralateral pixel intensities (I) in the axons ( $R = \log(I_{\text{ipsi}}/I_{\text{contra}})$ ). Unpaired t-test,  $p = 0.08$ . N=7 mice, 14 images (WT); n= 8 mice, 16 images (R451C).

## Organization and receptive field properties of visual cortical neurons

We characterized the basic organization and receptive field (RF) properties of visual cortical cells in NL3-R451C mutant and WT littermate mice using extracellular recordings from the binocular visual cortex (V1b). Young adult male mice were anesthetized and the activity of single excitatory cells was recorded in response to computer-generated visual stimuli. Basic firing properties were similar between the two groups. We recorded comparable rates of spontaneous activity (SA) in response to a blank stimulus and maximum evoked activity ( $R_{\max}$ ) in response to drifting black and white bars (Fig. 3.4A inset). As a result, there was no significant difference in the signal-to-noise ratio distribution, suggesting that evoked signals are equally effective over background noise in the NL3-R451C mutants (Fig. 3.4A).

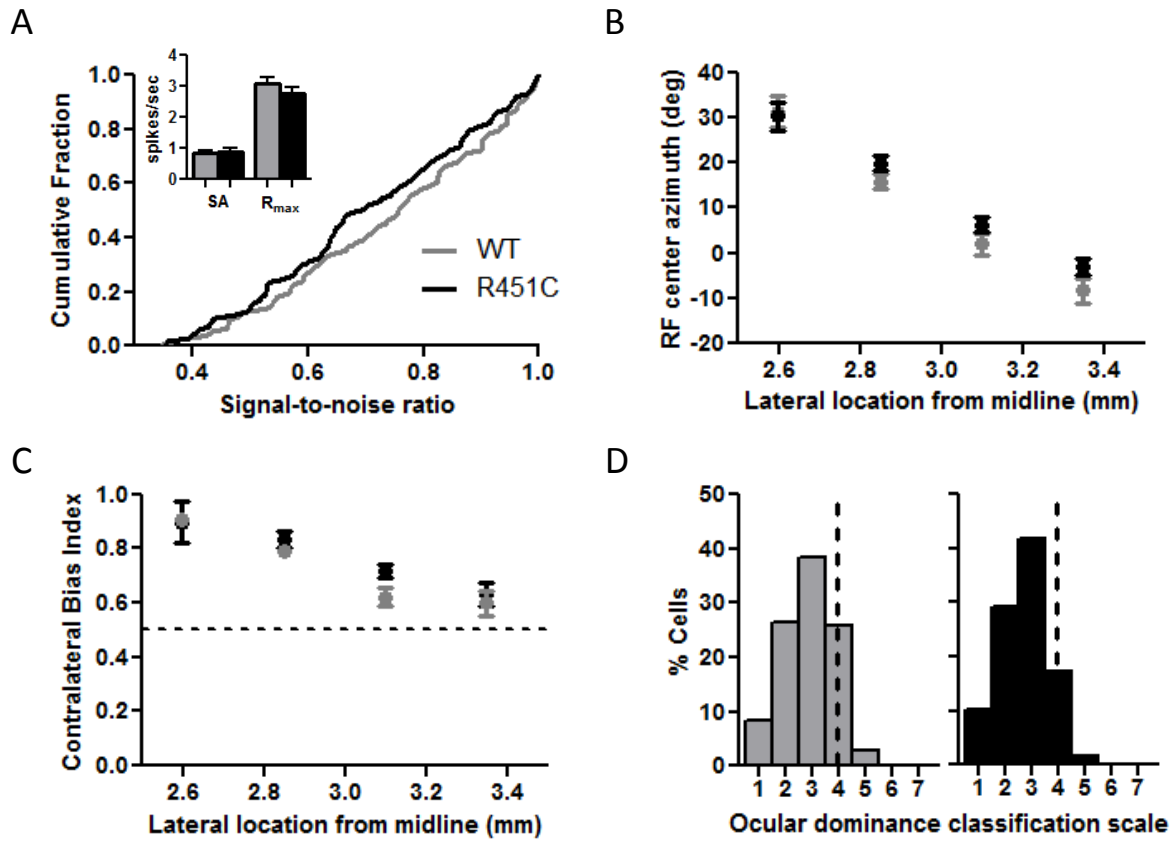
In order to determine if cortical organization was affected by the NL3-R451C mutation, we systematically mapped the RF azimuth locations and ocular dominance of neurons across V1b by analyzing each cell's response to a drifting bar of light. In WT mice, the RF location moved from the periphery to the center of the visual field as the recording site moved medial to lateral in the cortex (Fig. 3.4B, gray), as expected (Fig. 2.1). This organization was not significantly different in the NL3-R451C mutants, indicating a normal cortical representation of visual space (Fig. 3.4B, black).

Next, ocular dominance was evaluated by stimulating each eye independently with a drifting bar of light and assigning each cell a value on the 7-point ocular dominance classification scale based on the relative responsiveness of each eye (Hubel and Wiesel, 1962). The contralateral bias index (CBI), which is a weighted average of ocular dominance within a population of cells, was calculated for each recording location across the mediolateral V1b axis (see Chapter 2). For WT mice, the representation of the ipsilateral eye increased as the recording location moved laterally from the monocular zone to the binocular zone, as previously reported (Gordon and Stryker, 1996). This was reflected by a progressive decrease in the CBI from 1 (contralateral-dominated) to 0.5 (both eyes equal) (Fig. 3.4C, gray). The same

**Figure 3.4. Normal organization and receptive field properties of neurons in the binocular visual cortex of young adult NL3-R451C mutant mice.**

- A. The signal-to-noise ratio distribution was similar between genotypes. Signal-to-noise ratio was calculated as  $(R_{\max} - SA) / R_{\max}$ . Kolmogorov-Smirnov test,  $p=0.21$ . Inset: spontaneous activity (SA) and maximum evoked response ( $R_{\max}$ ) of cells remained at normal levels in mutant mice. Mann-Whitney test for each property, no significance. N=6 mice, 111 cells (WT); n=7 mice, 112 cells (R451C).
- B. Receptive field azimuth position in the contralateral visual field (in degrees lateral to the vertical meridian) is plotted against the location of the electrode lateral to the midline. There was no significant difference in receptive field organization between WT and mutant mice. 2-way ANOVA with Bonferroni post-tests, no significance. N=6 mice, 11-30 cells per location (WT); n=6 mice, 9-37 cells per location (R451C).
- C. The contralateral bias index (CBI; see Chapter 2) is plotted against the location of the electrode lateral to the midline for a subset of cells. The dashed line at CBI=0.5 indicates an equal response between the two eyes. There was no significant difference in the organization of ocular dominance between WT and mutant mice. 2-way ANOVA with Bonferroni post-tests, no significance. N=6 mice, 19-38 cells per location (WT); n=6 mice, 12-39 cells per location (R451C).
- D. Overall ocular dominance distribution on the 7-point ocular dominance classification scale was not significantly different from WT mice. The dashed line at 4 indicates an equal response between the two eyes. Chi-squared test,  $p=0.66$ . N=6 mice, 143 cells (WT); n=6 mice, 127 cells (R451C).

Figure 3.4 (Continued)



ocular dominance pattern was observed in the NL3-R451C mutants (Fig. 3.4C, black), further supporting that the organization of V1 is normal. In addition, when all cells were pooled together across V1b locations and mice for each genotype, the overall ocular dominance distribution was in favor of the contralateral eye (Fig. 3.4D), as expected, and not significantly different from the WT distribution. Therefore, the NL3-R451C mutation does not appear to affect the general organization of the visual cortex or the basic response properties of individual neurons.

We then analyzed the receptive field properties of orientation selectivity and direction selectivity. We presented the mice with drifting bars of 12 different orientations and directions (0-360°) and calculated an index that quantified the extent to which each cell modulated its firing based on orientation (OSI) or direction (DSI) (Fig. 3.5; see Chapter 2). These indices were near 0 for cells that were not selective and near 1 for cells that were highly selective. There was no difference in the OSI or DSI distribution between WT and NL3-R451C mutant mice (Fig. 3.5B and D, respectively).

### **Spatial acuity as a measure of the functional output of the visual system**

Spatial acuity, or the resolution of vision, is often used to assess local cortical processing. Acuity of the contralateral eye was measured *in vivo* in V1b of anesthetized mice using visual evoked potentials (VEPs). First, the response to a 0.05 cycles/degree (cpd) stimulus was recorded at different depths throughout the cortex. The location where we obtained the largest amplitude response, generally at 300-400  $\mu\text{m}$  (corresponding to the bottom of layer 3 or the top of layer 4), was then used for measuring acuity (Fig. 2.3; Porciatti et al., 1999). We tested acuity by progressively increasing the spatial frequency of the stimulus until a signal could no longer be detected. 2-3-month-old WT mice reached a threshold of spatial acuity at 0.5 cycles/degree (cpd) (Fig.3.6A, gray), which is in agreement with previous studies

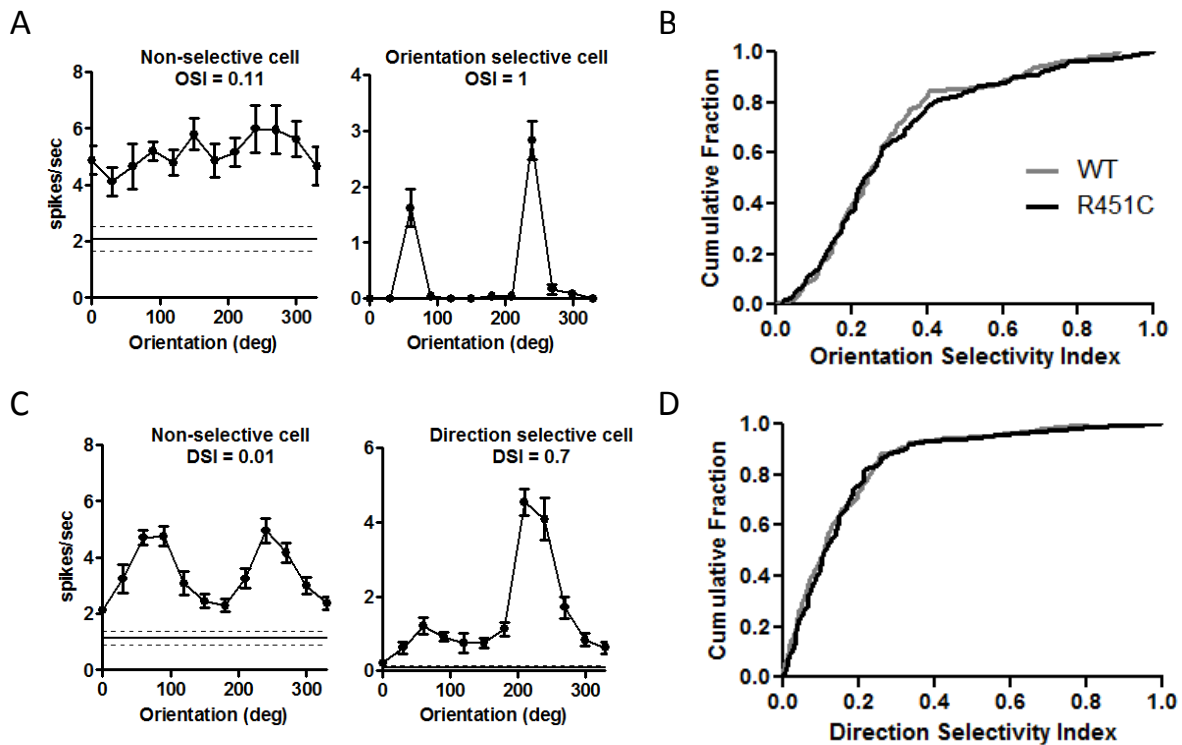


**Figure 3.5. Normal orientation and direction selectivity in young adult NL3-R451C mutant visual cortex.**

- Sample non-selective and orientation selective cell. Horizontal solid and dotted lines represent mean SA and SA SEM, respectively.
- The orientation selectivity index (OSI) distribution was similar between genotypes.  $OSI = (R_{max} - R_{ortho}) / (R_{max} + R_{ortho})$ , where  $R_{ortho}$  is the response to the orientation that is orthogonal ( $\pm 90^\circ$ ) to the preferred orientation. Kolmogorov-Smirnov test,  $p=0.87$ .  $N=6$  mice, 111 cells (WT);  $n=7$  mice, 112 cells (R451C).
- Sample non-selective and direction selective cell. Horizontal solid and dotted lines represent mean SA and SA SEM, respectively.
- The direction selectivity index (DSI) distribution was similar between genotypes.  $DSI = (R_{max} - R_{opp}) / (R_{max} + R_{opp})$ , where  $R_{opp}$  is the response to the direction that is opposite ( $\pm 180^\circ$ ) to the preferred direction. Kolmogorov-Smirnov test,  $p=0.91$ .  $N=6$  mice, 111 cells (WT);  $n=7$  mice, 112 cells (R451C).

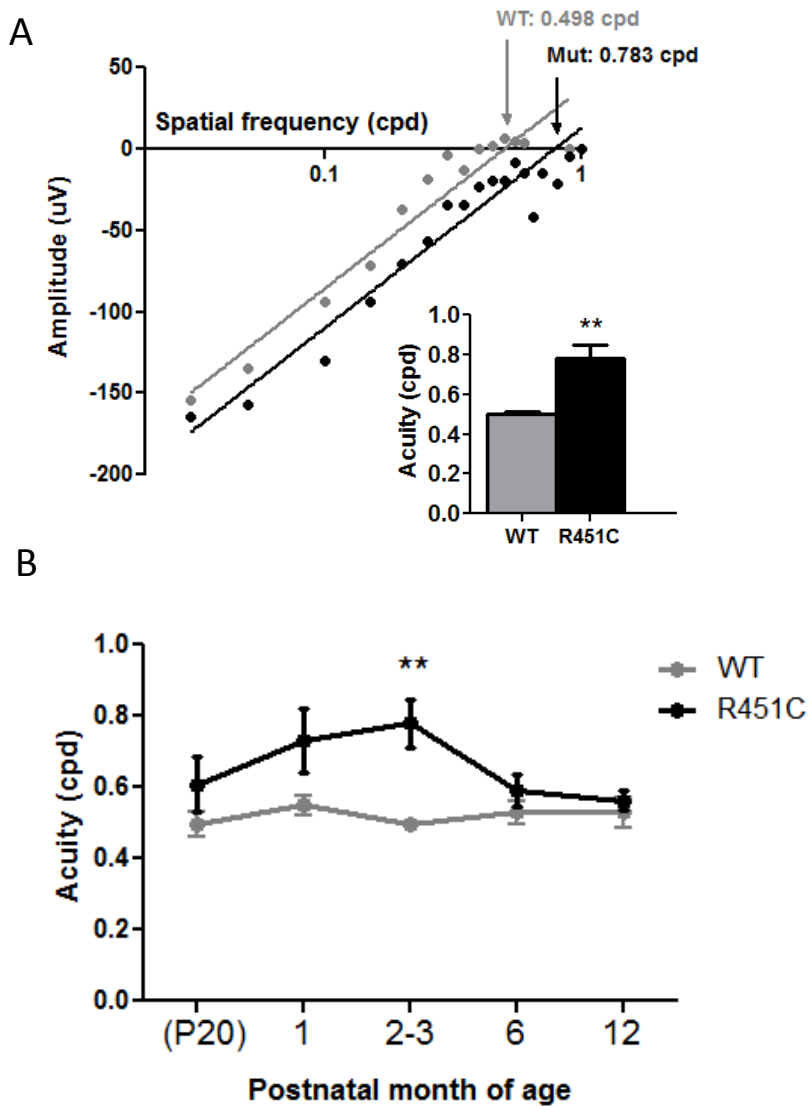


**Figure 3.6. Enhanced VEP spatial acuity in young adult NL3-R451C mutant mice.**

- A. Average acuity plots from 7 WT and 8 mutant mice are shown. Each point represents the mean response to multiple stimulus presentations across mice at that spatial frequency. The mean amplitude of the negative component of the waveform (NC) was plotted against the log of the spatial frequency, and the threshold of visual acuity was determined by linear extrapolation to 0 mV. Inset: Mean acuity at 2-3 months of age, Mann-Whitney test,  $**p=0.004$ . N=7 mice (WT); n=8 mice (R451C).
- B. Average acuity over development is shown. There was a significant but unstable increase in spatial acuity in 2-3 month-old mutant mice. Two-way ANOVA with Bonferroni post-tests,  $**p<0.01$  at 2-3 months. N=4-7 mice for each time point (WT); n=5-8 mice for each time point (R451C).

using both VEP (Porciatti et al., 1999) and behavioral tests (Prusky et al., 2000a). Strikingly, the visual spatial acuity of NL3-R451C mice measured in this way was significantly increased to approximately 0.77 cpd (Fig. 3.6A inset). In order to further investigate this phenotype, we measured acuity at different ages to characterize the developmental profile. In WT mice, spatial acuity was stable at 0.5 cpd from P20 until 1 year of age (Fig. 3.6B, gray). On the other hand, acuity in the mutants was high but variable early in life (P20 and 1 month), significantly increased at 2-3 months of age, and then decreased down to WT levels by 6 months of age (Fig. 3.6B, black). These results indicate a hypersensitivity of NL3-R451C mutant mice to high spatial frequencies that is unstable throughout development.

## DISCUSSION

NL3 transcript is expressed throughout the brain (<http://www.brain-map.org>), including the retina and LGN. Therefore, we considered that the R451C mutation may affect the visual system on a global level. Overall, the general structure and lamination of the retina appeared normal based on immunostaining for cellular and synaptic markers (Fig. 3.1, 3.2), but we cannot rule out the possibility that the NL3-R451C mutation may impact retinal processing. Interestingly, other isoforms of neuroligins have been found to play roles in information processing in the retina. Loss of NL2 protein also did not affect the basic organization of the retina (Hoon et al. 2009). However, because NL2 is preferentially localized to GABAergic synapses of the retina, NL2 knock-out mice exhibited reduced GABA<sub>A</sub> receptor clustering and subtle effects on retinal information processing (Hoon et al., 2009). In particular, oscillatory electroretinogram (ERG) potentials, which reflect the combined activity of glycinergic amacrine cells in the IPL, showed a trend towards smaller amplitudes at high light intensities. In addition RGCs showed increased baseline firing and impaired responses to light onset. NL4 is preferentially localized to glycinergic synapses in the retina, and loss of NL4 protein produced a reduction in



glycinergic receptor number, slower glycinergic mIPSCs, and altered glycinergic inhibition in the IPL, as shown by changes in RGC firing and ERG responses (Hoon et al., 2011). The exact synaptic location of NL3 in the retina is still unclear (Gilbert et al., 2001; Paraoanu et al., 2006), due to the poor quality of available antibodies. The development of better antibodies will help to predict if or how the NL3-R451C mutation might affect retinal processing. Furthermore, the role of NL3 in the retina could also be addressed using multielectrode array recordings of RGCs or electroretinogram recordings in NL3-R451C mutant mice.

Labeling contralateral and ipsilateral eye inputs in the LGN revealed no significant change in the segregation of the two eyes (Fig. 3.3). This process of segregation is activity-dependent and disruptions could indicate deficits in retinal waves or synaptic pruning mechanisms (reviewed in Torborg and Feller, 2005). There was a slight trend towards overlap in the mutants ( $p=0.08$ ). It could be worth performing a more in depth analysis of synaptic pruning by reconstructing retinogeniculate arbors or performing retinogeniculate recordings to further assess the functional pruning of afferents (reviewed in Hong and Chen, 2011). However, the ocular dominance distribution across multiple locations in the binocular cortex was not different from WT littermate mice or C57BL/6 animals (Fig. 3.4C and D; Gordon and Stryker, 1996). This suggests that any differences in LGN eye-specific segregation are subtle and do not transfer any major defect to the primary visual cortex. In addition, the retinotopic organization of V1 was conserved in the mutants (Fig. 3.4B), indicating that the representation of visual space was normal.

No differences were observed in the spontaneous and visually evoked firing rates of single neurons (Fig. 3.4A). In addition, mutant excitatory cells exhibited normal levels of orientation and direction selectivity (Fig. 3.5). Throughout the course of these experiments, some fast-spiking inhibitory neurons were also recorded. Unfortunately, because these only comprised about 5% of visually responsive cells (based on waveform analysis, Fig. 2.2), there were too few cells to reach conclusive

results. In the future, intracellular recording from excitatory and fast-spiking inhibitory cells *in vivo* (Yazaki-Sugiyama et al., 2009) could allow for a nuanced comparison of intrinsic and evoked responses in both types of cells.

Overall, these results suggest that NL3 does not play any role in setting up the components of the visual pathway, or in the development of response properties of visual cortical cells. Instead, it plays important roles in modulating circuit properties, as demonstrated by the increase in spatial acuity in young adult NL3-R451C mutants when measured with the VEP (Fig.3.6). This increased acuity threshold in the mutants may result from higher gain, as response amplitudes to all spatial frequencies are enhanced, resulting in similar best fit line slopes for averaged WT and mutant data. This could suggest an increased signal-to-noise ratio at the level of local field potentials. In light of this, we are currently testing other properties, like contrast sensitivity or temporal resolution, to see if enhanced functioning is a common feature of the mutant visual cortex.

To our knowledge, the only other manipulation consistently reported to enhance acuity is environmental enrichment (Prusky et al., 2000c; Cancedda et al., 2004; Sale et al., 2004; Beaulieu and Cynader, 1990). Environmental enrichment increases BDNF levels in the visual cortex (Cancedda et al. 2004; Sale et al., 2004), so it is possible that this mutation in NL3 positively impacts the BDNF-TrkB receptor signaling pathway. Alternatively, this mutation could render the cortex hypersensitive to stimuli, thereby simulating enriched surroundings. Interestingly, this enhanced acuity was unstable over development; acuity was high but variable in juveniles and then reduced back to WT levels at 6 months of age. This could suggest that having such high acuity is not sustainable and is perhaps maladaptive for the animal.

It is generally accepted that VEP acuity accurately reflects behavioral acuity (Porciatti et al., 2002), but we cannot rule out the possibility that this increase in VEP acuity reflects subthreshold

changes that do not impact behavior. However, it is interesting to note that the NL3-R451C mice performed better on the Morris water maze (Tabuchi et al., 2007), which could be attributed to increased acuity or visual plasticity, as this task relies heavily on visual cues. In addition, it is intriguing that enhanced visual acuity has been reported in autistic individuals (Ashwin et al., 2009a), but this result has been highly controversial and unable to be replicated by other groups (Bolte et al., 2012; but see Ashwin et al., 2009b). Several studies have concluded that children with autism focus more on local, detail-oriented aspects of visual stimuli because of a relative hyper-processing of high spatial frequency information (Deruelle et al., 2004; Deruelle et al., 2008; Vlamings et al., 2010). This abnormal processing could prevent autistic children from extracting the gestalt from socially-relevant visual stimuli, like faces (Behrmann et al., 2006).

It is clear that many different aspects of visual processing are affected in ASD in manners that vary depending on the individual (Behrmann et al., 2006; Simmons et al., 2009). Fortunately, excellent tools for noninvasively assessing visual function in children, like the visual evoked potential, are already being used to evaluate low and high level visual processing and screen for ASD risk (Jeste and Nelson, 2009; Jeste et al., 2012). Our results predict that vision may serve as an easily testable biomarker for autism, and emphasize the need for longitudinal studies in children at risk for developing autism.

## **CHAPTER 4**

### **THE CRITICAL PERIOD FOR OCULAR DOMINANCE PLASTICITY**

## INTRODUCTION

The brain has a remarkable ability to be shaped by experience, but this capacity generally decreases with age. Windows of heightened plasticity occur at distinct times for different modalities throughout early development (Fig. 1.1; reviewed in Hensch, 2004). These sensitive periods exist for complex phenomena, such as filial imprinting (Lorenz, 1958), acquisition of courtship song in birds (Doupe and Kuhl, 1999; Brainard and Doupe, 2002), sound localization (Knudsen et al., 2000), and fear extinction (Kim and Richardson, 2007; Gogolla et al., 2009a). They also occur for sensory modalities, such as tonotopic map refinement in the auditory cortex (Chang and Merzenich, 2003) and cortical barrel formation (Van Der Loos and Woolsey, 1973) and tuning to whisker stimulation (Fox, 1992; Stern et al., 2001) in rodent somatosensory cortex.

One of the most well-understood examples, present in both humans and animal models, is the critical period for ocular dominance plasticity. Compromised input to one eye permanently reduces vision from that eye unless corrected during childhood (Banks et al., 1975; Mitchell and Mackinnon, 2002). Hubel and Wiesel, in a series of Nobel Prize winning experiments in the 1960s, found that sewing one eye shut in kittens during a distinct period caused loss of acuity and reduced responsiveness to that eye in the visual cortex, despite no physical damage to the eye itself (Wiesel and Hubel, 1963; reviewed in Hubel and Wiesel, 1998). This occurs as a result of the nondeprived eye out-competing the deprived eye for cortical territory (LeVay et al., 1980; Antonini and Stryker, 1996). Further studies following these seminal experiments confirmed that a similar critical period exists in rodents as well (Drager, 1978; Fagiolini et al., 1994; Gordon and Stryker, 1996). Genetic manipulation in mice has allowed researchers to dissect the molecular mechanisms governing critical periods (Hensch, 2005).

Decades of experiments have suggested a unique role for inhibitory circuits in regulating critical period plasticity (reviewed in Hensch, 2005). Parvalbumin (PV) cells receive direct thalamic input, are

connected in networks with each other, envelop the soma of excitatory pyramidal cells, and can target many pyramidal cells at once (Lazarus and Huang, 2011). This connectivity develops with a late postnatal activity-dependent onset that follows the maturation of vision (Chattopadhyaya et al., 2004). PV cells are particularly suited to detect disparities between the two eyes and to control the output and synchrony of excitatory cells, thereby enabling experience-dependent plasticity (Lazarus and Huang, 2011). Accelerating PV cell development causes the critical period to occur prematurely, while delaying the maturation of PV cells also delays the onset of the critical period (reviewed in Levelt and Hubener, 2012; Le Magueresse and Monyer, 2013). In addition, manipulations that titrate the level of inhibition during adulthood can reopen the critical period and allow for juvenile-like plasticity (reviewed in Bavelier et al., 2010).

We hypothesized that the NL3-R451C mutation might alter critical periods by disrupting the balance of excitation and inhibition in the cortex. In order to test this, we challenged the visual system with monocular deprivation at different time points to determine if and when ocular dominance plasticity was possible in the R451C mutant mice. We used *in vivo* recording to measure visual acuity and the ocular dominance of single cells. In addition, we explored the effect of this mutation on E/I balance by quantifying synaptic protein levels, and we specifically investigated the effect on PV cells using confocal imaging of immunostained visual cortex.

## **RESULTS**

### **The effect of long and short-term monocular deprivation on ocular dominance in the visual cortex**

We first tested for the presence of ocular dominance plasticity throughout life by depriving input to one eye with long-term monocular deprivation (MD) from the time of eye-opening (P13) until

young adulthood (Fig. 4.1A). This is a well-characterized manipulation that has been shown to trigger circuit rewiring in contralateral V1b, resulting in a permanent reduction of acuity from the contralateral eye (Prusky and Douglas, 2003). We compared acuity in non-deprived and deprived animals with the VEP in adulthood. As expected, WT mice showed a significant loss of acuity after long-term MD that was not recoverable following a period of deprived eye reopening (Fig. 4.1B, gray). NL3-R451C mice also showed a permanent loss of acuity in response to long-term MD (Fig. 4.1B, black). It is interesting to note that the decrease from baseline adult acuity after long-term MD was actually larger in the NL3-R451C mutant mice (37%) than in the WT mice (17%), indicating that there may be either a larger capacity or longer window for plasticity (Fig. 4.1C).

Competition between the eyes is a necessary component of ocular dominance plasticity (Wiesel and Hubel, 1965). Closure of both eyes does not result in a loss of acuity because the two eyes are affected equally and neither has an advantage. Indeed, short-term 4-day binocular deprivation (BD) during the classical peak of ocular dominance plasticity (P24-30) did not affect acuity in WT mice, whereas 4-day MD did cause a significant decrease of acuity from the deprived eye (Fig. 4.2B, gray). We next tested if plasticity in mutant animals was similar in nature. Indeed, NL3-R451C mutant mice also demonstrated a specific effect of MD versus BD at this age (Fig. 4.2B, black). These results demonstrate two important points: First, mutant mice are plastic during the peak of the canonical critical period, i.e. 1 month of age; Second, this ocular dominance plasticity requires imbalanced input from the two eyes. A comparison of the magnitude of plasticity revealed that 4-day MD during the canonical critical period also elicited a more dramatic loss of acuity in the mutants than in WT mice, but this difference was smaller and not significant (Fig. 4.2C compared with 4.1C). This result indicates that the mutants may have a larger cumulative plastic effect after long-term deprivation due to a longer duration critical period. We tested this possibility next.

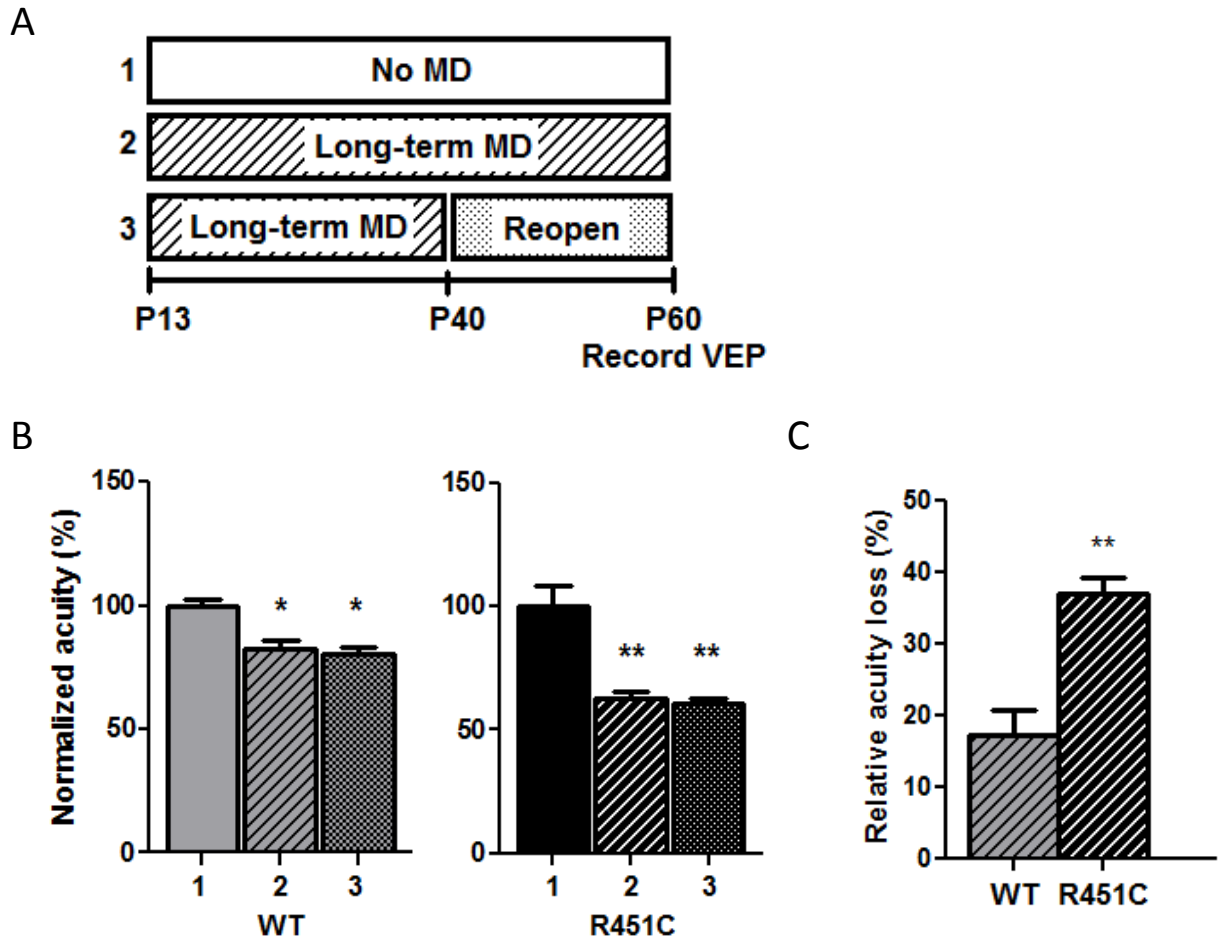


**Figure 4.1. Long-term monocular deprivation induces more robust ocular dominance plasticity in NL3-R451C mutant mice.**

- A. Acuity of the contralateral eye was measured with VEP at 2-3 months of age after 3 conditions: No MD, Long-term MD from eye-opening until adulthood, and long-term MD from eye-opening until P40, followed by reopening of the deprived eye until P60 (2-3 months of age).
- B. Acuity was normalized to the mean of the No MD condition for each genotype. For WT and mutant mice, loss of acuity was induced after long-term MD and recovery was impossible following reopening of the eye. One-way ANOVA (Kruskal-Wallis test with Dunn's comparison to No MD condition), comparisons were made within genotypes, \* $p < 0.05$ , \*\* $p < 0.01$ .  $N = 5-11$  mice for each group (WT);  $n = 8-13$  mice for each group (R451C).
- C. The magnitude of plasticity after long-term MD was compared by calculating the percent decrease of acuity from the No MD mean for each genotype. There was a larger decrease from baseline acuity in the mutants. One-way ANOVA with Bonferroni post-tests. WT+LTMD vs. R451C+LTMD, \*\* $p < 0.01$ .



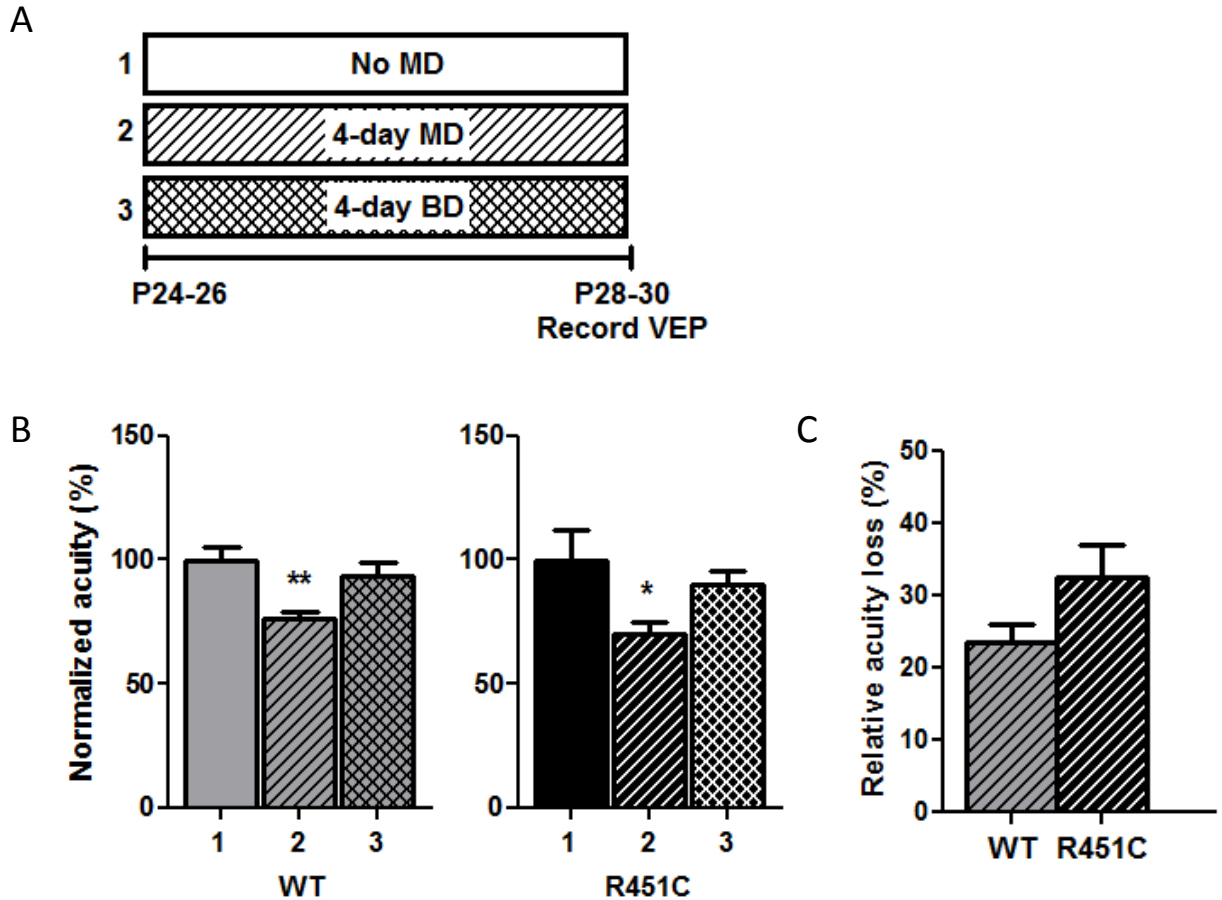


**Figure 4.2. Competition-induced ocular dominance plasticity is present during the peak of the canonical critical period.**

- A. Three conditions were compared during the canonical critical period: No MD, 4-day monocular deprivation (MD), and 4-day binocular deprivation (BD). Deprivation was performed between P24 and P30.
- B. For both WT and mutant mice, loss of acuity only occurred after MD and not BD. One-way ANOVA (Kruskal-Wallis test with Dunn's comparison to No MD condition), comparisons were made within genotypes, \* $p < 0.05$ , \*\* $p < 0.01$ .  $N = 4-6$  mice for each group (WT);  $n = 4-8$  mice for each group (R451C).
- C. The magnitude of plasticity after 4-day MD was compared by calculating the percent decrease of acuity from the No MD mean for each genotype. There was a trend towards a larger decrease from baseline acuity in the mutants but this was not significant. One-way ANOVA (Kruskal-Wallis test with Dunn's comparison), WT+MD vs. R451C+MD, not significant.

## Mapping the critical period for ocular dominance plasticity

In mice, the critical period for ocular dominance plasticity in response to brief MD opens after the third postnatal week, peaks around P24-28, and closes by P35 (Gordon and Stryker, 1996). We tested if ocular dominance plasticity in the mutant mice is restricted to this period by performing 4-day MD at different ages. Strikingly, while the critical period closed after 1 month of age in WT mice as expected, the mutants exhibited plasticity well into adulthood (Fig. 4.3). In fact, some degree of plasticity was present throughout the entire life of the mutant mice, though most strongly from 1 to 3 months of age and tapering off after 6 months. Therefore, the NL3-R451C mutation causes the critical period for ocular dominance plasticity to extend into adulthood.

Ocular dominance plasticity is also characterized by a shift in the responsiveness of individual cells towards the ipsilateral non-deprived eye (Wiesel and Hubel, 1963; Hensch et al., 1998). In order to confirm this presence of aberrant plasticity in adult NL3-R451C mutants, we tested the ocular dominance of single cells after 4-day MD using extracellular recording in young adulthood. We used two independent methods to quantify the relative responsiveness of each eye to a drifting bar of light. First, as previously described (Fig. 3.4C and D), we assigned each cell a value on the 7-point ocular dominance classification scale and compared the pooled ocular dominance distributions between deprived and non-deprived conditions. WT mice did not show any change, while mutants significantly shifted towards the ipsilateral non-deprived eye after MD (Fig. 4.4A). In order to assess the relative degree and variability of ocular dominance shift between mice, we calculated a contralateral bias index (CBI) for each mouse based on the 7-point values of their cells (see Chapter 2). This also revealed a significant shift in response to MD only in the mutants (Fig. 4.4B).

Second, we used a more quantitative method by calculating an ocular dominance score for each cell based on peak firing rates in response to stimulation of each eye (see Chapter 2), and we compared

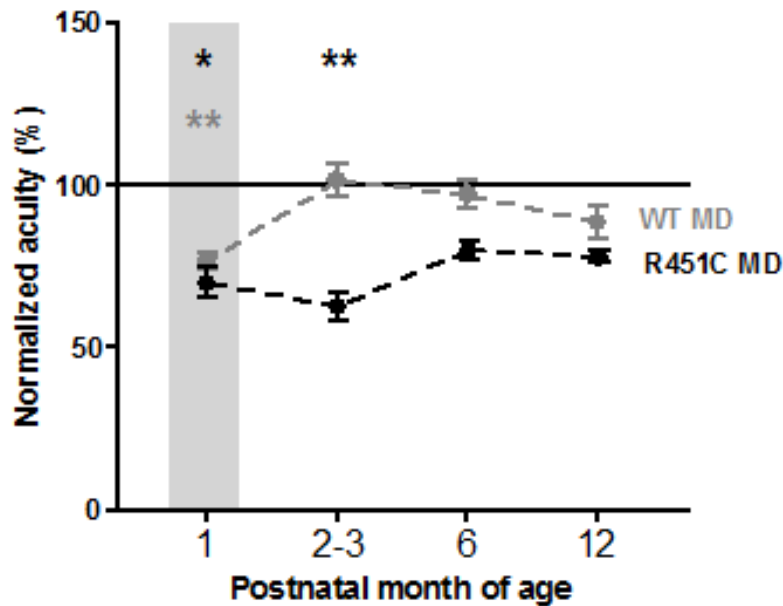


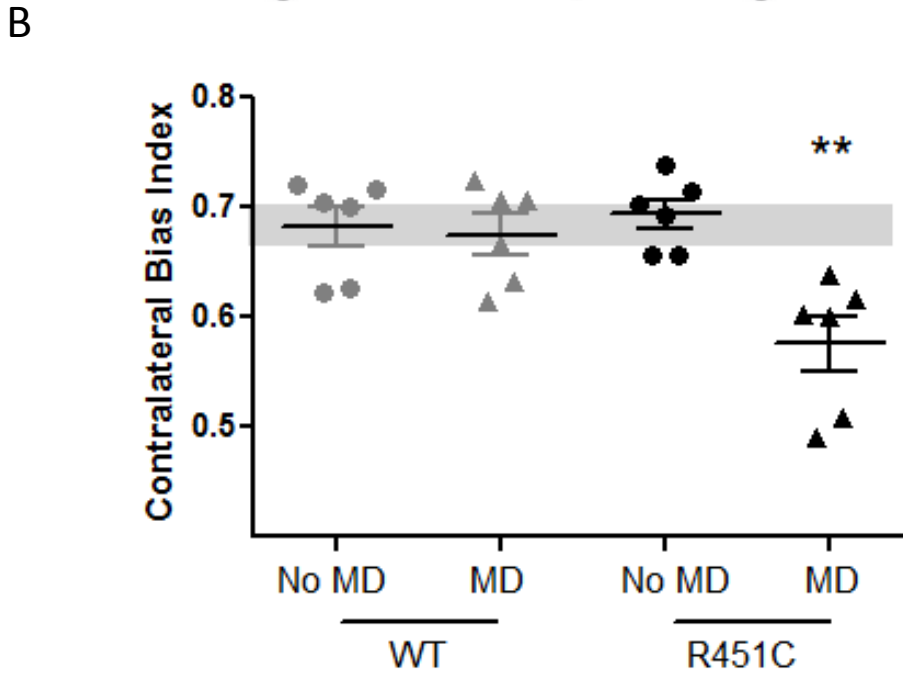
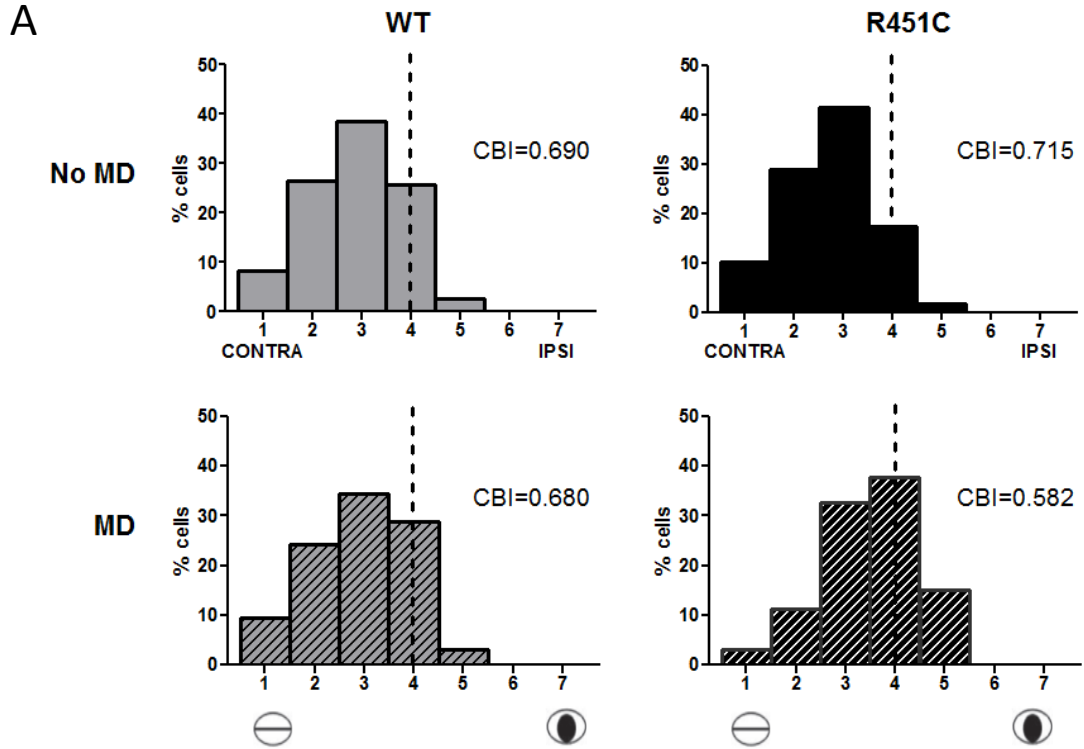
**Figure 4.3. The critical period is extended into adulthood in NL3-R451C mutant mice.**

Acuity was measured with VEP following 4-day MD at different ages. Acuity was normalized to the mean of the No MD condition for each genotype and time point (represented by solid black line at 100%). The gray column at 1 month of age represents the peak of the canonical critical period. There was a significant loss of acuity for both WT and mutant mice during the canonical critical period (1 month) but the mutants also exhibited a significant loss of acuity at 2-3 months of age. Two-way ANOVA with Bonferroni post-tests, all comparisons were made within genotype, \* $p < 0.05$ , \*\* $p < 0.01$  (gray asterisk=WT, black asterisk=R451C). N=4-7 mice for each time point (WT); n=5-8 mice for each time point (R451C).

**Figure 4.4. Young adult plasticity is confirmed at the single cell level in NL3-R451C mutant mice.**

- A. Ocular dominance distribution on the 7-point ocular dominance classification scale was significantly shifted towards the non-deprived eye after 4-day MD during young adulthood in mutant but not WT mice. Chi-squared test, WT vs. WT MD,  $p=0.87$ ; R451C vs. R451C MD,  $***p<0.001$ ; WT vs. R451C,  $p=0.66$ ; WT MD vs. R451C MD,  $***p=0.0002$ . N=6 mice, 143 cells (WT no MD); n=6 mice, 128 cells (WT MD); n=6 mice, 127 cells (R451C no MD); n=6 mice, 132 cells (R451C MD).
- B. Individual contralateral bias indexes (CBI; see Chapter 2) are plotted for each mouse. The shadowed area represents the mean  $\pm$  SEM for the WT no MD condition. There was a significant reduction in the CBI in mutants after MD, indicating an ocular dominance shift towards the ipsilateral non-deprived eye. One-way ANOVA (Kruskal-Wallis test with Dunn's comparisons), R451C no MD vs. R451C MD,  $**p<0.01$ . N=6 mice, 143 cells (WT no MD); n=6 mice, 128 cells (WT MD); n=6 mice, 127 cells (R451C no MD); n=6 mice, 132 cells (R451C MD).

Figure 4.4 (Continued)



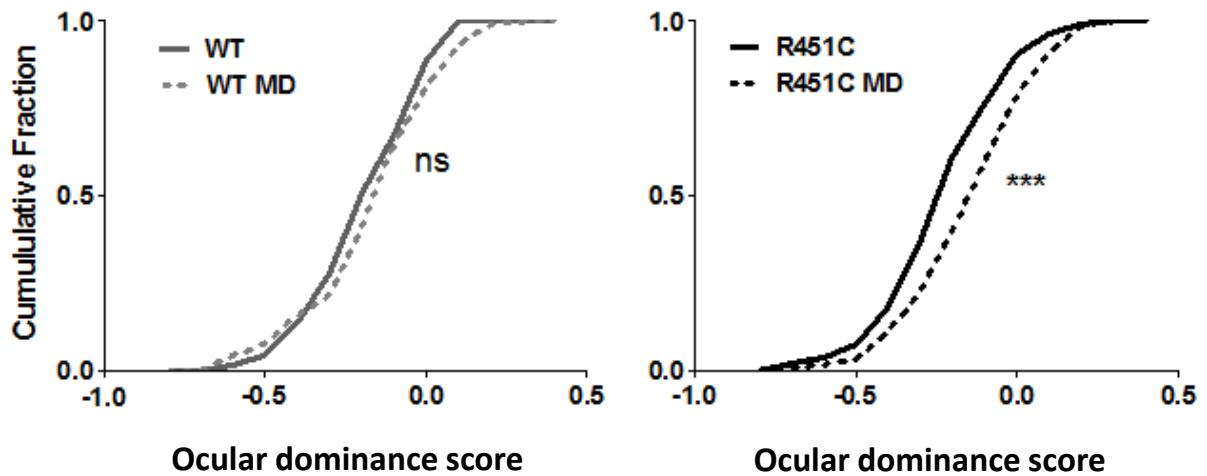


**Figure 4.5. Ocular dominance scores also show a shift towards the ipsilateral eye after short-term monocular deprivation in young adult mutant mice.**

The cumulative distribution of ocular dominance scores is plotted (see Chapter 2). Ocular dominance score =  $\frac{(PI-BI)-(PC-BC)}{[(PI-BI)+(PC-BC)]}$ , where P, peak; B, baseline; C, contralateral eye; I, ipsilateral eye. An ocular dominance score of -1 indicates complete dominance of the contralateral eye, and a score of 0 indicates equal responsiveness to both eyes. There was a significant difference after MD in mutant adults (right). Kolmogorov-Smirnov test within genotype, WT vs. WT MD:  $p=0.34$ ; R451C vs. R451C MD:  $***p<0.001$ . N=6 mice, 118 cells (WT); n=6 mice, 116 cells (WT MD); n=6 mice, 105 cells (R451C); n=6 mice, 130 cells (R451C MD).

the cumulative distributions in animals with and without MD. An ocular dominance score of -1 indicates complete dominance of the contralateral eye, and a score of 0 indicates equal responsiveness to both eyes. As expected, WT mice did not show any significant difference between non-deprived and MD conditions (Fig. 4.5, gray). Mutants, on the other hand, shifted the responsiveness of cells towards the ipsilateral non-deprived eye after MD (Fig. 4.5, black). To conclude, this data shows that the critical period for ocular dominance is extended into adulthood in the NL3-R451C mutant mice, and this can be measured by both a loss of acuity and a shift in the ocular dominance of single cells following MD.

### **Synaptic protein expression in the young adult binocular visual cortex**

The balance of excitation and inhibition is crucial for normal sensory processing and plasticity. The NL3-R451C mutation has been shown to differentially affect E/I balance depending on the specific brain region; inhibition is enhanced in the somatosensory cortex (Tabuchi et al., 2007), while excitation is enhanced in the hippocampus (Etherton et al., 2011). In order to begin to understand how the NL3-R451C mutation may affect E/I balance in the visual cortex, and how it may lead to the changes we see in the visual system, we next quantified the levels of different excitatory and inhibitory synaptic proteins in V1b homogenates from 2-3-month-old mice using western blot. NL3 protein levels were substantially decreased (Fig. 4.6A) as previously reported, because most of the protein is degraded upon failure to exit the endoplasmic reticulum (Tabuchi et al., 2007; De Jaco et al., 2006; De Jaco et al., 2010; Comoletti et al., 2004). NL1 levels were also decreased as previously reported (Tabuchi et al., 2007), most likely due to dimerization of a subset of NL1 with defective NL3 (Poulopoulos et al., 2012). NL2 protein levels were not significantly affected.

We next examined a variety of pre- and postsynaptic excitatory and inhibitory proteins. Excitatory protein levels were normal, including vesicular glutamate transporter 1 (Vglut1), postsynaptic

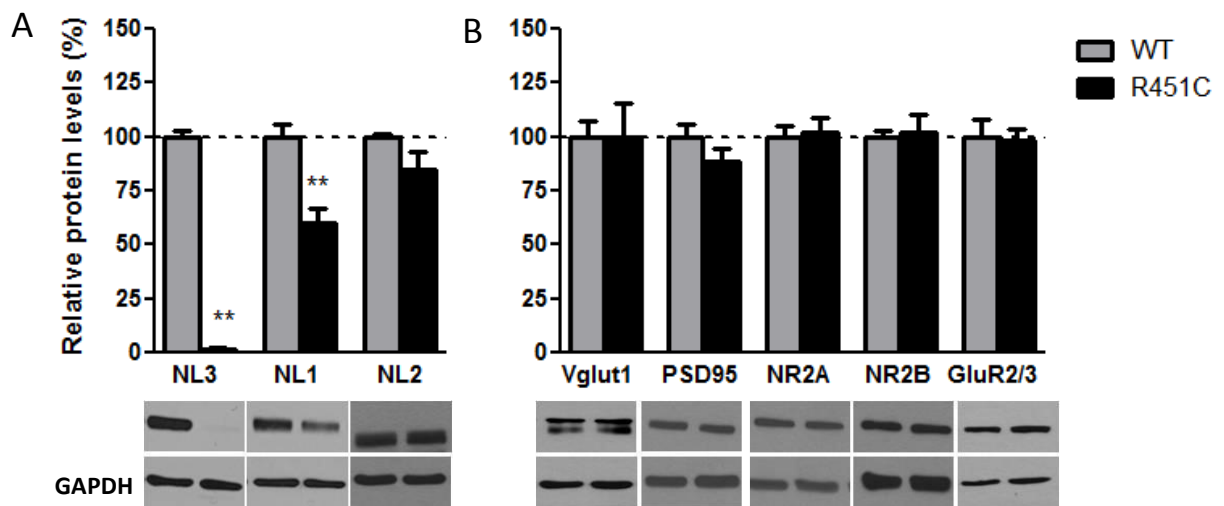


**Figure 4.6. Expression levels of neuroligins and excitatory synaptic proteins in young adult NL3-R451C binocular visual cortex.**

Protein levels in V1b are quantified by western blot and represented as the percent of WT levels. Representative blots are below, including GAPDH levels used for loading controls. Unpaired t-test or Mann-Whitney test was performed for each marker, \*\* $p < 0.01$ ,  $n = 4-8$  mice (WT);  $n = 4-8$  mice (R451C).

- A. NL3 and NL1 levels were decreased and NL2 was not significantly altered.
- B. Excitatory markers, including vesicular glutamate transporter 1 (Vglut1), postsynaptic density protein 95 (PSD95), NMDA receptor subunits NR2A and NR2B, and AMPA receptor subunits GluR2/3, were not significantly changed.



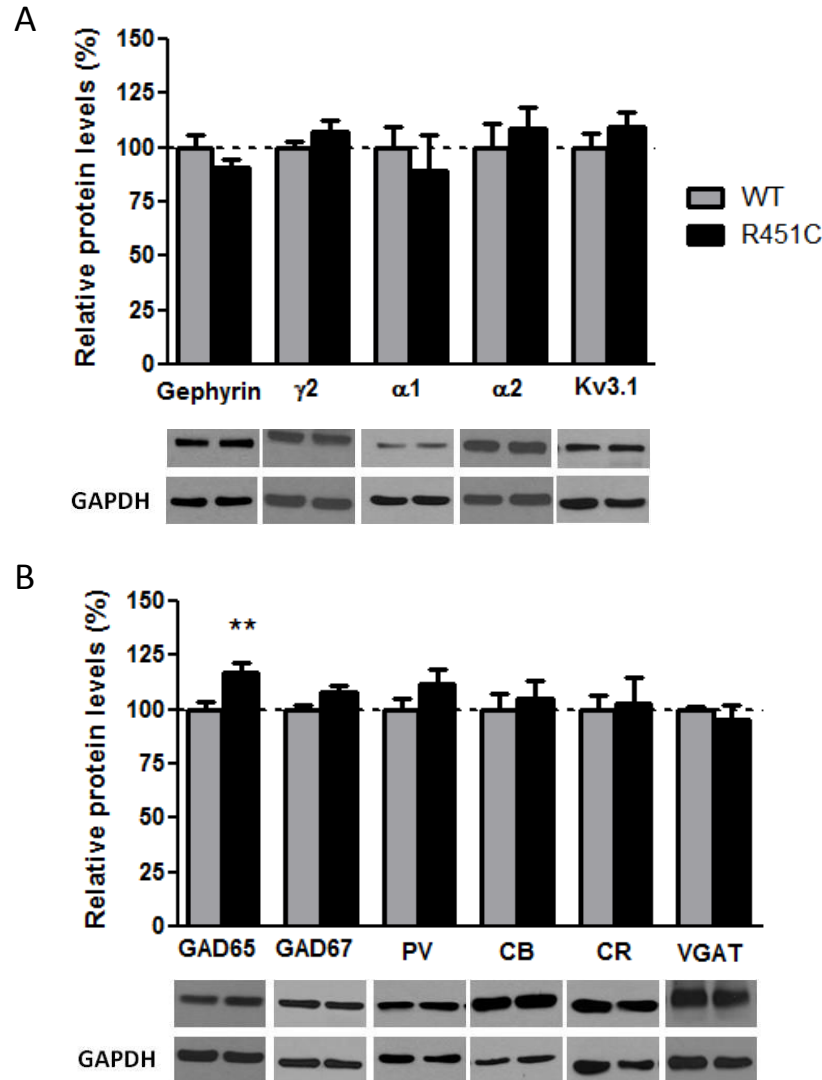


**Figure 4.7. Expression levels of presynaptic and postsynaptic inhibitory proteins in young adult NL3-R451C binocular visual cortex**

Protein levels in V1b are quantified by western blot and represented as the percent of WT levels. Representative blots are below, including GAPDH levels used for loading controls. Unpaired t-test or Mann-Whitney test was performed for each marker, \*\* $p < 0.01$ ,  $n = 4-9$  mice (WT);  $n = 4-11$  mice (R451C).

- A. Postsynaptic inhibitory markers were examined, including gephyrin, GABA<sub>A</sub> receptor subunits  $\gamma 2$ ,  $\alpha 1$ ,  $\alpha 2$ , and the potassium channel Kv3.1. There were no significant changes.
- B. Presynaptic inhibitory markers were examined, including glutamic acid decarboxylase 65 and 67 (GAD65, GAD67), parvalbumin (PV), calbindin (CB), calretinin (CR), and vesicular GABA transporter (VGAT). There was a significant increase in GAD65 levels.

density protein 95 (PSD95), NMDA receptor subunits NR2A and NR2B, and AMPA receptor subunits GluR2/3 (Fig. 4.6B). Postsynaptic inhibitory markers were normal, including the scaffolding protein Gephyrin and the GABA receptor subunits  $\gamma 2$ ,  $\alpha 1$ , and  $\alpha 2$  (Fig. 4.7A). There was no change in the expression of the potassium channel Kv3.1, which contributes to the fast-spiking ability of parvalbumin-positive interneurons (Rudy and McBain, 2001). Measuring the levels of calcium-binding proteins that are specific to different interneuron subsets revealed no change in calbindin (CB) or calretinin (CR), but a trend towards an increase in parvalbumin (PV) that did not reach significance (Fig. 4.7B). Interestingly, GAD65, which is the presynaptic activity-dependent GABA-synthesizing enzyme responsible for fast intrinsic inhibitory signaling (Soghomian and Martin, 1998), was significantly increased, suggesting an enhancement of presynaptic inhibition. Many studies have demonstrated that the development and activity of PV-positive basket cells regulates the timing of critical period plasticity (reviewed in Levelt and Hubener, 2012; Le Magueresse and Monyer, 2013). For this reason, we decided to further investigate PV synapses in NL3-R451C mice.

### **Parvalbumin-positive perisomatic innervation of pyramidal cells in young adult binocular visual cortex**

We analyzed parvalbumin circuitry in detail using confocal imaging of immunostained sections of adult V1b. The overall mean intensity of PV staining in NL3-R451C mice was not significantly different from WT levels (Fig. 4.8A). However, the intensity of GAD65 was significantly enhanced, suggesting a possible increase in synaptic inhibition (Fig. 4.8B). PV basket cells form perisomatic synapses onto excitatory pyramidal cells, which allows them to significantly control the precision of spiking and the engagement of plasticity (Fig. 4.9A and B; Lazarus and Huang, 2011). We analyzed these putative synapses by counting the number of PV-positive and GAD65-positive puncta surrounding NL3-R451C

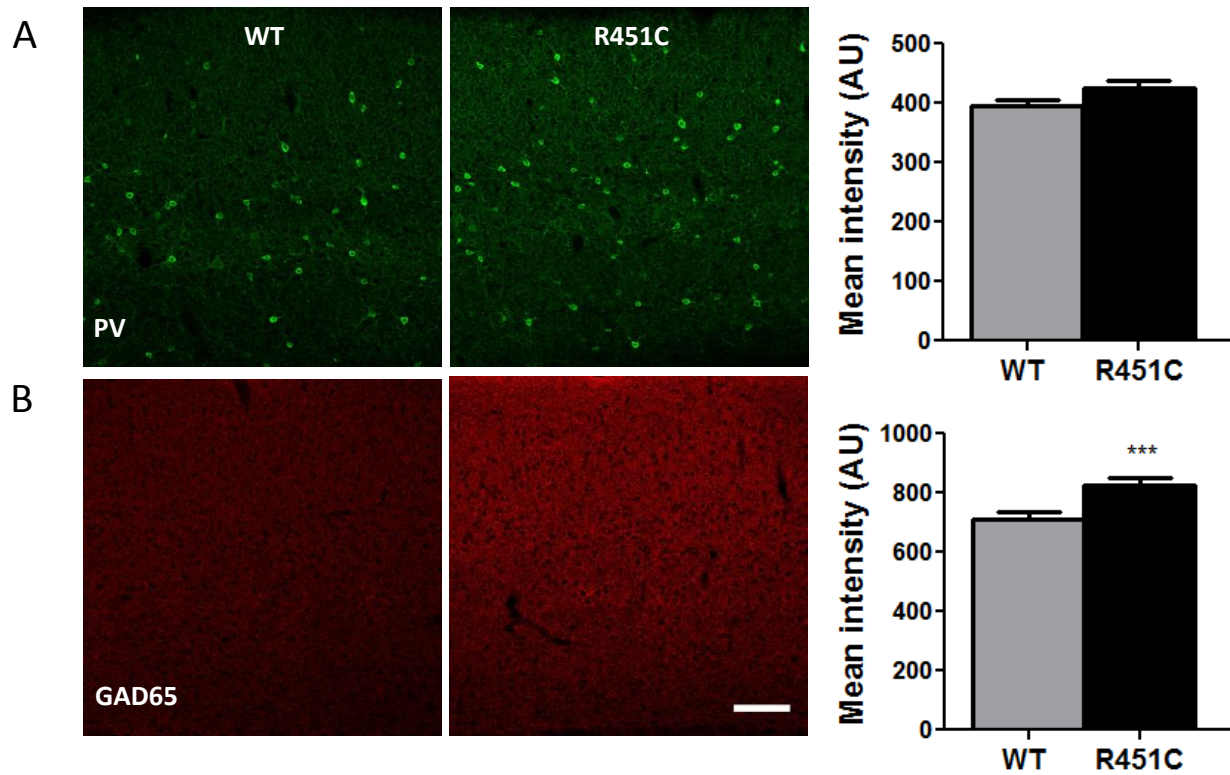


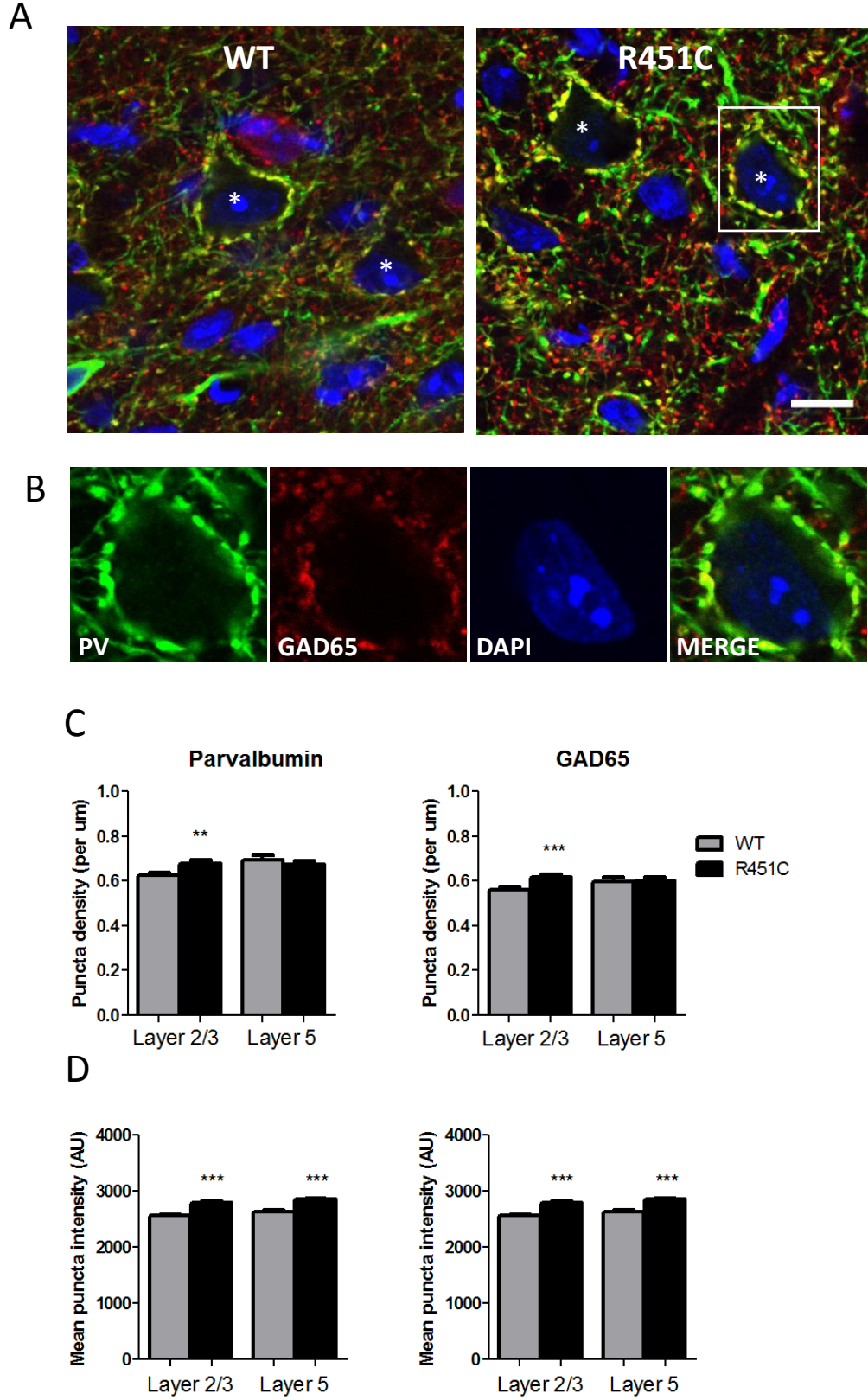
**Figure 4.8. Mean intensity of GAD65 is increased in immunostained visual cortical sections in NL3-R451C mice.**

- A. Sample 20X images from young adult V1b stained with PV (green). Mean PV intensity is quantified. AU, arbitrary units. Unpaired t-test,  $p=0.18$ ,  $n=6$  mice, 58 sections (WT);  $n=6$  mice, 53 sections (R451C).
- B. Sample 20X images from adult V1b stained with GAD65 (red). Scale bar=100  $\mu\text{m}$ . Mean GAD65 intensity is quantified. There is an increase in the level of GAD65 in mutant mice. Unpaired t-test,  $***p<0.001$ ,  $n=6$  mice, 58 sections (WT);  $n=6$  mice, 53 sections (R451C).

**Figure 4.9. Parvalbumin circuitry in young adult NL3-R451C mutant binocular visual cortex is enhanced and hyperconnected.**

- A. Sample 100X images of pyramidal cells surrounded by PV puncta. PV is in green, GAD65 is in red, and DAPI is in blue. The white asterisks indicate cells that would be included in the analysis. Scale bar=10  $\mu\text{m}$ .
- B. Zoomed in sample 100X images showing PV and GAD65 puncta surrounding the soma of a pyramidal cell.
- C. Quantification of the density of PV and GAD65 puncta surrounding pyramidal cells. There is a layer-specific (2/3) increase in PV and GAD65 puncta density. Mann-Whitney test within layer, \*\* $p < 0.01$ , \*\*\* $p < 0.001$ ,  $n = 6$  mice, 202 cells (WT);  $n = 6$  mice, 204 cells (R451C).
- D. Quantification of the mean intensity (AU, arbitrary units) of fluorescence in double-positive puncta. There is an increase in the intensity of PV and GAD65 in puncta on cells in layers 2/3 and 5. Mann-Whitney test within layer, \*\*\* $p < 0.001$ ,  $n = 6$  mice, 202 cells, 3095 puncta (WT);  $n = 6$  mice, 204 cells, 3256 puncta (R451C).

Figure 4.9 (Continued)



mutant pyramidal cell somas in superficial (2/3) and deeper (5) cortical layers. The density of PV-positive and GAD65-positive puncta were both increased specifically on layer 2/3 pyramidal cells (Fig. 4.9C). We also measured the mean intensity of GAD65 and PV content in double-positive puncta and found a consistent increase in intensity for both markers in layer 2/3 and layer 5 (Fig. 4.9D). Therefore, this analysis suggests that presynaptic inhibition at the PV-pyramidal cell synapse may be enhanced and this circuit may be hyperconnected.

### **VEP waveform shape may reflect *in vivo* E/I balance in the visual cortex**

Our western blot and immunostaining data support previous findings that cortical inhibition is increased in the NL3-R451C mutant mice (Tabuchi et al., 2007). Based on the firing properties of single V1 cells, we did not see any change in spontaneous or evoked activity that would indicate an increase in inhibition (Fig. 3.4A). However, analysis of the VEP waveform in response to a low spatial frequency stimulus revealed a dramatic change in local cortical processing. WT mice exhibited a classical response to a low spatial frequency stimulus (1 Hz alternating black and white bars at 0.05 cpd), consisting of an initial negative component (NC) as neurons were excited by the onset of the stimulus, and a subsequent positive component (PC) following the offset of the stimulus (Figure 4.10, gray; Porciatti et al., 1999). In the NL3-R451C mutants, NC latency was similar but there was a slight increase in NC amplitude and a dramatic increase in PC amplitude (Figure 4.10A, black and 4.10B). The NC and PC of the VEP waveform are believed to represent the engagement of excitatory and inhibitory circuits, respectively (Zemon et al., 1980; Haider et al., 2013). This result indicates an alteration in the way that the mutant cortex processes simple visual stimuli and suggests a potential increase in inhibition.

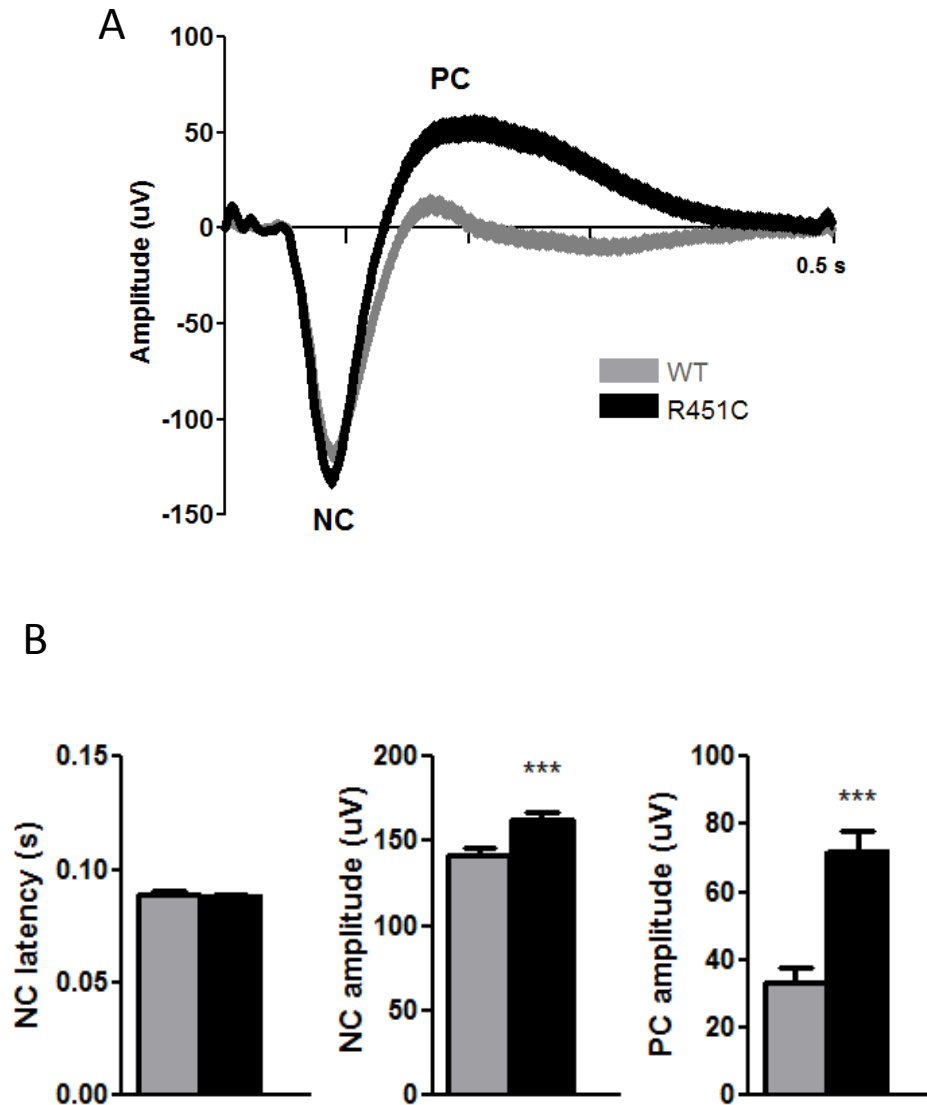


**Figure 4.10. Abnormal VEP waveform shape provides evidence of enhanced inhibition *in vivo* in NL3-R451C mutant mice.**

- A. Average VEP waveform in response to 0.05 cpd stimuli in young adult mice. The width of the trace represents mean  $\pm$  SEM. NC indicates the negative component and PC indicates the subsequent positive component. N=7 mice, 3500 individual contrast reversals (WT); n=8 mice, 4120 individual contrast reversals (R451C).
- B. The mean NC latency, absolute value of maximum NC amplitude, and maximum PC amplitude were quantified. NC latency was unaffected, whereas NC and PC amplitudes were enhanced in the mutants. Mann-Whitney test,  $p=0.97$  (NC latency),  $p=0.0002$  (NC amplitude),  $p=0.0007$  (PC amplitude).

## **Developmental changes in inhibition in the visual cortex**

We performed our analysis of E/I balance in the young adult brain (2-3 months old) because this is the age at which we saw the most dramatic phenotype, including significantly enhanced acuity and aberrant ocular dominance plasticity. In order to understand how or if this increased inhibition contributes to this phenotype, we also examined VEP waveform shape and PV circuitry in 1-month-old juvenile mice. Strikingly, although the NC amplitude was already slightly enhanced, we did not observe the same dramatic increase in PC amplitude that young adult mutants exhibited (Fig. 4.11A). In addition, the mean intensity of PV and GAD65 puncta was already increased (Fig. 4.11B). However, there was no change in PV puncta density and only a slight increase in GAD65 puncta density in layer 2/3 (Fig. 4.11C). Thus, we observe an increase in inhibition that was most prominent in adulthood, at a time when acuity is enhanced and the critical period is abnormally open.

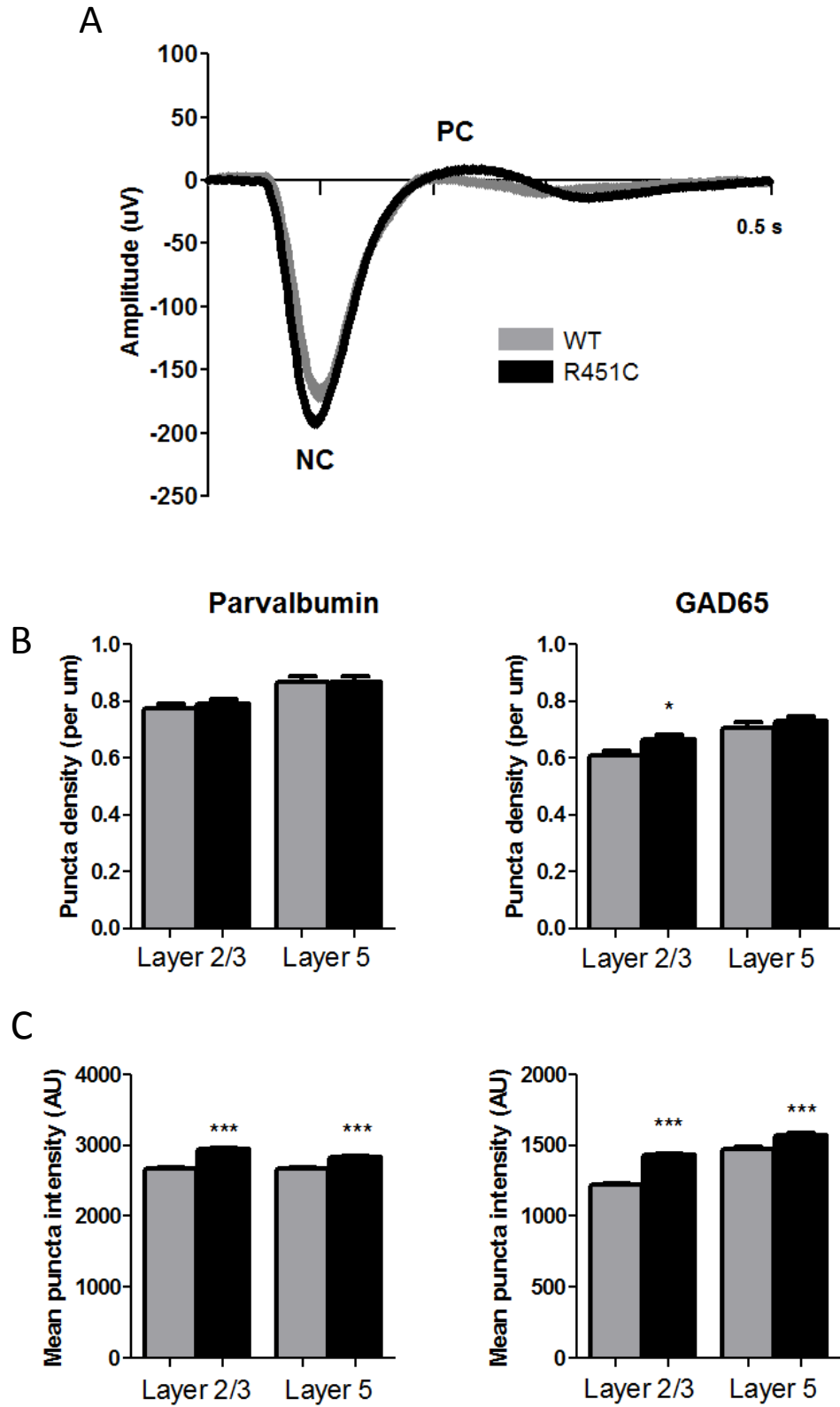
The most apparent difference between the two ages was an increase in PV synapse density on layer 2/3 cells in adults that was not present at 1 month (Fig. 4.12A and B). Interestingly, we found that there was a decrease in PV puncta density that occurred over development, from 1 month to 2-3 months, and this change was highly significant in both genotypes (Fig. 4.12C). This result presents novel evidence that PV synapses may undergo some form of pruning in young adulthood. Such a phenomenon has never before been investigated to our knowledge.



**Figure 4.11. Juvenile NL3-R451C mutant mice exhibit less evidence of increased inhibition.**

- A. Average VEP waveform in response to 0.05 cpd stimuli in 1-month-old mice. The width of the trace represents mean  $\pm$  SEM. NC indicates the negative component and PC indicates the subsequent positive component. N=6 mice, 3280 individual contrast reversals (WT); n=8 mice, 4100 individual contrast reversals (R451C). There are minimal differences between WT and mutant waveforms.
- B. Quantification of the density of PV and GAD65 puncta surrounding pyramidal cells in 1-month-old mice. There is no change in PV puncta density and a layer-specific (2/3) increase in GAD65 puncta density. Mann-Whitney test within layer, \* $p < 0.05$ , n=4 mice, 215 cells (WT); n=4 mice, 235 cells (R451C).
- C. Quantification of the mean intensity (AU, arbitrary units) of fluorescence in double-positive puncta. There is an increase in the intensity of PV and GAD65 in puncta on cells in layers 2/3 and 5. Mann-Whitney test within layer, \*\*\* $p < 0.001$ , n=4 mice, 215 cells, 4581 puncta (WT); n=4 mice, 235 cells, 5233 puncta (R451C).

Figure 4.11 (Continued)



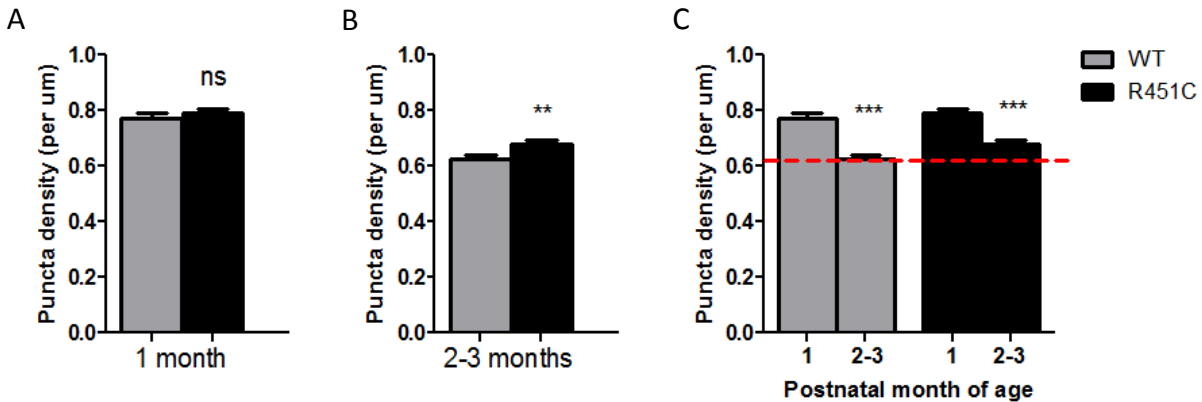


**Figure 4.12. Comparison of PV puncta density over development on layer 2/3 mutant pyramidal cells.**

- There is no change in PV puncta density on layer 2/3 cells at 1 month of age. Mann-Whitney test,  $p=0.47$ ;  $n=4$  mice, 215 cells (WT);  $n=4$  mice, 235 cells (R451C).
- There is a significant increase in PV puncta density on layer 2/3 cells at 2-3 months of age. Mann-Whitney test,  $**p<0.01$ ,  $n=6$  mice, 202 cells (WT);  $n=6$  mice, 204 cells (R451C).
- Both genotypes exhibit a significant decrease in PV puncta density with age. Red dotted line indicates the final puncta density reached in WT mice at 2-3 months of age. Kruskal-Wallis test, WT 1-month vs. WT 2-3-months,  $***p<0.0001$ ; R451C 1-month vs. R451C 2-3-months,  $***p<0.0001$ ; WT 1-month vs. R451C 1-month, not significant; WT 2-3-months vs. R451C 2-3-months, not significant.

## DISCUSSION

While alterations in ocular dominance plasticity have been reported in at least three different animal models of syndromic autism, including Angelman (Yashiro et al., 2009; Sato and Stryker, 2010), Rett (Tropea et al., 2009), and Fragile X syndrome (Dölen et al., 2007), none of these studies systematically mapped the critical period for ocular dominance plasticity over development. By performing a thorough characterization of ocular dominance plasticity in the NL3-R451C mice, we were able to assess the nature of this plasticity as well as the timing. We found that deprivation-induced loss of acuity was driven by competition and was permanent, as in WT mice. However, a careful mapping over development revealed that the critical period remained open in adult mutant mice.

The fact that the critical period does not close at the normal time suggests that there is a failure of the normal brakes on adult plasticity. Other mouse models that are reported to exhibit aberrant ocular dominance plasticity in adulthood are often also able to recover from amblyopia (reviewed in Morishita and Hensch, 2008). Therefore, it was surprising that the mutant mice were unable to regain acuity after a period of reopening following prolonged MD, considering that their critical period was still open as adults. Our study provides the first evidence to our knowledge that deprivation-induced loss of function and recovery from this loss of function may be two separable forms of plasticity that employ different mechanisms. Alternatively, it is possible that we did not optimize the conditions for recovery. Perhaps a shorter deprivation combined with a longer period of reopening could allow for some rescue of acuity. In addition, engaging competition by simultaneously closing the non-deprived eye and reopening the deprived eye (reverse suture) could prove more effective in stimulating similar mechanisms used for loss of acuity, in order to regain function.

We found evidence of enhanced inhibition in the binocular visual cortex at an age when the critical period was abnormally open. Quantification of synaptic protein levels in V1 revealed that GAD65

levels were significantly increased by approximately 20%, and there were no changes in excitatory markers. In comparison, Tabuchi et al. (2007) also found specific changes in inhibitory markers in these mice, but their results differed from ours in several ways. They did not quantify GAD65 or 67 levels and they did not look at calcium binding proteins. Instead, they found significant increases in both VGAT and gephyrin (approximately 20%), whereas we did not find similar changes. Discrepancies between the two studies are not unexpected, as Tabuchi et al. examined protein levels in the total brain and we specifically looked in the binocular visual cortex. Indeed, when the same group looked in the hippocampus, they found completely different results that supported an increase in excitation instead (Eherton et al., 2011). Therefore, it is clear that the R451C mutation has region-specific effects, indicating that NL3 may play different roles depending on the location or circuit type.

The shape of the local field potential waveform in response to visual stimuli provides valuable information about the speed and strength of excitatory and inhibitory circuit processing (Porciatti et al., 1999; Zemon et al., 1980). Topical bicuculline application during VEP recording in cats increased the equivalent of the NC peak and diminished the equivalent of the PC peak of the waveform (Zemon et al., 1980). As bicuculline is a GABA<sub>A</sub> receptor antagonist, this suggests that GABAergic inhibition normally dampens the NC and is responsible for the PC. We found that the amplitude of the excitatory negative VEP peak was slightly enhanced and the amplitude of the ensuing positive peak was strongly increased (Fig. 4.10). It is interesting that we see a slight increase in NC amplitude that accompanies the dramatic PC increase. If we interpret the PC increase to mean an increase in inhibition, we might also expect there to also be a decrease in NC. Perhaps there is compensation by the circuit in the presence of this increased inhibition that could explain why NC is increased and why we don't see any decrease in the spontaneous or evoked firing rate of single cells. It is interesting to note that a preliminary study on vision in girls with Rett Syndrome found distinct changes in the VEP waveform that correlate with the

severity of symptoms (DeGregorio, O. Khwaja, W. Kaufmann, M.F., and C.A. Nelson, unpublished data). Therefore, the VEP waveform shape could be used as a biomarker to test for autism risk.

Ongoing experiments in our lab are attempting to further investigate the role that inhibition (particularly parvalbumin-mediated inhibition) plays in generating the positive component of the VEP waveform. Some methods we are testing include acute administration of the GABA<sub>A</sub> receptor agonist diazepam, optogenetics to specifically and reversibly activate or depress PV cells, and the expression of DREADDs (Designer receptors exclusively activated by designer drugs) in PV cells to acutely silence or activate them with the administration of a drug (Armbruster et al., 2007).

Using confocal imaging of immunostained visual cortex, we found that PV cells formed more perisomatic boutons onto pyramidal cells, and these boutons contained more PV and GAD65 protein. This could reflect an enhancement of inhibition that allows excitatory cells to better discriminate changes in binocular input, allowing for continued plasticity after changes in visual experience in adulthood. Interestingly, juvenile mutant mice already exhibited enhanced GAD65 and PV content in perisomatic boutons, but did not show an increase in PV puncta number. Perhaps this early increase in GAD65 and PV intensity in juvenile mice serves to strengthen these synapses, thereby preventing some of the normal synaptic pruning of PV synapses that occurs with the closure of the critical period. Our results do not provide any direct evidence of defective pruning, as the difference in PV synapse density in young adulthood loses significance when tested in the context of development (Fig. 4.12C). However, this may be an interesting avenue to pursue in the future.

We do not know if the functional output of PV cells is actually enhanced, but the enhancement of the positive VEP component and previous analysis of inhibitory synaptic transmission by Tabuchi et al. (2007) in layer 2/3 of the cortex supports this conclusion. In the future, paired recordings from PV cells and pyramidal cells in an *in vitro* slice preparation could provide valuable insight into functional circuit-

specific changes. PV cells are also connected in networks with each other (Galarreta and Hestrin, 1999). Therefore, it would be interesting to examine PV synapses onto PV cells as well. In addition, although we found changes at PV synapses, we cannot rule out effects at other types of inhibitory synapses.

The maturation state of PV cells is a crucial factor in determining whether plasticity is possible or not. For example, the homeoprotein Otx2 is stimulated by visual experience to travel from the retina to PV cells in the visual cortex, promoting PV cell maturation and triggering the onset and closure of the ocular dominance critical period (Sugiyama et al., 2008). Beurdeley et al. (2012) recently showed that the perineuronal nets (PNNs) surrounding PV cells trap Otx2 and allow for its uptake. Disruption of Otx2 binding to PNNs in adult mice reduces PV and PNN expression, and reopens the critical period for ocular dominance. It may be that PV cells in the NL3-R451C mice are maintained in a juvenile-like state, and infusion of Otx2 could stimulate their full maturation and close the critical period. Alternatively, PNNs may not form completely around PV cells, preventing the proper uptake of Otx2, and thereby stalling PV cell maturation and the close of the critical period. These possibilities present interesting future directions to pursue in order to understand why the critical period does not close.

## **CHAPTER 5**

### **DISCUSSION AND CONCLUSIONS**



The onset of autism spectrum disorder (ASD) occurs early in life, during a period of heightened experience-dependent plasticity. We hypothesized that E/I imbalance during this sensitive postnatal phase of brain development alters the timing of critical periods, resulting in aberrant plasticity and atypical circuit refinement, ultimately leading to problems in sensory processing and cognitive behaviors. We found that the NL3-R451C autism-associated mutation enhanced GABAergic parvalbumin circuits in the mouse visual cortex, providing further evidence of a functional enhancement of cortical inhibitory signaling (Tabuchi et al., 2007). Although the basic response properties and organization of the visual cortex were grossly unaffected, the NL3-R451C mutation caused increases in visual acuity, the degree of ocular dominance plasticity, and the duration of the critical period.

The results of this study have furthered our understanding of how sensory processing and plasticity may be affected by E/I imbalance in some cases of autism, and lead to many interesting questions. Here, we will discuss how we might begin to synthesize our results in the broader context of experience-dependent cortical development and autism.

### **Role of inhibitory signaling in visual acuity**

In the young adult visual cortex, we found a simultaneous enhancement of spatial acuity (discussed in Chapter 3) and an increase in inhibition (discussed in Chapter 4) in the NL3-R451C mutant mice. We wondered if these phenotypes were related. In other words, does inhibition regulate acuity? For each mouse in which VEPs were recorded, we were able to obtain both an acuity value and an average waveform in response to low spatial frequency stimuli. We tested if changes in the shape of the waveform correlated with the level of acuity in each mouse. The NC amplitude, which is believed to represent excitatory signaling, was not correlated with acuity in WT mice but exhibited a negative correlation in the mutant mice (Fig. 5.1). The inhibitory PC amplitude exhibited a trend towards a

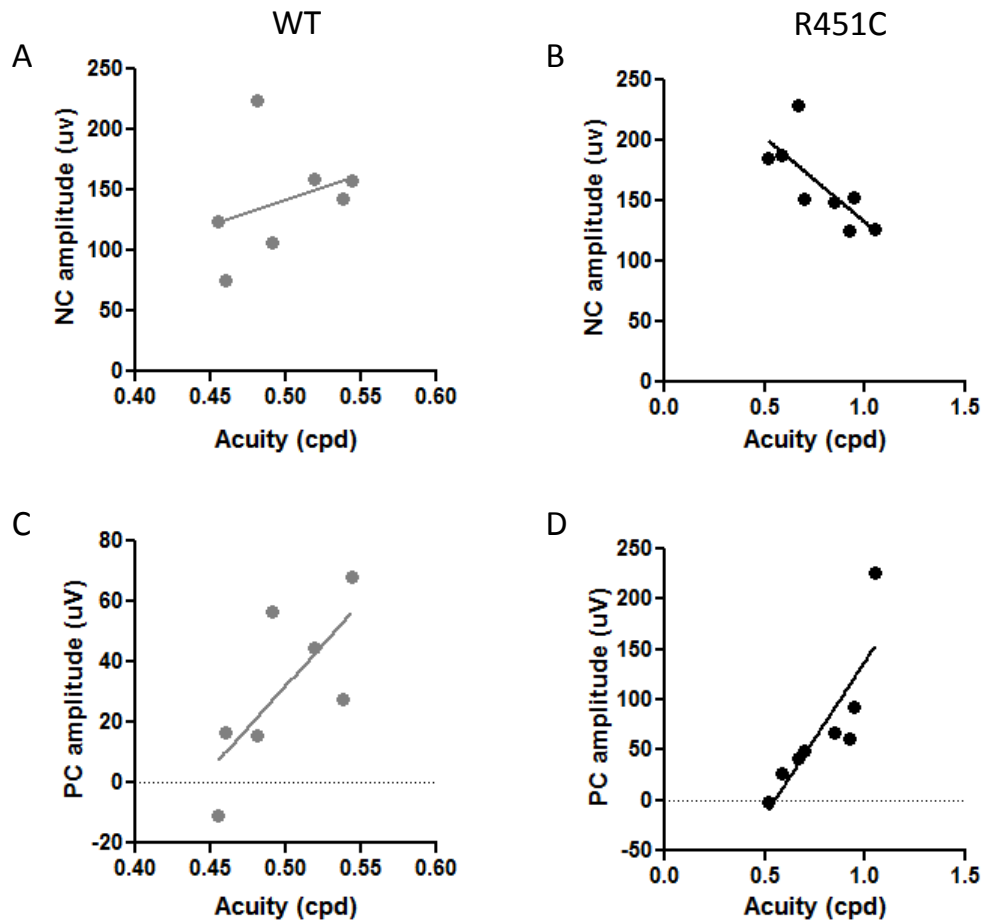


**Figure 5.1. The amplitude of the NC and PC VEP waveform peaks are correlated with acuity in young adult NL3-R451C mutant mice.**

- A. Correlation analysis of the amplitude of the NC with acuity in individual WT mice. There is no significant correlation. Pearson  $r$ ,  $p=0.48$ ;  $n=7$  pairs.
- B. Correlation analysis of the amplitude of the NC with acuity in individual R451C mutant mice. There is a significant negative correlation. Pearson  $r$ ,  $*p=0.03$ ;  $n=8$  pairs.
- C. Correlation analysis of the amplitude of the PC with acuity in individual WT mice. There is a trend but no significant correlation. Pearson  $r$ ,  $p=0.06$ ;  $n=7$  pairs.
- D. Correlation analysis of the amplitude of the PC with acuity in individual R451C mutant mice. There is a significant positive trend. Pearson  $r$ ,  $**p=0.009$ ;  $n=8$  pairs.

positive correlation in WT mice and a significant positive correlation in the mutants. This suggests that a decrease in the E/I ratio, due to a strong enhancement of inhibition, is likely to contribute to the increase in acuity that we see in the mutant mice.

A recent study from the Fagiolini lab on the *Mecp2* KO mouse model of Rett Syndrome found a decrease in adult visual acuity, while PV perisomatic puncta density was increased (Durand et al., 2012). This seems to be in apparent conflict with our results in the NL3-R451C mouse. However, several crucial differences exist between the two models. First, the PV hyperconnectivity in *Mecp2* KO mice was significantly enhanced already at eye opening and progressively increased throughout life, while other inhibitory circuits (calretinin and calbindin) and GAD65 in general decreased over development, perhaps as a compensatory mechanism to rebalance the level of inhibition. In the NL3-R451C mutant mice, PV hyperconnectivity is accompanied by enhanced GAD65 and presumably stronger perisomatic synapses onto pyramidal cells. This could result in more precise, targeted inhibition that enhances spatial discrimination. Indeed, juvenile NL3-R451C mutant mice have a less dramatic change in acuity, and they do not yet exhibit any change in PV synapse density. Second, in the *Mecp2* KO mice, the expression of NMDA receptor subunits was misregulated, resulting in an increase in the ratio of NR2A to NR2B subunits. Acuity was rescued by crossing *Mecp2* KO mice with mice heterozygous for NR2A, thus normalizing this ratio. Therefore, the disruption of acuity in the *Mecp2* KO mice may involve complex changes in both excitatory and inhibitory circuits. The NL3-R451C mice, on the other hand, do not appear to have altered expression of excitatory markers, suggesting a more selective impact on inhibitory circuits.

Our results suggest that there may be a relationship between inhibition and acuity. It would be informative to measure mean PV puncta density and acuity within the same NL3-R451C mutant mice and see if they are also correlated. What remains to be tested is whether this increase in PV synapse

density represents more convergence of input from multiple different PV cells or simply more input from the same PV cell. A distinction between these two scenarios could help us to understand how the nature of inhibition is changing on a network level. In fact, the exact reciprocal connectivity of PV and pyramidal cells is still unclear, and several studies that have attempted to address this *in vitro* have found conflicting results (for example, Wang et al., 2002; Holmgren et al., 2003; Yoshimura and Callaway, 2005; Thomson and Lamy, 2007; Packer and Yuste, 2011). While it is generally accepted that one PV cell can innervate many pyramidal cells, it is unclear how many PV cells target a single pyramidal cell. In order to investigate PV-pyramidal cell connectivity more thoroughly, we are currently generating mice in which *Brainbow* is expressed exclusively in PV cells in the NL3-R451C mice (Livet et al., 2007) to distinguish inputs from multiple PV cells in different fluorescent colors.

The contribution of PV-mediated inhibition to sensory processing has not been fully elucidated, but tools are now being developed to address this question. One study found that optogenetic activation of PV cells *in vivo* sharpened direction and orientation selectivity of nearby excitatory cells, and enhanced orientation discrimination in awake behaving mice (Lee et al., 2012). In contrast, two other groups used optogenetics to modify the activity of PV cells *in vivo*, and showed that PV cells linearly transform the response of pyramidal cells by modulating cortical gain, with only modest effects on stimulus selectivity (Attalah et al., 2012; Wilson et al., 2012). According to Lee et al. (2012), this discrepancy could result in part from the relatively low level of PV activation used in the latter two studies.

### **More thorough investigation of excitatory/inhibitory balance is warranted**

Based on the critical period phenotype observed in the NL3-R451C mutant mice, we chose to investigate potential alterations in parvalbumin cells as a first step because of their known role in

regulating plasticity. However, it is possible that other interneuron subtypes are also affected. In the future, we would like to do a similar analysis of the connectivity of interneurons expressing somatostatin, calbindin, and calretinin. In this way, we could determine if the hyperconnectivity of PV neurons is specific or general to all GABAergic cells. In addition, it is imperative to determine if the changes we observed using immunostaining techniques actually reflect functional increases in inhibition. In order to properly test this in the future, a comprehensive analysis of mIPSC and mEPSC frequency and amplitude in visual cortex slices at different ages will be conducted. In addition, paired recordings from excitatory and inhibitory neurons would reveal if there is a true functional hyperconnectivity in the visual cortex of the mutant mice. Finally, intracellular recording from excitatory and fast-spiking inhibitory cells *in vivo* (Yazaki-Sugiyama et al., 2009) could allow for a nuanced comparison of intrinsic and evoked responses in both types of cells.

Our experiments revealed a clear extension of the critical period for ocular dominance plasticity, accompanied by evidence of increased inhibition in the adult visual cortex. This result is actually quite surprising and counterintuitive based on the critical period literature. Many studies have found a correlation between decreased adult inhibition and adult ocular dominance plasticity. For example, two different direct methods for reducing inhibition - infusion of the GAD inhibitor 3-mercaptopropionic acid (MPA) and infusion of the GABA<sub>A</sub> receptor antagonist picrotoxin - allowed for weak but significant ocular dominance plasticity after 7 days of monocular deprivation in adult rats (Harauzov et al., 2010). In addition, other manipulations, including treatment with the antidepressant drug fluoxetine (Maya Vetencourt et al., 2008), dark exposure (He et al., 2006), environmental enrichment (Sale et al., 2007; Baroncelli et al., 2010), and genetic ablation of lynx1 (Morishita et al., 2010), have all been shown to promote adult ocular dominance plasticity and reduce inhibition. Notably, enhancing inhibition with diazepam is able to preclude the effects of all of these manipulations on adult plasticity.

One theory that exists in the critical period field is that there is an optimal level of inhibitory circuit maturation that allows for plasticity during a specific time window. Transplantation of embryonic inhibitory cells into the visual cortex opens a second critical period when the cells reach a stage of maturation that is equivalent to endogenous inhibitory neurons during the normal critical period (Southwell et al., 2010). A possible explanation for the extended critical period in the NL3-R451C mice could be that PV cells are maintained in a critical period-like maturation state throughout early adulthood. Although we have not directly tested this hypothesis, it is interesting to note that we see a reduction of PV bouton density with age in WT mice, and this may be less pronounced in the mutants because they have a higher PV bouton density at 2-3 months of age. More in-depth analysis of how PV puncta density changes with development, as well as investigation of other factors that directly regulate PV cell maturation, like Otx2 and perineuronal nets, could help us to better understand the maturation state of PV cells in the NL3-R451C mutant mice.

### **BDNF-TrkB pathway as a possible alternative explanation for extended critical period**

Alternatively, the changes we see in inhibition could be unrelated or secondary to the visual phenotype of the NL3-R451C mutant mouse. One intriguing alternative explanation for our data, accounting for increased acuity, extended critical period, and enhanced parvalbumin circuits, could be an upregulation of the BDNF-TrkB signaling pathway. BDNF (brain-derived neurotrophic factor) is a secreted neurotrophin that signals through its receptor, TrkB (tyrosine-related kinase B). This pathway is of particular interest because upregulation of BDNF is implicated in autism (Nishimura et al., 2007; Miyazaki et al., 2004; Tsai et al., 2005; Correia et al., 2010). In addition, many studies implicate BDNF signaling in the regulation of acuity. To our knowledge, the only manipulation reported to enhance acuity is environmental enrichment. Environmental enrichment upregulates BDNF levels and induces

precocious development of acuity (Cancedda et al., 2004; Sale et al., 2004). It also results in increased adult acuity, as measured with behavior (Prusky et al., 2000c; Cancedda et al., 2004; Sale et al., 2004), VEP (Cancedda et al., 2004; Sale et al., 2004), and enhances the spatial frequency preference of single cells (Beaulieu and Cynader, 1990). Genetic overexpression of BDNF results in precocious development of acuity (Huang et al., 1999). In addition, activity-dependent BDNF transcription plays a role in the enhancement of acuity following conditioning with visual stimulation in developing *Xenopus* (Schwartz et al., 2011). On the other hand, overexpression of a dominant-negative TrkB protein in pyramidal cells reduces visual acuity (Heimel et al., 2010). Interestingly, monocular deprivation during the critical period reduces acuity (Prusky et al., 2000b) and concurrently reduces BDNF mRNA and protein levels (Bozzi et al., 1995; Rossi et al., 1999) in the contralateral visual cortex.

This pathway is also implicated in regulation of the critical period for ocular dominance. BDNF mRNA levels increase during development with the opening of the critical period, and then decrease following the closure of the critical period after P40 (Kato-Semba et al., 1998, Gorba et al., 1999). Artificially increasing BDNF levels early in life in transgenic mice shifts the critical period earlier (Huang et al., 1999; Hanover et al., 1999), whereas increasing BDNF in adulthood by cortical infusion or treatment with the antidepressant drug fluoxetine reopens the critical period (Maya Vetencourt et al., 2008). In addition, environmental enrichment during adulthood increases BDNF and allows for recovery from amblyopia (Sale et al., 2007). Therefore, recreating the high BDNF environment of the critical period can allow for adult plasticity.

Finally, the BDNF-TrkB pathway regulates the development of inhibition, and in particular, of parvalbumin-positive interneurons (Rutherford et al., 1997; Seil and Drake-Baumann, 2000; Hartman et al., 2006; Marty et al., 2000; Rico et al., 2002; Patz et al., 2004; Hong et al., 2008; Sakata et al., 2009). BDNF overexpression increases GAD65 expression, PV cell number, and IPSC amplitude (Huang et al.,

1999), and increasing BDNF levels via environmental enrichment increases GAD65/67 protein levels (Sale et al., 2004; Cancedda et al., 2004). Disrupting this signaling pathway in layer 2/3 pyramidal cells by knocking out *BDNF* (Kohara et al., 2007) or overexpression of a dominant-negative TrkB receptor (Heimel et al., 2010) reduces the number of parvalbumin-positive perisomatic synapses on the manipulated cells. In order to begin to test the possibility that this pathway is altered in the NL3-R451C mutant mice, we could quantify levels of BDNF and TrkB mRNA with RT-PCR or protein with western blot or ELISA as a first step.

#### **Other possible alternative explanations for extended critical period**

One physical mechanism believed to mediate ocular dominance plasticity is deprived eye spine loss as a result of proteolysis of the extracellular matrix. Following 2 days of monocular deprivation, there is increased spine motility due to proteolytic activity by tissue-type plasminogen (tPA) in the binocular visual cortex of mice (Mataga et al., 2002; Mataga et al., 2004; Oray et al., 2004). Genetic deletion of tPA prevents MD-induced spine loss and ocular dominance plasticity (Mataga et al., 2004). Interestingly, tPA release appears to be regulated upstream by GAD65, as knocking-out GAD65 abolishes MD-induced tPA activity, spine motility, and ocular dominance plasticity (Mataga et al., 2002). One theory to explain adult ocular dominance plasticity in the NL3-R451C mice could be that tPA activity is elevated due to increased GAD65 levels in the NL3-R451C mutant mice. This could render the cortex more sensitive to changes in experience due to the ability to respond to monocular deprivation with structural changes, even as adults. A first step to investigate this possibility would be to compare proteolytic activity using a chromogenic assay kit in baseline and post-MD juvenile and adult NL3-R451C WT and mutant binocular visual cortex. Future studies could delve into this question deeper by imaging dendritic spines *in vivo* with two-photon microscopy.



The extended critical period in the NL3-R451C mutants could also result from changes in hebbian homosynaptic plasticity. One explanation for MD-induced ocular dominance plasticity lies in the rapid LTD-induced weakening of the deprived eye and subsequent strengthening of the open eye through LTP (reviewed in Smith et al., 2009). In the normal adult visual cortex, prolonged MD can still induce LTP of inputs from the open eye, but LTD of deprived-eye inputs fails to occur. It is possible that NL3-R451C mutant mice still retain the capacity for LTD in adulthood, thus maintaining ocular dominance plasticity past the normal closure of the critical period. To our knowledge, LTD has never been tested in the NL3-R451C mice, but they were found to have enhanced NMDA receptor-dependent LTP in the CA1 region of the hippocampus (Etherton et al., 2011). Interestingly, in mice in which the NL3 has been completely knocked out, there is an misregulation of mGluR-dependent LTD in the cerebellum (Baudouin et al., 2012). Misregulation of LTD appears to be a common theme in autism, present in mouse models of Fragile-X syndrome and Tuberous sclerosis (Auerbach et al., 2011), and therefore may merit investigation in the NL3-R451C mutant mice.

### **Specific effect of the autism-associated R451C mutation**

In order to begin to understand how this particular mutation may lead to altered visual function and plasticity, we considered the effect of the R451C mutation on neuroligin-3 protein. While the R451C point mutation was identified in genetic studies of autistic individuals, complete loss of the *NL3* gene has not been linked to ASD. However, the R451C destabilizes the protein and results in almost complete intracellular retention and degradation of the NL3 protein (Fig. 4.6A; Chih et al., 2004; Comoletti et al., 2004; Chubykin et al., 2005; De Jaco et al., 2006). Previous studies have compared the NL3-R451C and NL3 knock-out (KO) mice and found changes in behavior and synaptic transmission in the R451C mutants

that were completely absent in the KO mice (Tabuchi et al., 2007; Etherton et al., 2011). This suggests that the R451C mutation exerts gain-of-function effects.

This held true in the visual system as well. KO mice were indistinguishable from their WT littermates. They had normal baseline acuity and no ocular dominance plasticity at 2-3 months (Fig. 5.2B), and there was no dramatic difference in the shape of the VEP waveform (Fig. 5.2A). Therefore, our results confirm previous findings that, unlike R451C mice, NL3 KO mice do not have an increase of inhibition in the cortex (Tabuchi et al., 2007). How might this specific point mutation result in gain-of-function effects? The small percent of the protein that reaches the cell surface (about 10%) is still able to induce synapse formation (Chubykin et al., 2005) and form heterodimers with NL1 (Poulopoulos et al., 2012). However, one study found a decrease in the ability of NL3 to bind with presynaptic NX1 $\beta$  (Comoletti et al., 2004). One possibility is that the R451C mutation causes aberrant binding with other presynaptic partners. Alternatively, the small amount of protein that is left could prevent homeostatic compensation that may occur in the complete absence of NL3.

It is quite possible that NL3 protein is either restricted to particular types of synapses or plays distinct roles at different synapses. There is evidence that NL3 can be found at both excitatory and inhibitory synapses (Budreck and Scheiffle, 2007; Heller, 2012), but due to the insufficient quality of available antibodies, this still remains debated. We might expect from our results that NL3 would be located at perisomatic synapses formed by PV cells onto layer 2/3 pyramidal cells, due to the increase in perisomatic puncta that we observed. Heller et al. (2012) isolated inhibitory synaptosomes from deeper layer cortical pyramidal cells and confirmed the presence of both NL2 and NL3 at inhibitory synapses. Interestingly, they found some evidence that NL2 and NL3 may be preferentially localized to synapses on the soma and on the base of apical dendrites of pyramidal cells, respectively. Further support for NL2 being localized to synapses on the soma comes from a paper that showed that deletion of NL2

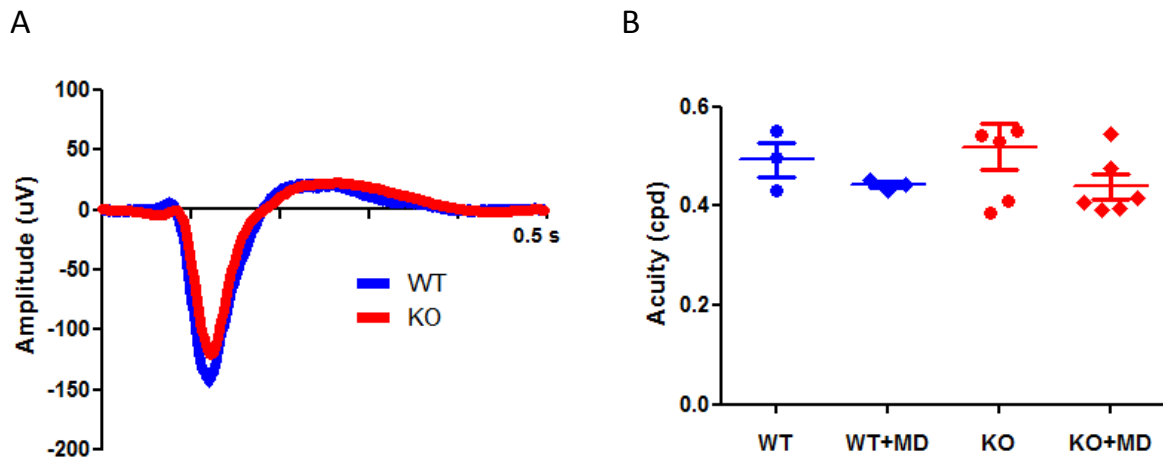


**Figure 5.2. Young adult NL3 KO mice do not show changes in VEP waveform shape or baseline visual acuity, and do not exhibit adult ocular dominance plasticity.**

- A. Average VEP waveform in response to many repetitions of a 0.05 cpd stimulus. There is no increase in the positive component of the waveform, as was seen in the R451C mutants (see Fig. 4.10A). N=3 mice, 1520 individual contrast reversals (WT); n=5 mice, 2080 individual contrast reversals (KO).
- B. Acuity was measured in response to non-deprived and deprived situations. There was no difference in baseline acuity, and there was no plasticity after 4 days of monocular deprivation at 2-3 months of age. One-way ANOVA (Kruskal-Wallis test with Dunn's comparisons), no significance. N=3 mice (WT); n=5-6 mice (KO).

onto pyramidal cells in the somatosensory cortex (Gibson et al., 2009). If NL3 is not at PV synapses, it could also be that it is localized to synapses that receive input from other types of inhibitory cells, like somatostatin cells. In fact, layer 4 somatostatin cells actually inhibit PV cells, which themselves inhibit pyramidal cells (Xu et al., 2013). Therefore, altered NL3 activity at somatostatin synapses could decrease inhibition of PV cells, which could in turn increase PV cells' innervation of pyramidal cells.

### **Disrupted critical period expression in autism**

What might altered parvalbumin circuitry and critical periods in the visual system mean for the brain in general? Interestingly, similar mechanisms appear to regulate critical periods across brain regions. For example, the maturation of PV cells in the barrel cortex peaks during the critical period for whisker tuning (del Rio et al., 1994). Whisker trimming exclusively during this critical period in mice results in decreased PV expression and reduced inhibitory transmission in vitro (Jiao et al., 2006). In the zebra finch, brain regions dedicated to singing exhibit progressive perineuronal net formation around PV cells with a time course that parallels the critical period (Balmer et al., 2009). The maturity of the song correlates with the percentage of PV cells that are enwrapped in PNNs, and this can be manipulated with experience by altering exposure to tutor song. In the rodent auditory cortex, spectrally limited noise exposure prevents the closure of the critical period for regions of auditory cortex that selectively respond to those interrupted frequencies, and PV cell number is also reduced in those regions (De Villers-Sidani et al., 2008). In the rodent, conditioned fear can be eliminated during early life but is protected from erasure in adulthood (Kim and Richardson, 2007). A developmental progression of PNN formation around PV cells coincides with this switch and enzymatic degradation of PNNs allows juvenile-like fear extinction in adulthood (Gogolla et al., 2009a), similar to the reopening of ocular dominance plasticity in the adult visual cortex (Pizzorusso et al., 2002). In light of these findings, it is interesting to

note that at least nine different mouse models of autism share common alterations in PV cells (Gogolla et al., 2009b). Therefore, we believe that the failure to properly regulate critical periods may be a general feature of the autistic brain.

Constant plasticity that persists into adulthood may be advantageous in normal environments, but a weakness when an individual is challenged by deprivation or abnormal experience. This could lead to a large spectrum of phenotypes, varying in severity depending on the individual. Indeed, two brothers carrying the same R451C mutation in NL3 exhibited drastically different functional outcomes; one brother was diagnosed at 3-years-old with typical autism, severe mental retardation, and epilepsy, while the other was diagnosed at 10 years of age with more mild Asperger's syndrome (Jamain et al., 2003). This highlights the importance of experience in understanding and managing autism. If the autistic brain is indeed hyperplastic, it would be prudent to keep the environment as stable as possible to avoid overstimulation and instability of brain function. In fact, it has been suggested that autism is an "intense world syndrome", where hypersensitivity to stimuli can ultimately render an individual debilitated unless these symptoms can be managed (Markram et al., 2007). On the other end of the spectrum, the autistic brain may be hypoplastic in some individuals, and in this case, enriching the environment as much as possible may help the brain to gain the necessary experience to properly refine its circuitry. It must also be considered that one of the core symptoms of autism includes repetitive behaviors and restricted interests early in life. Therefore, as a result of these types of behaviors, a child could end up deprived of necessary experiences during critical periods.

It would be interesting to manipulate the environment of the NL3-R451C mice, for example by dark-rearing, and see how brain function is affected. We might hypothesize that by reducing sensory input with dark rearing, we could prevent enhancement of inhibition and thereby renormalize acuity and plasticity and allow for closure of the critical period. Indeed, this type of sensory deprivation has

been shown to rescue symptoms in other mouse models of autism (Yashiro et al., 2009; Durand et al., 2012).

## **Conclusion**

The careful regulation of critical periods indicates that their precise expression is crucial for normal development. For the first time, we have demonstrated robust evidence that critical periods are misregulated in autism. A brain that is too plastic at the wrong times could result in noisy and unstable processing of external inputs. On the other hand, a brain that lacks the right level of plasticity early in life might remain hyper- or hypo-connected and unsuited to its surroundings. Together with the existing literature, our results support the necessity and value of a systematic investigation of sensory function in ASD and associated neurodevelopmental disorders. Screening for sensory function should be included in ongoing studies of children at risk for developing ASD due to affected siblings in the family. By first understanding basic circuit processing in autism, a cumulative chain reaction of abnormalities could be prevented early on and save consequent behavior. Further investigation of sensory processing in mouse models of autism will clarify the underlying molecular mechanisms and bring us closer to developing effecting treatments for autism.

## REFERENCES

- Abrahams, B.S., and Geschwind, D.H. (2008). Advances in autism genetics: on the threshold of a new neurobiology. *Nature Reviews. Genetics* 9, 341–355.
- American Psychiatric Association. (1994). *Diagnostic and Statistical Manual of Mental Disorders: DSM-IV*. 4th ed. (Washington, DC).
- American Psychiatric Association. *Proposed Draft Revisions to DSM Disorders and Criteria: A 09 Autism Spectrum Disorder*. Arlington, VA: American Psychiatric Association; 2011. Available at: <http://www.dsm5.org/ProposedRevision/Pages/proposedrevision.aspx?rid=94>. Revised January 26, 2011. Accessed November 13, 2012.
- Amir, R.E., Van den Veyver, I.B., Wan, M., Tran, C.Q., Francke, U., and Zoghbi, H.Y. (1999). Rett syndrome is caused by mutations in X-linked MECP2, encoding methyl-CpG-binding protein 2. *Nature Genetics* 23, 185–188.
- Antonini, A., and Stryker, M.P. (1996). Plasticity of geniculocortical afferents following brief or prolonged monocular occlusion in the cat. *The Journal of Comparative Neurology* 369, 64–82.
- Antonini, A., Fagiolini, M., and Stryker, M.P. (1999). Anatomical correlates of functional plasticity in mouse visual cortex. *The Journal of Neuroscience* 19, 4388–4406.
- Antonini, A., Gillespie, D.C., Crair, M.C., and Stryker, M.P. (1998). Morphology of single geniculocortical afferents and functional recovery of the visual cortex after reverse monocular deprivation in the kitten. *The Journal of Neuroscience* 18, 9896–9909.
- Armbruster, B.N., Li, X., Pausch, M.H., Herlitze, S., and Roth, B.L. (2007). Evolving the lock to fit the key to create a family of G protein-coupled receptors potentially activated by an inert ligand. *Proceedings of the National Academy of Sciences of the United States of America* 104, 5163–5168.
- Ashwin, E. (2009b). Eagle-eyed Visual Acuity in Autism, Correspondence. *Biological Psychiatry* 66, e23–e24.
- Ashwin, E., Ashwin, C., Rhydderch, D., Howells, J., and Baron-Cohen, S. (2009a). Eagle-eyed visual acuity: an experimental investigation of enhanced perception in autism. *Biological Psychiatry* 65, 17–21.
- Atallah, B. V, Bruns, W., Carandini, M., and Scanziani, M. (2012). Parvalbumin-expressing interneurons linearly transform cortical responses to visual stimuli. *Neuron* 73, 159–170.
- Auerbach, B.D., Osterweil, E.K., and Bear, M.F. (2011). Mutations causing syndromic autism define an axis of synaptic pathophysiology. *Nature* 480, 63–68.
- Badea, T.C., Cahill, H., Ecker, J., Hattar, S., and Nathans, J. (2009). Distinct roles of transcription factors *brn3a* and *brn3b* in controlling the development, morphology, and function of retinal ganglion cells. *Neuron* 61, 852–864.
- Balmer, T.S., Carels, V.M., Frisch, J.L., and Nick, T.A. (2009). Modulation of perineuronal nets and parvalbumin with developmental song learning. *The Journal of Neuroscience* 29, 12878–12885.

- Banks, M.S, Aslin, R.N.,and Letson, R.D. Sensitive period for the development of human binocular vision. (1975). *Science* 190, 675–677.
- Bansal, A., Singer, J.H., Hwang, B.J., Xu, W., Beaudet, A., and Feller, M.B. (2000). Mice lacking specific nicotinic acetylcholine receptor subunits exhibit dramatically altered spontaneous activity patterns and reveal a limited role for retinal waves in forming ON and OFF circuits in the inner retina. *The Journal of Neuroscience* 20, 7672–7681.
- Bardin, J. (2012). Unlocking the brain. *Nature* 487, 24-26.
- Baroncelli, L., Sale, A., Viegi, A., Maya Vetencourt, J.F., De Pasquale, R., Baldini, S., and Maffei, L. (2010). Experience-dependent reactivation of ocular dominance plasticity in the adult visual cortex. *Experimental Neurology* 226, 100–109.
- Barthó, P., Hirase, H., Monconduit, L., Zugaro, M., Harris, K.D., and Buzsáki, G. (2004). Characterization of neocortical principal cells and interneurons by network interactions and extracellular features. *Journal of Neurophysiology* 92, 600–608.
- Baudouin, S.J., Gaudias, J., Gerharz, S., Hatstatt, L., Zhou, K., Punnakkal, P., Tanaka, K.F., Spooren, W., Hen, R., De Zeew, C.I., Vogt, K., Scheiffele, P. (2012). Shared synaptic pathophysiology in syndromic and nonsyndromic rodent models of autism. *Science* 228, 128-32.
- Bavelier, D., Levi, D.M., Li, R.W., Dan, Y., and Hensch, T.K. (2010). Removing Brakes on Adult Brain Plasticity: From Molecular to Behavioral Interventions. *Journal of Neuroscience* 30, 14964–14971.
- Beaulieu, C., and Cynader, M. (1990). Effect of the richness of the environment on neurons in cat visual cortex. II. Spatial and temporal frequency characteristics. *Brain Research. Developmental Brain Research* 53, 82–88.
- Behrmann, M., Thomas, C., and Humphreys, K. (2006). Seeing it differently: visual processing in autism. *Trends in Cognitive Sciences* 10, 258–264.
- Belichenko, P.V., Oldfors, A., Hagberg, B. and Dahlstrom, A. (1994). Rett syndrome: 3-D confocal microscopy of cortical pyramidal dendrites and afferents. *NeuroReport* 5, 1509–1513.
- Belmonte, M.K., Cook, E.H., Anderson, G.M., Rubenstein, J.L.R., Greenough, W.T., Beckel-Mitchener, a, Courchesne, E., Boulanger, L.M., Powell, S.B., Levitt, P.R., et al. (2004). Autism as a disorder of neural information processing: directions for research and targets for therapy. *Molecular Psychiatry* 9, 646–663.
- Ben-Sasson, A., Hen, L., Fluss, R., Cermak, S. a, Engel-Yeger, B., and Gal, E. (2009). A meta-analysis of sensory modulation symptoms in individuals with autism spectrum disorders. *Journal of Autism and Developmental Disorders* 39, 1–11.
- Berardi, N., Pizzorusso, T., and Maffei, L. (2000). Critical periods during sensory development. *Current Opinion in Neurobiology* 10, 138–145.



- Betancur, C., Sakurai, T., and Buxbaum, J.D. (2009). The emerging role of synaptic cell-adhesion pathways in the pathogenesis of autism spectrum disorders. *Trends in Neurosciences* 32, 402–412.
- Beurdeley, M., Spatazza, J., Lee, H.H.C., Sugiyama, S., Bernard, C., Nardo, A.A. Di, Hensch, T.K., and Prochiantz, A. (2012). Otx2 Binding to Perineuronal Nets Persistently Regulates Plasticity in the Mature Visual Cortex. *The Journal of Neuroscience* 32, 9429–9437.
- Blasi, F., Bacchelli, E., Pesaresi, G., Carone, S., Bailey, A.J., Maestrini, E., and IMGSAC. (2006). Absence of coding mutations in the X-linked genes *neuroligin 3* and *neuroligin 4* in individuals with autism from the IMGSAC collection. *American Journal of Medical Genetics. Part B, Neuropsychiatric Genetics* 141B, 220–221.
- Blue, M.E., Naidu, S., and Johnston, M. V (1999). Altered development of glutamate and GABA receptors in the basal ganglia of girls with Rett syndrome. *Experimental Neurology* 156, 345–352.
- Blundell, J., Blaiss, C.A., Etherton, M.R., Espinosa, F., Tabuchi, K., Walz, C., Bolliger, M.F., Südhof, T.C., and Powell, C.M. (2010). *Neuroligin-1* deletion results in impaired spatial memory and increased repetitive behavior. *The Journal of Neuroscience* 30, 2115–2129.
- Bogdashina, O. (2003). *Sensory Perceptual Issues in Autism and Asperger Syndrome: Different Sensory Experiences, Different Perceptual Worlds* (London, UK: Jessica Kingsley).
- Bölte, S., Schlitt, S., Gapp, V., Hainz, D., Schirman, S., Poustka, F., Weber, B., Freitag, C., Ciaramidaro, A., and Walter, H. (2012). A close eye on the eagle-eyed visual acuity hypothesis of autism. *Journal of Autism and Developmental Disorders* 42, 726–733.
- Bozzi, Y., Pizzorusso, T., Cremisi, F., Rossi, F.M., Barsacchi, G., and Maffei, L. (1995). Monocular deprivation decreases the expression of messenger RNA for brain-derived neurotrophic factor in the rat visual cortex. *Neuroscience* 69, 1133–1144.
- Brainard, M.S. and Doupe, A.J. (2002). What songbirds teach us about learning. *Nature* 417, 351–358.
- Bruneau, N., Bonnet-Brilhault, F., Gomot, M., Adrien, J.L., and Barthelemy, C. (2003). Cortical auditory processing and communication in children with autism: electrophysiological/behavioral relations. *International Journal of Psychophysiology* 51, 17–25.
- Budreck, E.C., and Scheiffele, P. (2007). *Neuroligin-3* is a neuronal adhesion protein at GABAergic and glutamatergic synapses. *The European Journal of Neuroscience* 26, 1738–1748.
- Bukalo, O., and Dityatev, A. (2012). Synaptic cell adhesion molecules. *Synaptic Plasticity Advances in Experimental Medicine and Biology* 970, 97-128.
- Cancedda, L., Putignano, E., Sale, A., Viegi, A., Berardi, N., and Maffei, L. (2004). Acceleration of visual system development by environmental enrichment. *The Journal of Neuroscience* 24, 4840–4848.
- Carulli, D., Pizzorusso, T., Kwok, J.C.F., Putignano, E., Poli, A., Forostyak, S., Andrews, M.R., Deepa, S.S., Glant, T.T., and Fawcett, J.W. (2010). Animals lacking link protein have attenuated perineuronal nets and persistent plasticity. *Brain : a Journal of Neurology* 133, 2331–2347.

- Casanova, M.F., Buxhoeveden, D., and Gomez, J. (2003). Disruption in the inhibitory architecture of the cell minicolumn: implications for autism. *The Neuroscientist* 9, 496–507.
- Casanova, M.F., Buxhoeveden, D.P., Switala, A.E., and Roy, E. (2002). Minicolumnar pathology in autism. *Neurology* 58, 428–432.
- Cascio, C.J. (2010). Somatosensory processing in neurodevelopmental disorders. *Journal of Neurodevelopmental Disorders* 2, 62–69.
- Chadman, K.K., Gong, S., Scattoni, M.L., Boltuck, S.E., Gandhi, S.U., Heintz, N., and Crawley, J.N. (2008). Minimal aberrant behavioral phenotypes of neuroligin-3 R451C knockin mice. *Autism Research* 1, 147–158.
- Chang, E.F., and Merzenich, M.M. (2003). Environmental noise retards auditory cortical development. *Science* 300, 498–502.
- Chapleau, C. a, Calfa, G.D., Lane, M.C., Albertson, A.J., Larimore, J.L., Kudo, S., Armstrong, D.L., Percy, A.K., and Pozzo-Miller, L. (2009). Dendritic spine pathologies in hippocampal pyramidal neurons from Rett syndrome brain and after expression of Rett-associated MECP2 mutations. *Neurobiology of Disease* 35, 219–233.
- Chapman, B. (2000). Necessity for Afferent Activity to Maintain Eye-Specific Segregation in Ferret Lateral Geniculate Nucleus. *Science* 287, 2479–2482.
- Chattopadhyaya, B., Di Cristo, G., Higashiyama, H., Knott, G.W., Kuhlman, S.J., Welker, E., and Huang, Z.J. (2004). Experience and activity-dependent maturation of perisomatic GABAergic innervation in primary visual cortex during a postnatal critical period. *The Journal of Neuroscience* 24, 9598–9611.
- Chen, J.L., and Nedivi, E. (2010). Neuronal structural remodeling: is it all about access? *Current Opinion in Neurobiology* 20, 557–562.
- Chen, J.L., Lin, W.C., Cha, J.W., So, P.T., Kubota, Y., and Nedivi, E. (2011). Structural basis for the role of inhibition in facilitating adult brain plasticity. *Nature Neuroscience* 14, 587–594.
- Chih, B., Afridi, S.K., Clark, L., and Scheiffele, P. (2004). Disorder-associated mutations lead to functional inactivation of neuroligins. *Human Molecular Genetics* 13, 1471–1477.
- Chih, B., Engelman, H., and Scheiffele, P. (2005). Control of excitatory and inhibitory synapse formation by neuroligins. *Science* 307, 1324–1328.
- Chubykin, A. a, Atasoy, D., Etherton, M.R., Brose, N., Kavalali, E.T., Gibson, J.R., and Südhof, T.C. (2007). Activity-dependent validation of excitatory versus inhibitory synapses by neuroligin-1 versus neuroligin-2. *Neuron* 54, 919–931.
- Chubykin, A. a, Liu, X., Comoletti, D., Tsigelny, I., Taylor, P., and Südhof, T.C. (2005). Dissection of synapse induction by neuroligins: effect of a neuroligin mutation associated with autism. *The Journal of Biological Chemistry* 280, 22365–22374.

- Collins, A.L., Ma, D., Whitehead, P.L., Martin, E.R., Wright, H.H., Abramson, R.K., Hussman, J.P., Haines, J.L., Cuccaro, M.L., Gilbert, J.R., et al. (2006). Investigation of autism and GABA receptor subunit genes in multiple ethnic groups. *Neurogenetics* 7, 167–174.
- Comoletti, D., De Jaco, A., Jennings, L.L., Flynn, R.E., Gaietta, G., Tsigelny, I., Ellisman, M.H., and Taylor, P. (2004). The Arg451Cys-neuroigin-3 mutation associated with autism reveals a defect in protein processing. *The Journal of Neuroscience* 24, 4889–4893.
- Correia, C.T., Coutinho, A.M., Sequeira, A.F., Sousa, I.G., Venda, L., Almeida, J.P., Abreu, R.L., Lobo, C., Miguel, T.S., Conroy, J., et al. (2010). Increased BDNF levels and NTRK2 gene association suggest a disruption of BDNF/TrkB signaling in autism. *Genes, Brain, and Behavior* 9, 841–848.
- Coskun, M.A., Varghese, L., Reddoch, S., Castillo, E.M., Pearson, D.A., Loveland, K.A., Papanicolaou, A.C., and Sheth, B.R. (2009). How somatic cortical maps differ in autistic and typical brains. *Neuroreport* 20, 175–179.
- Crawley, J.N. (2004). Designing mouse behavioral tasks relevant to autistic-like behaviors. *Mental Retardation and Developmental Disabilities Research Reviews* 10, 248–258.
- Crawley, J.N. (2012). Translational animal models of autism and neurodevelopmental disorders. *Clinical Research* 293–305.
- Cruikshank, S. J., Lewis, T. J., and Connors, B.W. (2007). Synaptic basis for intense thalamocortical activation of feedforward inhibitory cells in neocortex. *Nature Neuroscience* 10, 462–468.
- Curia, G., Papouin, T., Séguéla, P., and Avoli, M. (2009). Downregulation of tonic GABAergic inhibition in a mouse model of fragile X syndrome. *Cerebral Cortex* 19, 1515–1520.
- Dakin, S., and Frith, U. (2005). Vagaries of visual perception in autism. *Neuron* 48, 497–507.
- Dalva, M.B., McClelland, A.C., and Kayser, M.S. (2007). Cell adhesion molecules: signalling functions at the synapse. *Nature Reviews. Neuroscience* 8, 206–220.
- Dani, V.S., and Nelson, S.B. (2009). Intact long-term potentiation but reduced connectivity between neocortical layer 5 pyramidal neurons in a mouse model of Rett syndrome. *The Journal of Neuroscience* 29, 11263–11270.
- Dani, V.S., Chang, Q., Maffei, A., Turrigiano, G.G., Jaenisch, R., and Nelson, S.B. (2005). Reduced cortical activity due to a shift in the balance between excitation and inhibition in a mouse model of Rett syndrome. *Proceedings of the National Academy of Sciences of the United States of America* 102, 12560–12565.
- Daoud, H., Bonnet-Brilhault, F., Védrine, S., Demattéi, M.-V., Vourc’h, P., Bayou, N., Andres, C.R., Barthélémy, C., Laumonnier, F., and Briault, S. (2009). Autism and nonsyndromic mental retardation associated with a de novo mutation in the NLGN4X gene promoter causing an increased expression level. *Biological Psychiatry* 66, 906–910.
- Daw, N.W., Fox, K., Sato, H., and Czepita, D. (1992). Critical period for monocular deprivation in the cat visual cortex. *Journal of Neurophysiology* 67, 197–202.

- De Jaco, A., Comoletti, D., Kovarik, Z., Gaietta, G., Radic, Z., Lockridge, O., Ellisman, M.H., and Taylor, P. (2006). A mutation linked with autism reveals a common mechanism of endoplasmic reticulum retention for the alpha,beta-hydrolase fold protein family. *The Journal of Biological Chemistry* *281*, 9667–9676.
- De Jaco, A., Lin, M.Z., Dubi, N., Comoletti, D., Miller, M., Camp, S., Ellisman, M., Butko, M.T., Tsien, R.Y., and Taylor, P. (2010). Neuroligin trafficking deficiencies arising from mutations in the {alpha}/{beta}-hydrolase fold protein family. *The Journal of Biological Chemistry* *285*, 28674 – 28682.
- De Villers-Sidani, E., Simpson, K.L., Lu, Y.-F., Lin, R.C.S., and Merzenich, M.M. (2008). Manipulating critical period closure across different sectors of the primary auditory cortex. *Nature Neuroscience* *11*, 957–965.
- Dean, C., Scholl, F.G., Choih, J., DeMaria, S., Berger, J., Isacoff, E., and Scheiffele, P. (2003). Neurexin mediates the assembly of presynaptic terminals. *Nature Neuroscience* *6*, 708–716.
- Defelipe, J., and Farinas, I. (1992). The pyramidal neuron of the cerebral cortex: morphological and chemical characteristics of the synaptic inputs. *Progress in Neurobiology* *39*, 563–607.
- Del Rio, J., De Lecea, L., Ferrer, I., and Soriano, E. (1994). The development of parvalbumin-immunoreactivity in the neocortex of the mouse. *Brain Research. Developmental Brain Research* *81*, 247–259.
- Deruelle, C., Rondan, C., Gepner, B., and Tardif, C. (2004). Spatial frequency and face processing in children with autism and Asperger syndrome. *Journal of Autism and Developmental Disorders* *34*, 199–210.
- Deruelle, C., Rondan, C., Salle-Collemiche, X., Bastard-Rosset, D., and Da Fonséca, D. (2008). Attention to low- and high-spatial frequencies in categorizing facial identities, emotions and gender in children with autism. *Brain and Cognition* *66*, 115–123.
- Desai, N.S., Casimiro, T.M., Gruber, S.M., and Vanderklish, P.W. (2006). Early postnatal plasticity in neocortex of Fmr1 knockout mice. *Journal of Neurophysiology* *96*, 1734–1745.
- Dhossche, D., Applegate, H., Abraham, A., Maertens, P., Bland, L., Bencsath, A., and Martinez, J. (2002). Elevated plasma gamma-aminobutyric acid (GABA) levels in autistic youngsters: stimulus for a GABA hypothesis of autism. *Med Sci Monit* *8*, PR1–6.
- Dhossche, D.M., Song, Y., and Liu, Y. (2005). Is there a connection between autism, Prader-Willi syndrome, catatonia, and GABA? *International Review* *71*, 189–216.
- Di Cristo, G., Chattopadhyaya, B., Kuhlman, S.J., Fu, Y., Bélanger, M.-C., Wu, C.Z., Rutishauser, U., Maffei, L., and Huang, Z.J. (2007). Activity-dependent PSA expression regulates inhibitory maturation and onset of critical period plasticity. *Nature Neuroscience* *10*, 1569–1577.
- Dindot, S. V, Antalffy, B.A., Bhattacharjee, M.B., and Beaudet, A.L. (2008). The Angelman syndrome ubiquitin ligase localizes to the synapse and nucleus, and maternal deficiency results in abnormal dendritic spine morphology. *Human Molecular Genetics* *17*, 111–118.

- Dölen, G., Osterweil, E., Rao, B.S.S., Smith, G.B., Auerbach, B.D., Chattarji, S., and Bear, M.F. (2007). Correction of fragile X syndrome in mice. *Neuron* *56*, 955–962.
- Doupe, A.J., and Kuhl, P.K. (1999). Birdsong and human speech: common themes and mechanisms. *Annual Review of Neuroscience* *22*, 567–631.
- Dräger, U.C. (1975). Receptive fields of single cells and topography in mouse visual cortex. *The Journal of Comparative Neurology* *160*, 269–290.
- Drager, U.C. (1978). Observations on monocular deprivation in mice. *Journal of Neurophysiology* *41*, 28–42.
- Durand, S., Patrizi, A., Quast, K.B., Hachigian, L., Pavlyuk, R., Saxena, A., Carninci, P., Hensch, T.K., and Fagiolini, M. (2012). NMDA receptor regulation prevents regression of visual cortical function in the absence of *Mecp2*. *Neuron* *76*, 1078–1090.
- Etherton, M., Földy, C., Sharma, M., Tabuchi, K., Liu, X., Shamloo, M., Malenka, R.C., and Sudhof, T.C. (2011). Autism-linked neuroligin-3 R451C mutation differentially alters hippocampal and cortical synaptic function. *Proceedings of the National Academy of Sciences of the United States of America* *108*, 13764–13769.
- European Chromosome 16 Tuberous Sclerosis Consortium. (1993). Identification and characterization of the tuberous sclerosis gene on chromosome 16. *Cell* *75*, 1305–1315.
- Fagiolini, M., and Hensch, T.K. (2000). Inhibitory threshold for critical-period activation in primary visual cortex. *Nature* *404*, 183–186.
- Fagiolini, M., Fritschy, J., Low, K., Mohler, H., Rudolph, U., and Hensch, T. (2004). Specific GABAA Circuits for Visual Cortical Plasticity. *Science* *303*, 1681–1683.
- Fagiolini, M., Pizzorusso, T., Berardi, N., Domenici, L., and Maffei, L. (1994). Functional Postnatal Development of the Rat Primary Visual Cortex and the Role of Visual Experience : Dark Rearing and Monocular Deprivation. *Vision Research* *34*, 709–720.
- Fatemi, S., Reutiman, T., Folsom, T.D., and Thuras, P.D. (2009a). GABA A Receptor Downregulation in Brains of Subjects with Autism. *Journal of Autism and Developmental Disorders* *39*, 223–230.
- Fatemi, S.H., Folsom, T.D., Reutiman, T.J., and Thuras, P.D. (2009b). Expression of GABA(B) receptors is altered in brains of subjects with autism. *Cerebellum* *8*, 64–69.
- Fatemi, S.H., Halt, A.R., Stary, J.M., Kanodia, R., Schulz, S.C., and Realmuto, G.R. (2002). Glutamic Acid Decarboxylase 65 and 67 kDa Proteins are Reduced in Autistic Parietal and Cerebellar Cortices. *Biological Psychiatry* *52*.
- Fatemi, S.H., Reutiman, T.J., Folsom, T.D., Rooney, R.J., Patel, D.H., and Thuras, P.D. (2010). mRNA and protein levels for GABAAalpha4, alpha5, beta1 and GABABR1 receptors are altered in brains from subjects with autism. *Journal of Autism and Developmental Disorders* *40*, 743–750.

- Ferri, R., Elia, M., Agarwal, N., Lanuzza, B., Musumeci, S.A., and Pennisi, G. (2003). The mismatch negativity and the P3a components of the auditory event-related potentials in autistic low-functioning subjects. *Clinical Neurophysiology* *114*, 1671–1680.
- Fox, K. (1992). A Critical Period for Experience-dependent Barrel Cortex Synaptic Plasticity in Rat. *The Journal of Neuroscience* *12*, 1826–1838.
- Fox, M.A., and Sanes, J.R. (2007). Synaptotagmin I and II Are Present in Distinct Subsets of Central Synapses. *The Journal of Comparative Neurology* *503*, 280–296.
- Galarreta, M., and Hestrin, S. (1999). A network of fast-spiking cells in the neocortex connected by electrical synapses. *Nature* *402*, 72–75.
- Gatto, C.L., Broadie, K., and Cline, H. (2010). Genetic controls balancing excitatory and inhibitory synaptogenesis in neurodevelopmental disorder models. *Frontiers in Synaptic Neuroscience* *2*, 1–19.
- Gauthier, J., Bonnel, A., St-Onge, J., Karemera, L., Laurent, S., Mottron, L., Fombonne, E., Joober, R., and Rouleau, G.A. (2005). NLGN3/NLGN4 gene mutations are not responsible for autism in the Quebec population. *American Journal of Medical Genetics. Part B, Neuropsychiatric Genetics* *132B*, 74–75.
- Geschwind, D.H. (2008). Essay Autism : Many Genes , Common Pathways ? *Cell* *135*, 391–395.
- Gibson, J.R., Bartley, A.F., Hays, S.A., and Huber, K.M. (2009a). Imbalance of Neocortical Excitation and Inhibition and Altered UP States Reflect Network Hyperexcitability in the Mouse Model of Fragile X Syndrome. *Journal of Neurophysiology* *100*, 2615–2626.
- Gibson, J.R., Huber, K.M., and Südhof, T.C. (2009b). Neuroligin-2 deletion selectively decreases inhibitory synaptic transmission originating from fast-spiking but not from somatostatin-positive interneurons. *The Journal of Neuroscience* *29*, 13883–13897.
- Gilbert, M., Smith, J., Roskams, A.J., and Auld, V.J. (2001). Neuroligin 3 is a vertebrate gliotactin expressed in the olfactory ensheathing glia, a growth-promoting class of macroglia. *Glia* *34*, 151–164.
- Gillberg, C., and Billstedt, E. (2000). Autism and Asperger syndrome: coexistence with other clinical disorders. *Acta Psychiatrica Scandinavica* *102*, 321–330.
- Glessner, J.T., Wang, K., Cai, G., Korvatska, O., Kim, C.E., Wood, S., Zhang, H., Estes, A., Brune, C.W., Bradfield, J.P., et al. (2009). Autism genome-wide copy number variation reveals ubiquitin and neuronal genes. *Nature* *459*, 569–573.
- Godement, P., Salaün, J., and Imbert, M. (1984). Prenatal and postnatal development of retinogeniculate and retinocollicular projections in the mouse. *The Journal of Comparative Neurology* *230*, 552–575.
- Gogolla, N., Caroni, P., Luthi, A., and Herry, C. (2009a). Perineuronal Nets Protect Fear Memories from Erasure. *Science* *325*, 1258–1261.

- Gogolla, N., LeBlanc, J.J., Quast, K.B., Südhof, T.C., Fagiolini, M., and Hensch, T.K. (2009b). Common circuit defect of excitatory-inhibitory balance in mouse models of autism. *Journal of Neurodevelopmental Disorders* *1*, 172–181.
- Gorba, T., Klostermann, O., and Wahle, P. (1999). Development of neuronal activity and activity-dependent expression of brain-derived neurotrophic factor mRNA in organotypic cultures of rat visual cortex. *Cerebral Cortex* *9*, 864–877.
- Gordon, J.A., and Stryker, M.P. (1996). Experience-dependent plasticity of binocular responses in the primary visual cortex of the mouse. *The Journal of Neuroscience* *16*, 3274–3286.
- Graf, E.R., Zhang, X., Jin, S.-X., Linhoff, M.W., and Craig, A.M. (2004). Neurexins induce differentiation of GABA and glutamate postsynaptic specializations via neuroligins. *Cell* *119*, 1013–1026.
- Grandin, T. (1992). An Inside View of Autism. In *High-Functioning Individuals with Autism* E. Schopler and G. Mesibov (New York, NY: Plenum Press), pp. 105-126.
- Grandin, T. (2009). Visual abilities and sensory differences in a person with autism. *Biological Psychiatry* *65*, 15–16.
- Guptill, J., Booker, A., Gibbs, T.T., Kemper, T.L., Bauman, M.L., and Blatt, G.J. (2007). [ 3 H ] - Flunitrazepam-labeled Benzodiazepine Binding Sites in the Hippocampal Formation in Autism : A Multiple Concentration Autoradiographic Study. *Journal of Autism and Developmental Disorders* *37*, 911–920.
- Haider, B., Häusser, M., and Carandini, M. (2013). Inhibition dominates sensory responses in the awake cortex. *Nature* *493*, 97–100.
- Hanover, J.L., Huang, Z.J., Tonegawa, S., and Stryker, M.P. (1999). Brain-derived neurotrophic factor overexpression induces precocious critical period in mouse visual cortex. *The Journal of Neuroscience* *19*, RC40.
- Happé, F., and Frith, U. (2006). The weak coherence account: detail-focused cognitive style in autism spectrum disorders. *Journal of Autism and Developmental Disorders* *36*, 5–25.
- Harauzov, A., Spolidoro, M., DiCristo, G., De Pasquale, R., Cancedda, L., Pizzorusso, T., Viegi, A., Berardi, N., and Maffei, L. (2010). Reducing intracortical inhibition in the adult visual cortex promotes ocular dominance plasticity. *The Journal of Neuroscience* *30*, 361–371.
- Harlow, H., Dodsworth, R.O., and Harlow, M.K. (1965). Total social isolation in monkeys. *Proceedings of the National Academy of Sciences of the United States of America* *54*, 90–97.
- Harrison, R. V, Gordon, K. a, and Mount, R.J. (2005). Is there a critical period for cochlear implantation in congenitally deaf children? Analyses of hearing and speech perception performance after implantation. *Developmental Psychobiology* *46*, 252–261.
- Hartman, K.N., Pal, S.K., Burrone, J., and Murthy, V.N. (2006). Activity-dependent regulation of inhibitory synaptic transmission in hippocampal neurons. *Nature Neuroscience* *9*, 642–649.

- Hasenstaub, A., Shu, Y., Haider, B., Kraushaar, U., Duque, A., and McCormick, D.A. (2005). Inhibitory postsynaptic potentials carry synchronized frequency information in active cortical networks. *Neuron* 47, 423–435.
- Haverkamp, S., and Wassle, H. (2000). Immunocytochemical Analysis of the Mouse Retina. *The Journal of Comparative Neurology* 424, 1–23.
- He, H., Hodos, W., and Quinlan, E.M. (2006). Visual Deprivation Reactivates Rapid Ocular Dominance Plasticity in Adult Visual Cortex. *The Journal of Neuroscience* 26, 2951–2955.
- Heimel, J.A., Saiepour, M.H., Chakravarthy, S., Hermans, J.M., and Levelt, C.N. (2010). Contrast gain control and cortical TrkB signaling shape visual acuity. *Nature Neuroscience* 13, 642–648.
- Heller, E.A., Zhang, W., Selimi, F., Earnheart, J.C., Ślimak, M.A., Santos-Torres, J., Ibañez-Tallon, I., Aoki, C., Chait, B.T., and Heintz, N. (2012). The biochemical anatomy of cortical inhibitory synapses. *PLoS One* 7, e39572.
- Hensch, T.K. (2004). Critical period regulation. *Annual Review of Neuroscience* 27, 549–579.
- Hensch, T.K. (2005). Critical period plasticity in local cortical circuits. *Nature Reviews. Neuroscience* 6, 877–888.
- Hensch, T.K., Fagiolini, M., Mataga, N., Stryker, M.P., Baekkeskov, S., and Kash, S. (1998). Local GABA Circuit Control of Experience-Dependent Plasticity in Developing Visual Cortex. *Science* 282, 1504–1508.
- Hinton, V.J., Brown, W.T., Wisniewski, K., and Rudelli, R.D. (1991). Analysis of neocortex in three males with the fragile X syndrome. *American Journal of Medical Genetics* 41, 289–294.
- Holmgren, C., Harkany, T., Svennenfors, B., and Zilberter, Y. (2003). Pyramidal cell communication within local networks in layer 2/3 of rat neocortex. *The Journal of Physiology* 551, 139–153.
- Hong, E.J., McCord, A.E., and Greenberg, M.E. (2008). A biological function for the neuronal activity-dependent component of Bdnf transcription in the development of cortical inhibition. *Neuron* 60, 610–624.
- Hong, Y.K., and Chen, C. (2011). Wiring and rewiring of the retinogeniculate synapse. *Current Opinion in Neurobiology* 21, 228–237.
- Hong, Y.K., Kim, I.-J., and Sanes, J.R. (2011). Stereotyped axonal arbors of retinal ganglion cell subsets in the mouse superior colliculus. *The Journal of Comparative Neurology* 519, 1691–1711.
- Hoon, M., Bauer, G., Fritschy, J.-M., Moser, T., Falkenburger, B.H., and Varoqueaux, F. (2009). Neuroligin 2 controls the maturation of GABAergic synapses and information processing in the retina. *The Journal of Neuroscience* 29, 8039–8050.
- Hoon, M., Soykan, T., Falkenburger, B., Hammer, M., Patrizi, A., Schmidt, K.-F., Sassoè-Pognetto, M., Löwel, S., Moser, T., Taschenberger, H., et al. (2011). Neuroligin-4 is localized to glycinergic



- postsynapses and regulates inhibition in the retina. *Proceedings of the National Academy of Sciences of the United States of America* *108*, 3053–3058.
- Huang, Z.J., Kirkwood, a, Pizzorusso, T., Porciatti, V., Morales, B., Bear, M.F., Maffei, L., and Tonegawa, S. (1999). BDNF regulates the maturation of inhibition and the critical period of plasticity in mouse visual cortex. *Cell* *98*, 739–755.
- Hubel, D.H., and Wiesel, T.N. (1962) Receptive fields, binocular interaction and functional architecture in the cat's visual cortex. *J Physiol* *160*, 106–154.
- Hubel, D., and Wiesel, T.N. (1970). The period of susceptibility to the physiological effects of unilateral eye closure in kittens. *Journal of Physiology* *206*, 419–436.
- Hubel, D.H., and Wiesel, T.N. (1998). Early Exploration of the Visual Cortex. *Neuron* *20*, 401–412.
- Hübener, M. (2003). Mouse visual cortex. *Current Opinion in Neurobiology* *13*, 413–420.
- Hutsler, J.J., and Zhang, H. (2010). Increased dendritic spine densities on cortical projection neurons in autism spectrum disorders. *Brain Research* *1309*, 83–94.
- Huttenlocher, P.R. (1990). Morphometric study of human cerebral cortex development. *Neuropsychologia* *28*, 517–527.
- Ichtchenko, K., Nguyen, T., and Südhof, T.C. (1996). Structures, alternative splicing, and neuroligin binding of multiple neuroligins. *The Journal of Biological Chemistry* *271*, 2676–2682.
- Irwin, S. a, Galvez, R., and Greenough, W.T. (2000). Dendritic spine structural anomalies in fragile-X mental retardation syndrome. *Cerebral Cortex* *10*, 1038–1044.
- Jamain, S., Quach, H., Betancur, C., Rastam, M., Gillberg, I.C., Söderström, H., Giros, B., Leboyer, M., Gillberg, C., Bourgeron, T., et al. (2003). Mutations of the X-linked genes encoding neuroligins NLGN3 and NLGN4 are associated with autism. *Nature Genetics* *34*, 27–29.
- Jeste, S.S., Hirsch, S., Vogel-Farley, V., Norona, A., Navalta, M.-C., Gregas, M.C., Prabhu, S.P., Sahin, M., and Nelson, C.A. (2012). Atypical Face Processing in Children With Tuberous Sclerosis Complex. *Journal of Child Neurology* *00*, 1-8.
- Jeste, S.S., and Nelson, C.A. (2009). Event related potentials in the understanding of autism spectrum disorders: an analytical review. *Journal of Autism and Developmental Disorders* *39*, 495–510.
- Jiao, Y., Zhang, C., Yanagawa, Y., and Sun, Q.-Q. (2006). Major effects of sensory experiences on the neocortical inhibitory circuits. *The Journal of Neuroscience* *26*, 8691–8701.
- Jun-Yu, X., Qiang-Qiang, X., and Jun, X. (2012). A review on the current neuroligin mouse models. *Acta Physiologica Sinica* *64*, 550–562.
- Kanner, L. (1943). Autistic disturbances of affective contact. *Pathology* *217–250*.

- Katagiri, H., Fagiolini, M., and Hensch, T.K. (2007). Optimization of Somatic Inhibition at Critical Period Onset in Mouse Visual Cortex. *Neuron* 53, 805–812.
- KatoH-Semba, R., Semba, R., Takeuchi, I.K., and Kato, K. (1998). Age-related changes in levels of brain-derived neurotrophic factor in selected brain regions of rats, normal mice and senescence-accelerated mice: a comparison to those of nerve growth factor and neurotrophin-3. *Neuroscience Research* 31, 227–234.
- Katz, L.C, and Shatz, C.J. (1996). Synaptic activity and the construction of cortical circuits. *Science* 274, 1133–1138.
- Kawaguchi, Y., and Kubota, Y. (1997). GABAergic cell subtypes and their synaptic connections in rat frontal cortex. *Cerebral Cortex* 7, 476–486.
- Kim, I.-J., Zhang, Y., Meister, M., and Sanes, J.R. (2010). Laminar restriction of retinal ganglion cell dendrites and axons: subtype-specific developmental patterns revealed with transgenic markers. *The Journal of Neuroscience* 30, 1452–1462.
- Kim, J.H., and Richardson, R. (2007). A developmental dissociation in reinstatement of an extinguished fear response in rats. *Neurobiology of Learning and Memory* 88, 48–57.
- Kishino, T., Lalande, M., and Wagstaff, J. (1997). UBE3A/E6-AP mutations cause Angleman syndrome. *Nature Genetics* 15, 70–73.
- Klausberger, T. (2009). GABAergic interneurons targeting dendrites of pyramidal cells in the CA1 area of the hippocampus. *The European Journal of Neuroscience* 30, 947–957.
- Klausberger, T., Roberts, J.D.B., and Somogyi, P. (2002). Cell type- and input-specific differences in the number and subtypes of synaptic GABA(A) receptors in the hippocampus. *The Journal of Neuroscience* 22, 2513–2521.
- Klin, A., Lin, D.J., Gorrindo, P., Ramsay, G., and Jones, W. (2009). Two-year-olds with autism orient to non-social contingencies rather than biological motion. *Nature* 459, 257–261.
- Knudsen, E.I., Zheng, W., and DeBello, W.M. (2000). Traces of learning in the auditory localization pathway. *Proceedings of the National Academy of Sciences of the United States of America* 97, 11815–11820.
- Koehnke, J., Katsamba, P.S., Ahlsen, G., Bahna, F., Vendome, J., Honig, B., Shapiro, L., and Jin, X. (2010). Splice Form Dependence of b-Neurexin / Neuroligin Binding Interactions. *Neuron* 67, 61–74.
- Kohara, K., Yasuda, H., Huang, Y., Adachi, N., Sohya, K., and Tsumoto, T. (2007). A local reduction in cortical GABAergic synapses after a loss of endogenous brain-derived neurotrophic factor, as revealed by single-cell gene knock-out method. *The Journal of Neuroscience* 27, 7234–7244.
- Laumonnier, F., Bonnet-Brilhault, F., Gomot, M., Blanc, R., David, A., Moizard, M.-P., Raynaud, M., Ronce, N., Lemonnier, E., Calvas, P., et al. (2004). X-linked mental retardation and autism are associated with a mutation in the NLGN4 gene, a member of the neuroligin family. *American Journal of Human Genetics* 74, 552–557.

- Lawson-Yuen, A., Saldivar, J.-S., Sommer, S., and Picker, J. (2008). Familial deletion within NLGN4 associated with autism and Tourette syndrome. *European Journal of Human Genetics* *16*, 614–618.
- Lazarus, M.S., and Huang, Z.J. (2011). Distinct maturation profiles of perisomatic and dendritic targeting GABAergic interneurons in the mouse primary visual cortex during the critical period of ocular dominance plasticity. *Journal of Neurophysiology* *106*, 775–787.
- Le Magueresse, C., and Monyer, H. (2013). GABAergic Interneurons Shape the Functional Maturation of the Cortex. *Neuron* *77*, 388–405.
- LeBlanc, J.J., and Fagiolini, M. (2011). Autism: a “critical period” disorder? *Neural Plasticity* *2011*, 1–17.
- Lee, S., Kwan, A.C., Zhang, S., Phoumthippavong, V., Flannery, J.G., Masmanidis, S.C., Taniguchi, H., Huang, Z.J., Zhang, F., Boyden, E.S., et al. (2012). Activation of specific interneurons improves V1 feature selectivity and visual perception. *Nature* *488*, 379–83.
- Lehmann, K., Schmidt, K.-F., and Löwel, S. (2012). Vision and visual plasticity in ageing mice. *Restorative Neurology and Neuroscience* *30*, 161–178.
- LeVay, S., Stryker, M.P., and Shatz, C.J. (1978). Ocular dominance columns and their development in layer IV of the cat’s visual cortex: a quantitative study. *The Journal of Comparative Neurology* *179*, 223–244.
- LeVay, S., Wiesel, T.N., and Hubel, D.H. (1980). The development of ocular dominance columns in normal and visually deprived monkeys. *The Journal of Comparative Neurology* *191*, 1–51.
- Levelt, C.N., and Hübener, M. (2012). Critical-period plasticity in the visual cortex. *Annual Review of Neuroscience* *35*, 309–330.
- Levinson, J.N., and El-Husseini, A. (2005). New players tip the scales in the balance between excitatory and inhibitory synapses. *Molecular Pain* *1*, 1–12.
- Levinson, J.N., Li, R., Kang, R., Moukhles, H., El-Husseini, a, and Bamji, S.X. (2010). Postsynaptic scaffolding molecules modulate the localization of neuroligins. *Neuroscience* *165*, 782–793.
- Lewis, T.L., and Maurer, D. (2009). Effects of early pattern deprivation on visual development. *Optometry and Vision Science* *86*, 640–646.
- Li, J., Pelletier, M.R., Perez Velazquez, J.-L., and Carlen, P.L. (2002). Reduced cortical synaptic plasticity and GluR1 expression associated with fragile X mental retardation protein deficiency. *Molecular and Cellular Neurosciences* *19*, 138–151.
- Lidierth, M. (2009). sigTOOL: A MATLAB-based environment for sharing laboratory-developed software to analyze biological signals. *Journal of Neuroscience Methods* *178*, 188–196.
- Livet, J., Weissman, T.A., Kang, H., Draft, R.W., Lu, J., Bennis, R.A., Sanes, J.R., and Lichtman, J.W. (2007). Transgenic strategies for combinatorial expression of fluorescent proteins in the nervous system. *Nature* *450*, 56–62.

- Loos, H. Van Der, and Woolsey, T.A. (1973). Somatosensory Cortex : Structural Alterations following Early Injury to Sense Organs. *Science* 179, 395–398.
- Maffei, A., and Fontanini, A. (2009). Network homeostasis: a matter of coordination. *Current Opinion in Neurobiology* 19, 168–173.
- Magenis, R.E., Brown, M.G., Lacy, D.A., Budden, S., and LaFranchi, S. (1987). Is angelman syndrome an alternate result of del(15)(q11q13)? *American Journal of Medical Genetics* 28, 829–838.
- Marco, E.J., Hinkley, L.B.N., Hill, S.S., and Nagarajan, S.S. (2011). Sensory processing in autism: a review of neurophysiologic findings. *Pediatric Research* 69, 48R–54R.
- Markram, H., Rinaldi, T., and Markram, K. (2007). The intense world syndrome--an alternative hypothesis for autism. *Frontiers in Neuroscience* 1, 77–96.
- Markram, H., Toledo-Rodriguez, M., Wang, Y., Gupta, A., Silberberg, G., and Wu, C. (2004). Interneurons of the neocortical inhibitory system. *Nature Reviews. Neuroscience* 5, 793–807.
- Martineau, J., Garreau, B., Barthelemy, C., and Lelord, G. (1984). Evoked potentials and P300 during sensory conditioning in autistic children. *Annals of the New York Academy of Sciences* 425, 362–369.
- Marty, S., Wehrli, R., and Sotelo, C. (2000). Neuronal activity and brain-derived neurotrophic factor regulate the density of inhibitory synapses in organotypic slice cultures of postnatal hippocampus. *The Journal of Neuroscience* 20, 8087–8095.
- Mataga, N., Nagai, N., and Hensch, T.K. (2002). Permissive proteolytic activity for visual cortical plasticity. *Proceedings of the National Academy of Sciences of the United States of America* 99, 7717–7721.
- Mataga, N., Mizuguchi, Y., and Hensch, T.K. (2004). Experience-dependent pruning of dendritic spines in visual cortex by tissue plasminogen activator. *Neuron* 44, 1031–1041.
- Matsuura, T., Sutcliffe, J., Fang, P., Galjaard, R.-J., Jiang, Y., Benton, C., Rommens, J., and Beaudet, A. (1997). De novo truncating mutations in E6-AP ubiquitin-protein ligase gene (UBE3A) in Angelman syndrome. *Nature Genetics* 15, 74–77.
- Maya Vetencourt, J.F., Sale, A., Viegi, A., Baroncelli, L., De Pasquale, R., O’Leary, O.F., Castrén, E., and Maffei, L. (2008). The antidepressant fluoxetine restores plasticity in the adult visual cortex. *Science* 320, 385–388.
- McGee, A.W., Yang, Y., Fischer, Q.S., Daw, N.W., and Strittmatter, S.M. (2005). Experience-driven plasticity of visual cortex limited by myelin and Nogo receptor. *Science* 309, 2222–2226.
- Medrihan, L., Tantalaki, E., Aramuni, G., Sargsyan, V., Dudanova, I., Missler, M., and Zhang, W. (2008). Early defects of GABAergic synapses in the brain stem of a MeCP2 mouse model of Rett syndrome. *Journal of Neurophysiology* 99, 112–121.

- Meikle, L., Talos, D.M., Onda, H., Pollizzi, K., Rotenberg, A., Sahin, M., Jensen, F.E., and Kwiatkowski, D.J. (2007). A mouse model of tuberous sclerosis: neuronal loss of Tsc1 causes dysplastic and ectopic neurons, reduced myelination, seizure activity, and limited survival. *The Journal of Neuroscience* 27, 5546–5558.
- Mitchell, D.E., and MacKinnon, S. (2002). The present and potential impact of research on animal models for clinical treatment of stimulus deprivation amblyopia. *Clinical & Experimental Optometry* 85, 5–18.
- Mitchell, J.F., Sundberg, K. a, and Reynolds, J.H. (2007). Differential attention-dependent response modulation across cell classes in macaque visual area V4. *Neuron* 55, 131–141.
- Miyazaki, K., Narita, N., Sakuta, R., Miyahara, T., Naruse, H., Okado, N., and Narita, M. (2004). Serum neurotrophin concentrations in autism and mental retardation: a pilot study. *Brain & Development* 26, 292–295.
- Miyazaki, M., Fujii, E., Saijo, T., Mori, K., Hashimoto, T., Kagami, S., and Kuroda, Y. (2007). Short-latency somatosensory evoked potentials in infantile autism: evidence of hyperactivity in the right primary somatosensory area. *Developmental Medicine and Child Neurology* 49, 13–17.
- Moretti, P., Levenson, J.M., Battaglia, F., Atkinson, R., Teague, R., Antalffy, B., Armstrong, D., Arancio, O., Sweatt, J.D., and Zoghbi, H.Y. (2006). Learning and memory and synaptic plasticity are impaired in a mouse model of Rett syndrome. *The Journal of Neuroscience* 26, 319–327.
- Morishita, H., and Hensch, T.K. (2008). Critical period revisited: impact on vision. *Current Opinion in Neurobiology* 18, 101–107.
- Morishita, H., Miwa, J.M., Heintz, N., and Hensch, T.K. (2010). Lynx1, a cholinergic brake, limits plasticity in adult visual cortex. *Science* 330, 1238–1240.
- Moser, S.J., Weber, P., and Lütsch, J. (2007). Rett syndrome: clinical and electrophysiologic aspects. *Pediatric Neurology* 36, 95–100.
- Mottron, L., Dawson, M., Soulières, I., Hubert, B., and Burack, J. (2006). Enhanced perceptual functioning in autism: an update, and eight principles of autistic perception. *Journal of Autism and Developmental Disorders* 36, 27–43.
- Nam, C.I., and Chen, L. (2005). Postsynaptic assembly induced by neurexin-neuroigin interaction and neurotransmitter. *Proceedings of the National Academy of Sciences of the United States of America* 102, 6137–6142.
- Nelson, C. a, Zeanah, C.H., Fox, N. a, Marshall, P.J., Smyke, A.T., and Guthrie, D. (2007). Cognitive recovery in socially deprived young children: the Bucharest Early Intervention Project. *Science* 318, 1937–1940.
- Niell, C.M., and Stryker, M.P. (2008). Highly selective receptive fields in mouse visual cortex. *The Journal of Neuroscience* 28, 7520–7536.

- Nishimura, K., Nakamura, K., Anitha, a, Yamada, K., Tsujii, M., Iwayama, Y., Hattori, E., Toyota, T., Takei, N., Miyachi, T., et al. (2007). Genetic analyses of the brain-derived neurotrophic factor (BDNF) gene in autism. *Biochemical and Biophysical Research Communications* 356, 200–206.
- Nosyreva, E.D., and Huber, K.M. (2006). Metabotropic receptor-dependent long-term depression persists in the absence of protein synthesis in the mouse model of fragile X syndrome. *Journal of Neurophysiology* 95, 3291–3295.
- Nusser, Z., Sieghart, W., Benke, D., Fritschy, J. M. and Somogyi, P. (1996). Differential synaptic localization of two major  $\gamma$ -aminobutyric acid type A receptor  $\alpha$  subunits on hippocampal pyramidal cells. *Proc. Natl Acad. Sci.* 93, 11939–11944.
- Oram Cardy, J.E., Flagg, E.J., Roberts, W., and Roberts, T.P.L. (2008). Auditory evoked fields predict language ability and impairment in children. *International Journal of Psychophysiology* 68, 170–175.
- Oray, S., Majewska, A., and Sur, M. (2004). Dendritic spine dynamics are regulated by monocular deprivation and extracellular matrix degradation. *Neuron* 44, 1021–1030.
- Packer, A.M., and Yuste, R. (2011). Dense, unspecific connectivity of neocortical parvalbumin-positive interneurons: a canonical microcircuit for inhibition? *The Journal of Neuroscience* 31, 13260–13271.
- Paraoanu, L.E., Becker-Roeck, M., Christ, E., and Layer, P.G. (2006). Expression patterns of neurexin-1 and neuroligins in brain and retina of the chick embryo: Neuroligin-3 is absent in retina. *Neuroscience Letters* 395, 114–117.
- Patz, S., Grabert, J., Gorba, T., Wirth, M., and Wahle, P. (2004). Parvalbumin Expression in Visual Cortical Interneurons Depends on Neuronal Activity and TrkB Ligands during an Early Period of Postnatal Development. *Cerebral Cortex* 14, 342–351.
- Paxinos, G., and Franklin, K. (2001). *The Mouse Brain in Stereotaxic Coordinates* 2nd. (Academic Press).
- Peça, J., and Feng, G. (2012). Cellular and synaptic network defects in autism. *Current Opinion in Neurobiology* 22, 866–872.
- Peça, J., Feliciano, C., Ting, J.T., Wang, W., Wells, M.F., Venkatraman, T.N., Lascola, C.D., Fu, Z., and Feng, G. (2011). Shank3 mutant mice display autistic-like behaviours and striatal dysfunction. *Nature* 472, 437–442.
- Penn, A., Riquelme, P., Feller, M., and Shatz, C. (1998). Competition in Retinogeniculate Patterning Driven by Spontaneous Activity. *Science* 279, 2108–2112.
- Pizzorusso, T., Medini, P., Berardi, N., Chierzi, S., Fawcett, J., and Maffei, L. (2002). Reactivation of Ocular Dominance Plasticity in the Adult Visual Cortex. *Science* 298, 1248–1251.
- Pizzorusso, T., Medini, P., Landi, S., Baldini, S., Berardi, N., and Maffei, L. (2006). Structural and functional recovery from early monocular deprivation in adult rats. *Proceedings of the National Academy of Sciences of the United States of America* 103, 8517–8522.

- Popescu, M. V, and Polley, D.B. (2010). Monaural deprivation disrupts development of binaural selectivity in auditory midbrain and cortex. *Neuron* 65, 718–731.
- Porciatti, V., Pizzorusso, T., and Maffei, L. (1999). The visual physiology of the wild type mouse determined with pattern VEPs. *Vision Research* 39, 3071–3081.
- Porciatti, V., Pizzorusso, T., and Maffei, L. (2002). Electrophysiology of the postreceptoral visual pathway in mice. *Documenta Ophthalmologica. Advances in Ophthalmology* 104, 69–82.
- Poulopoulos, A., Aramuni, G., Meyer, G., Soykan, T., Hoon, M., Harvey, K., Jedlicka, P., Papadopoulos, T., Zhang, M., Paarmann, I., et al. (2009). Neuroligin 2 Drives Postsynaptic Assembly at Perisomatic Inhibitory Synapses through Gephyrin and Collybistin. *Neuron* 63, 628–642.
- Poulopoulos, A., Soykan, T., Tuffy, L.P., Varoqueaux, F., and Brose, N. (2012). Homodimerization and isoform-specific heterodimerization of neuroligins. *Biochemical Journal* 446, 321-30.
- Prange, O., Wong, T.P., Gerrow, K., Wang, Y.T., and El-Husseini, A. (2004). A balance between excitatory and inhibitory synapses is controlled by PSD-95 and neuroligin. *Proceedings of the National Academy of Sciences of the United States of America* 101, 13915–13920.
- Prusky, G.T., and Douglas, R.M. (2003). Developmental plasticity of mouse visual acuity. *European Journal of Neuroscience* 17, 167–173.
- Prusky, G.T., Reidel, C., and Douglas, R.M. (2000c). Environmental enrichment from birth enhances visual acuity but not place learning in mice. *Behavioural Brain Research* 114, 11–15.
- Prusky, G.T., West, P.W., and Douglas, R.M. (2000a). Behavioral assessment of visual acuity in mice and rats. *Vision Research* 40, 2201–2209.
- Prusky, G.T., West, P.W., and Douglas, R.M. (2000b). Experience-dependent plasticity of visual acuity in rats. *The European Journal of Neuroscience* 12, 3781–3786.
- Quina, L. a, Pak, W., Lanier, J., Banwait, P., Gratwick, K., Liu, Y., Velasquez, T., O’Leary, D.D.M., Goulding, M., and Turner, E.E. (2005). Brn3a-expressing retinal ganglion cells project specifically to thalamocortical and collicular visual pathways. *The Journal of Neuroscience* 25, 11595–11604.
- Rico, B., Xu, B., and Reichardt, L. (2002). TrkB receptor signaling is required for establishment of GABAergic synapses in the cerebellum. *Nature Neuroscience* 5, 225–233.
- Roberts, T.P.L., Khan, S.Y., Rey, M., Monroe, J.F., Cannon, K., Blaskey, L., Woldoff, S., Qasmieh, S., Gandal, M., Schmidt, G.L., et al. (2010). MEG detection of delayed auditory evoked responses in autism spectrum disorders: towards an imaging biomarker for autism. *Autism Research* 3, 8–18.
- Robertson, H., and Feng, G. (2011). Transgenic mouse models of childhood onset psychiatric disorders. *J Child Psychol Psychiatry* 52, 442–475.
- Rossi, F.M., Bozzi, Y., Pizzorusso, T., and Maffei, L. (1999). Monocular deprivation decreases brain-derived neurotrophic factor immunoreactivity in the rat visual cortex. *Neuroscience* 90, 363–368.

- Rossi, F.M., Pizzorusso, T., Porciatti, V., Marubio, L.M., Maffei, L., and Changeux, J.P. (2001). Requirement of the nicotinic acetylcholine receptor beta 2 subunit for the anatomical and functional development of the visual system. *Proceedings of the National Academy of Sciences of the United States of America* *98*, 6453–6458.
- Rubenstein, J.L.R., and Merzenich, M.M. (2003). Model of autism : increased ratio of excitation / inhibition in key neural systems. *Genes, Brain, and Behavior* *2*, 255–267.
- Rudy, B., and McBain, C.J. (2001). Kv3 channels: voltage-gated K<sup>+</sup> channels designed for high-frequency repetitive firing. *Trends in Neurosciences* *24*, 517–526.
- Rutherford, L.C., DeWan, A., Lauer, H.M., and Turrigiano, G.G. (1997). Brain-derived neurotrophic factor mediates the activity-dependent regulation of inhibition in neocortical cultures. *The Journal of Neuroscience* *17*, 4527–4535.
- Sakata, K., Woo, N.H., Martinowich, K., Greene, J.S., Schloesser, R.J., Shen, L., and Lu, B. (2009). Critical role of promoter IV-driven BDNF transcription in GABAergic transmission and synaptic plasticity in the prefrontal cortex. *Proceedings of the National Academy of Sciences of the United States of America* *106*, 5942–5947.
- Sale, A., Berardi, N., Spolidoro, M., Baroncelli, L., and Maffei, L. (2010). GABAergic inhibition in visual cortical plasticity. *Frontiers in Cellular Neuroscience* *4*, 1–10.
- Sale, A., Maya Vetencourt, J.F., Medini, P., Cenni, M.C., Baroncelli, L., De Pasquale, R., and Maffei, L. (2007). Environmental enrichment in adulthood promotes amblyopia recovery through a reduction of intracortical inhibition. *Nature Neuroscience* *10*, 679–681.
- Sale, A., Putignano, E., Cancedda, L., Landi, S., Cirulli, F., Berardi, N., and Maffei, L. (2004). Enriched environment and acceleration of visual system development. *Neuropharmacology* *47*, 649–660.
- Sanes, J.R., and Zipursky, S. (2010). Design Principles of Insect and Vertebrate Visual Systems. *Neuron* *66*, 15–36.
- Sato, M., and Stryker, M.P. (2008). Distinctive features of adult ocular dominance plasticity. *The Journal of Neuroscience* *28*, 10278–10286.
- Sato, M., and Stryker, M.P. (2010). Genomic imprinting of experience-dependent cortical plasticity by the ubiquitin ligase gene *Ube3a*. *Proceedings of the National Academy of Sciences of the United States of America* *107*, 5611–5616.
- Scheiffele, P., Fan, J., Choih, J., Fetter, R., and Serafini, T. (2000). Neuroligin expressed in nonneuronal cells triggers presynaptic development in contacting axons. *Cell* *101*, 657–669.
- Schuett, S., Bonhoeffer, T., and Hübener, M. (2002). Mapping retinotopic structure in mouse visual cortex with optical imaging. *The Journal of Neuroscience* *22*, 6549–6559.
- Schwartz, N., Schohl, A., and Ruthazer, E.S. (2011). Activity-dependent transcription of BDNF enhances visual acuity during development. *Neuron* *70*, 455–467.



- Seil, F.J., and Drake-Baumann, R. (2000). TrkB receptor ligands promote activity-dependent inhibitory synaptogenesis. *The Journal of Neuroscience* 20, 5367–5373.
- Selby, L., Zhang, C., and Sun, Q.-Q. (2007). Major defects in neocortical GABAergic inhibitory circuits in mice lacking the fragile X mental retardation protein. *Neuroscience Letters* 412, 227–232.
- Schatz, C.J., and Kirkwood, P.A. (1984). Prenatal development of functional connections in the cat's retinogeniculate pathway. *The Journal of Neuroscience* 4, 1378–1397.
- Schatz, C.J., and Stryker, M.P. (1988). Prenatal Tetrodotoxin Infusion Blocks Segregation of Retinogeniculate Afferents. *Science* 242, 87–89.
- Simmons, D.R., Robertson, A.E., McKay, L.S., Toal, E., McAleer, P., and Pollick, F.E. (2009). Vision in autism spectrum disorders. *Vision Research* 49, 2705–2739.
- Smith, G.B., Heynen, A.J., and Bear, M.F. (2009). Bidirectional synaptic mechanisms of ocular dominance plasticity in visual cortex. *Philosophical Transactions of the Royal Society of London. Series B, Biological Sciences* 364, 357–367.
- Soghomonian, J.J., and Martin, D.L. (1998). Two isoforms of glutamate decarboxylase: why? *Trends in Pharmacological Sciences* 19, 500–505.
- Somogyi, P., Tamás, G., Lujan, R., and Buhl, E.H. (1998). Salient features of synaptic organisation in the cerebral cortex. *Brain Research. Brain Research Reviews* 26, 113–135.
- Song, J.Y., Ichtchenko, K., Südhof, T.C., and Brose, N. (1999). Neuroligin 1 is a postsynaptic cell-adhesion molecule of excitatory synapses. *Proceedings of the National Academy of Sciences of the United States of America* 96, 1100–1105.
- Southwell, D.G., Froemke, R.C., Alvarez-Buylla, A., Stryker, M.P., and Gandhi, S.P. (2010). Cortical plasticity induced by inhibitory neuron transplantation. *Science* 327, 1145–1148.
- Stern, E. a, Maravall, M., and Svoboda, K. (2001). Rapid development and plasticity of layer 2/3 maps in rat barrel cortex in vivo. *Neuron* 31, 305–315.
- Südhof, T.C. (2008). Neuroligins and neurexins link synaptic function to cognitive disease. *Nature* 455, 903–911.
- Sugiyama, S., Di Nardo, A. a, Aizawa, S., Matsuo, I., Volovitch, M., Prochiantz, A., and Hensch, T.K. (2008). Experience-dependent transfer of Otx2 homeoprotein into the visual cortex activates postnatal plasticity. *Cell* 134, 508–520.
- Svirsky, M.A, Teoh, S.W., and Neuburger, H. (2004). Development of language and speech perception in congenitally, profoundly deaf children as a function of age at cochlear implantation. *Audiology and Neuro-Otology* 9, 224–233.
- Tabuchi, K., Blundell, J., Etherton, M.R., Hammer, R.E., Liu, X., Powell, C.M., and Südhof, T.C. (2007). A Neuroligin-3 Mutation Implicated in Autism Increases Inhibitory Synaptic Transmission in Mice. *Science* 318, 71–76.

- Talebizadeh, Z., Lam, D.Y., Theodoro, M.F., Bittel, D.C., Lushington, G.H., and Butler, M.G. (2006). Novel splice isoforms for NLGN3 and NLGN4 with possible implications in autism. *Journal of Medical Genetics* 43, e21.
- Thomson, A.M., and Lamy, C. (2007). Functional maps of neocortical local circuitry. *Frontiers in Neuroscience* 1, 19–42.
- Tommerdahl, M., Tannan, V., Cascio, C.J., Baranek, G.T., and Whitsel, B.L. (2007). Vibrotactile adaptation fails to enhance spatial localization in adults with autism. *Brain Research* 1154, 116–123.
- Torborg, C.L., and Feller, M.B. (2004). Unbiased analysis of bulk axonal segregation patterns. *Journal of Neuroscience Methods* 135, 17–26.
- Torborg, C.L., and Feller, M.B. (2005). Spontaneous patterned retinal activity and the refinement of retinal projections. *Progress in Neurobiology* 76, 213–235.
- Tropea, D., Giacometti, E., Wilson, N.R., Beard, C., McCurry, C., Fu, D.D., Flannery, R., Jaenisch, R., and Sur, M. (2009). Partial reversal of Rett Syndrome-like symptoms in MeCP2 mutant mice. *Proceedings of the National Academy of Sciences of the United States of America* 106, 2029–2034.
- Tsai, P.T., Hull, C., Chu, Y., Greene-Colozzi, E., Sadowski, A.R., Leech, J.M., Steinberg, J., Crawley, J.N., Regehr, W.G., and Sahin, M. (2012). Autistic-like behaviour and cerebellar dysfunction in Purkinje cell Tsc1 mutant mice. *Nature* 488, 647–651.
- Tsai, S.-J. (2005). Is autism caused by early hyperactivity of brain-derived neurotrophic factor? *Medical Hypotheses* 65, 79–82.
- Turrigiano, G.G., and Nelson, S.B. (2004). Homeostatic plasticity in the developing nervous system. *Nature Reviews. Neuroscience* 5, 97–107.
- van Slegtenhorst, M., et al. (1997). Identification of the Tuberous Sclerosis Gene TSC1 on Chromosome 9q34. *Science* 277, 805–808.
- Van Spronsen, M., and Hoogenraad, C.C. (2010). Synapse pathology in psychiatric and neurologic disease. *Current Neurology and Neuroscience Reports* 10, 207–214.
- Varoqueaux, F., Aramuni, G., Rawson, R.L., Mohrmann, R., Missler, M., Gottmann, K., Zhang, W., Brose, N., and Su, T.C. (2006). Neuroligins Determine Synapse Maturation and Function. *Neuron* 51, 741–754.
- Varoqueaux, F., Jamain, S., and Brose, N. (2004). Neuroligin 2 is exclusively localized to inhibitory synapses. *European Journal of Cell Biology* 83, 449–456.
- Verkerk, A., Pieretti, M., Sutcliffe, J., Fu, Y.-H., Kuhl, D., Pixxuti, A., Refner, O., Richards, S., Victoria, M.F., Zhang, F., et al. (1991). Identification of a Gene (FMR -1) Containing a CGG Repeat Coincident with a Breakpoint Cluster Region Exhibiting Length Variation in Fragile X Syndrome. *Cell* 65, 905–914.

- Vincent, J.B., Kolozsvari, D., Roberts, W.S., Bolton, P.F., Gurling, H.M.D., and Scherer, S.W. (2004). Mutation screening of X-chromosomal neuroligin genes: no mutations in 196 autism probands. *American Journal of Medical Genetics. Part B, Neuropsychiatric Genetics* 129B, 82–84.
- Vlamings, P.H.J.M., Jonkman, L.M., Van Daalen, E., Van der Gaag, R.J., and Kemner, C. (2010). Basic abnormalities in visual processing affect face processing at an early age in autism spectrum disorder. *Biological Psychiatry* 68, 1107–1113.
- Walsh, C.A., Morrow, E.M., and Rubenstein, J.L.R. (2008). Autism and Brain Development. *Cell* 135, 396–400.
- Wang, Q., and Burkhalter, A. (2007). Area Map of Mouse Visual Cortex. *The Journal of Comparative Neurology* 502, 339–357.
- Wang, Y., Gupta, A., Toledo-Rodriguez, M., Wu, C.Z., and Markram, H. (2002). Anatomical, physiological, molecular and circuit properties of nest basket cells in the developing somatosensory cortex. *Cerebral Cortex* 12, 395–410.
- Wässle, H. (2004). Parallel processing in the mammalian retina. *Nature Reviews. Neuroscience* 5, 747–757.
- Wermter, A.-K., Kamp-Becker, I., Strauch, K., Schulte-Körne, G., and Remschmidt, H. (2008). No evidence for involvement of genetic variants in the X-linked neuroligin genes NLGN3 and NLGN4X in probands with autism spectrum disorder on high functioning level. *American Journal of Medical Genetics. Part B, Neuropsychiatric Genetics* 147B, 535–537.
- Wiesel, T.N., and Hubel, D.H. (1963). Single-cell Responses in Striate Cortex of Kittens Deprived of Vision in One Eye. *Journal of Neurophysiology* 26, 1003–1017.
- Wiesel, T.N., and Hubel, D.H. (1965). Comparison of the effects of unilateral and bilateral eye closure on cortical unit responses in kittens. *Journal of Neurophysiology* 28, 1029–1040.
- Williams, D. (1998). The remarkable autobiography of an autistic girl. In *Nobody Nowhere* (London, UK: Jessica Kingsley).
- Wilson, B.M., and Cox, C.L. (2007). Absence of metabotropic glutamate receptor-mediated plasticity in the neocortex of fragile X mice. *Proceedings of the National Academy of Sciences of the United States of America* 104, 2454–2459.
- Wilson, N.R., Runyan, C.A., Wang, F.L., and Sur, M. (2012). Division and subtraction by distinct cortical inhibitory networks in vivo. *Nature* 488, 343–348.
- Xiang, M., Zhou, L., Macke, J.P., Yoshioka, T., Hendry, S.H., Eddy, R.L., Shows, T.B., and Nathans, J. (1995). The Brn-3 family of POU-domain factors: primary structure, binding specificity, and expression in subsets of retinal ganglion cells and somatosensory neurons. *The Journal of Neuroscience* 15, 4762–4785.
- Xu, H., Jeong, H.-Y., Tremblay, R., and Rudy, B. (2013). Neocortical somatostatin-expressing GABAergic interneurons disinhibit the thalamorecipient layer 4. *Neuron* 77, 155–167.

- Yan, J., Feng, J., Schroer, R., Li, W., Skinner, C., Schwartz, C.E., Cook, E.H., and Sommer, S.S. (2008). Analysis of the neuroligin 4Y gene in patients with autism. *Psychiatric Genetics* 18, 204–207.
- Yan, J., Oliveira, G., Coutinho, a, Yang, C., Feng, J., Katz, C., Sram, J., Bockholt, a, Jones, I.R., Craddock, N., et al. (2005). Analysis of the neuroligin 3 and 4 genes in autism and other neuropsychiatric patients. *Molecular Psychiatry* 10, 329–332.
- Yanagi, K., Kaname, T., Wakui, K., Hashimoto, O., Fukushima, Y., and Naritomi, K. (2012). Identification of Four Novel Synonymous Substitutions in the X-Linked Genes Neuroligin 3 and Neuroligin 4X in Japanese Patients with Autistic Spectrum Disorder. *Autism Research and Treatment* 2012.
- Yashiro, K., Riday, T.T., Condon, K.H., Roberts, A.C., Bernardo, D.R., Prakash, R., Weinberg, R.J., Ehlers, M.D., and Philpot, B.D. (2009). Ube3a is required for experience-dependent maturation of the neocortex. *Nature Neuroscience* 12, 777–783.
- Yazaki-sugiyama, Y., Kang, S., Cateau, H., Fukai, T., and Hensch, T.K. (2009). Bidirectional plasticity in fast-spiking GABA circuits by visual experience. *Nature* 462, 218–222.
- Ye, H., Liu, J., and Wu, J.Y. (2010). Cell adhesion molecules and their involvement in autism spectrum disorder. *Neuro-Signals* 18, 62–71.
- Yip, J., Soghomonian, J.-J., and Blatt, G.J. (2007). Decreased GAD67 mRNA levels in cerebellar Purkinje cells in autism: pathophysiological implications. *Acta Neuropathologica* 113, 559–568.
- Ylisaukko-oja, T., Rehnström, K., Auranen, M., Vanhala, R., Alen, R., Kempas, E., Ellonen, P., Turunen, J. a, Makkonen, I., Riikonen, R., et al. (2005). Analysis of four neuroligin genes as candidates for autism. *European Journal of Human Genetics : EJHG* 13, 1285–1292.
- Yoshimura, Y., and Callaway, E.M. (2005). Fine-scale specificity of cortical networks depends on inhibitory cell type and connectivity. *Nature Neuroscience* 8, 1552–1559.
- Yu, J., He, X., Yao, D., Li, Z., Li, H., and Zhao, Z. (2011). A sex-specific association of common variants of neuroligin genes (NLGN3 and NLGN4X) with autism spectrum disorders in a Chinese Han cohort. *Behavioral and Brain Functions* 7, 13.
- Zemon, V., Kaplan, E., and Ratliff, F. (1980). Bicuculline enhances a negative component and diminishes a positive component of the visual evoked cortical potential in the cat. *Proceedings of the National Academy of Sciences of the United States of America* 77, 7476–7478.
- Zhang, C., Milunsky, J.M., Newton, S., Ko, J., Zhao, G., Maher, T.A., Tager-Flusberg, H., Bolliger, M.F., Carter, A.S., Boucard, A.A., et al. (2009). A neuroligin-4 missense mutation associated with autism impairs neuroligin-4 folding and endoplasmic reticulum export. *The Journal of Neuroscience* 29, 10843–10854.
- Zhang, Y.Q., Bailey, A.M., Matthies, H.J., Renden, R.B., Smith, M.A., Speese, S.D., Rubin, G.M., and Broadie, K. (2001). *Drosophila* fragile X-related gene regulates the MAP1B homolog Futsch to control synaptic structure and function. *Cell* 107, 591–603.

Zhao, M.-G., Toyoda, H., Ko, S.W., Ding, H.-K., Wu, L.-J., and Zhuo, M. (2005). Deficits in trace fear memory and long-term potentiation in a mouse model for fragile X syndrome. *The Journal of Neuroscience* 25, 7385–7392.

Zoghbi, H.Y., and Bear, M.F. (2012). Synaptic Dysfunction in Neurodevelopmental Disorders Associated with Autism and Intellectual Disabilities. *Cold Spring Harbor Perspectives in Biology* 4, a009886–a009886.